Reversible Enolization of β-Amino Carboxamides by Lithium Hexamethyldisilazide

Anne J. McNeil and David B. Collum*

Baker Laboratory, Department of Chemistry and Chemical Biology, Cornell University, Ithaca, New York 14853-1301

Supporting Information

Structure Chart

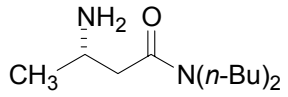

1

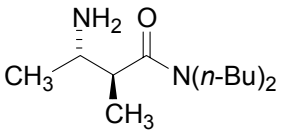

2

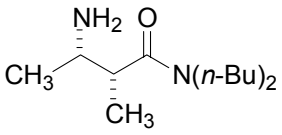

3

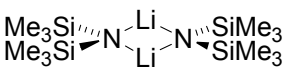

5

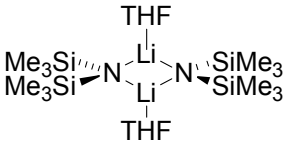

6

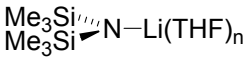

7; n = 3
8; n = 4

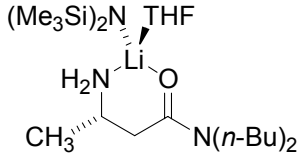

9

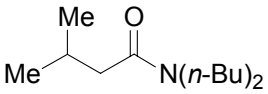

10

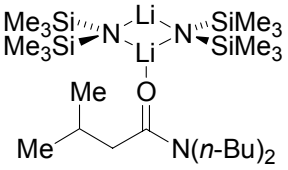

11

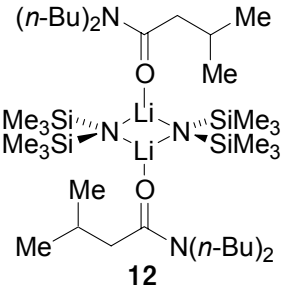

12

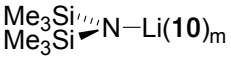

13

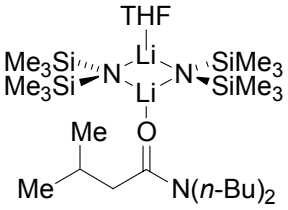

14

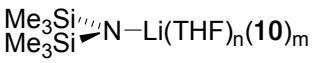

15

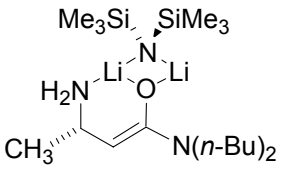

16

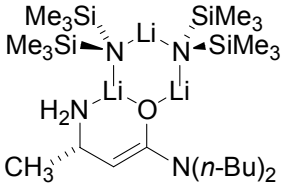

17

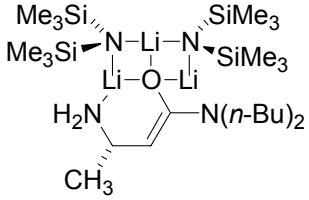

18

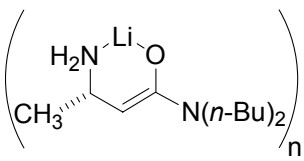

19

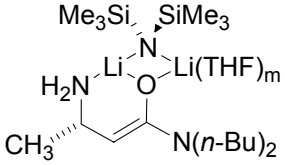

20

Structure Chart (continued)

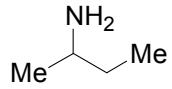

23

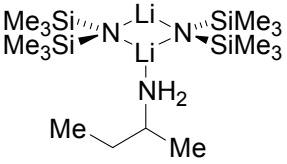

24

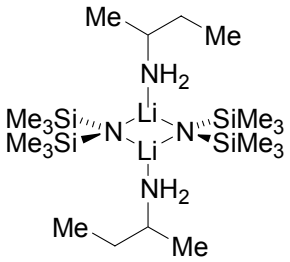

25

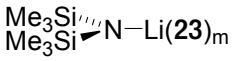

26

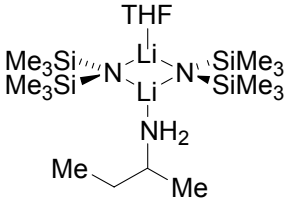

27

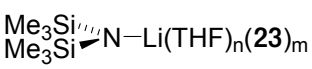

28

Procedure for the synthesis of 1 and [^{15}N]1.

(Adapted from the procedure used to couple an amino acid with a diazoketone by the Arndt-Eistert protocol, see Podlech, J.; Seebach, D. *Angew. Chem., Int. Ed. Engl.* **1995**, *34*, 471-472)

N-(*tert*-butoxycarbonyl)-L-alanine (2.5 g, 13.1 mmol) or [^{15}N] *N*-(*tert*-butoxycarbonyl)-L-alanine was dissolved in THF (60 mL) and cooled to 0 ^{o}C. Et_3N (1.89 mL, 13.1 mmol) and ethyl chloroformate (1.26 mL, 13.1 mmol) were added to the flask. A white precipitate formed on stirring. Diazomethane was prepared from Diazald (5.61 g, 26.2 mmol) dissolved in Et_2O (50 mL) and distilled from a basic solution of KOH (5.7 g) in EtOH (95%, 11 mL) and H_2O (9 mL). The ethereal diazomethane solution was poured into the THF solution containing the mixed anhydride and the ice-water bath was removed. After stirring for 2-3 h or until evolution of N_2 had ceased, EtOAc (50 mL) was added to the reaction mixture and the heterogeneous mixture was extracted with aqueous solutions of $NaHCO_3$ (50 mL), NH_4Cl (50 mL), and NaCl (50 mL), dried over $MgSO_4$, and concentrated to give a yellow solid. The crude product was purified by silica gel chromatography (2/1 petroleum ether/EtOAc) to give the diazoketone (2.46 g, 88% yield). ^{1}H NMR (400 MHz, $CDCl_3$): δ 1.30 (d, J = 6.8 Hz, 3H), 1.42 (s, 9H), 4.19 (bm, 1H), 5.12 (bm, 1H), 5.42 (s, 1 H).

The diazoketone (2.46 g, 11.5 mmol) was dissolved in THF (40 mL) and the flask was wrapped with a dark cloth to exclude light. The homogeneous solution was cooled to -45 ^{o}C, and a solution of silver benzoate (0.29 g, 1.27 mmol) dissolved in Bu_2NH was added. The reaction was allowed to reach room temperature over 3-4 h. Et_2O (50 mL) was added to the reaction and the mixture was washed with a 1 M HCl solution (2 x 25 mL) followed by extraction with saturated solutions of $NaHCO_3$ (50 mL), NH_4Cl (50 mL),

and NaCl (50 mL). The organic layer was dried over $MgSO_4$ and concentrated to give a yellow oil. The crude product was purified by silica gel chromatography (5/1 petroleum ether/EtOAc) to give the *N*-Boc-carboxamide (3.28 g, 91% yield). See Figure S1 for ^1H and ^{13}C NMR spectra.

The *N*-Boc-carboxamide (3.28 g, 10.4 mmol) was dissolved in MeOH (25 mL) and $TsOH \cdot H_2O$ (1.98 g, 10.4 mmol) was added. The solution was refluxed for 3 h until evolution of CO_2 has ceased. The MeOH is partially removed via rotary evaporation and CH_2Cl_2 (50 mL) was added followed by concentration. This procedure was repeated until the MeOH was completely removed as shown via ^1H NMR spectroscopy. ^1H NMR (300 MHz, $CDCl_3$): δ 0.92 (t, J = 7.2 Hz, 3H), 0.93 (t, J = 7.2 Hz, 3H), 1.28 (m, 4H), 1.44 (m, 4H), 1.48 (d, J = 6.6 Hz, 3 H), 2.38 (s, 3H), 2.66 (dd, J = 3.9, 17.1 Hz, 1H), 2.79 (dd, J = 8.7, 17.4 Hz, 1H), 3.13 (m, 2H), 3.26 (t, J = 7.5 Hz, 2H), 3.71 (bm, 1H), 7.19 (d, J = 8.1 Hz, 2H), 7.76 (d, J = 8.1 Hz, 2H), 8.07 (bs, 3H).

Anhydrous NH_3 (15 mL) was condensed in a 100 mL RBF equipped with a dry ice-acetone condenser. The ammonium tosylate salt was dissolved in CH_2Cl_2 (10 mL) and added to the flask via syringe. The mixture was refluxed for 15 min. Anhydrous Et_2O (50 mL) distilled from Na/benzophenone was then added, and the excess NH_3 is evaporated. The NH_4OTs salt was removed via filtration and the solution was concentrated to give **1** (1.28 g, 46% overall yield from amino acid).

Optical rotation measurements (MeOH) for (*R*)-**1** and (*S*)-**1** are -0.0239 and +0.0223, respectively.

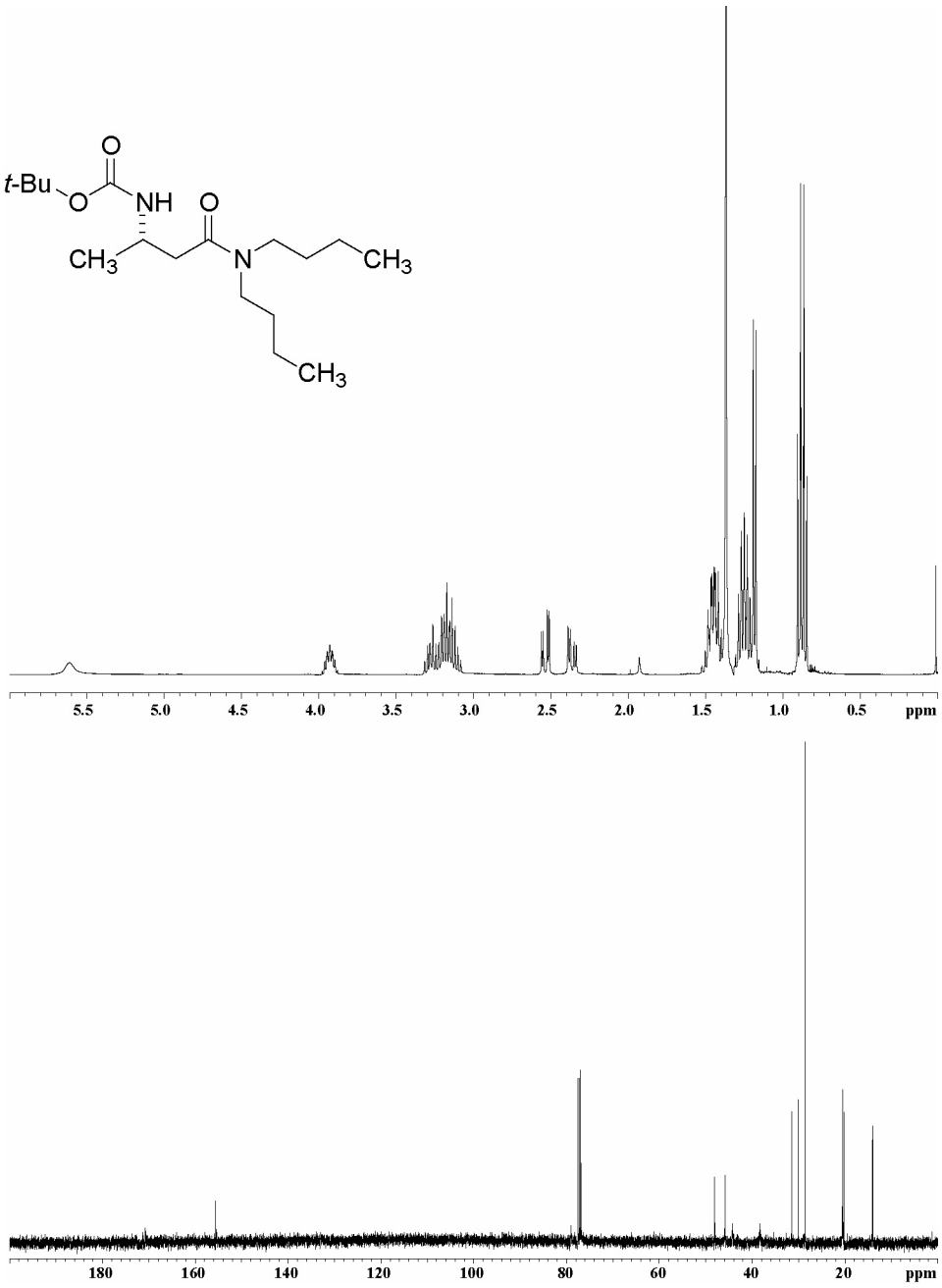

Figure S1. ^{1}H NMR (400 MHz, $CDCl_3$): δ 0.87 (t, J = 7.6 Hz, 3H), 0.89 (t, J = 7.2 Hz, 3H), 1.18 (d, J = 6.4 Hz, 3H), 1.25 (sept, J = 7.2 Hz, 4H), 1.37 (s, 9H), 1.45 (m, 4H), 2.36 (dd, J = 5.6, 15.2 Hz, 1H), 2.54 (dd, J = 4.4, 15.2 Hz, 1H), 3.17 (m, 2H), 3.26 (m, 2H), 3.93 (m, 1H), 5.61 (bs, 1H). ^{13}C NMR (100 MHz, $CDCl_3$): δ 14.0, 14.1, 20.3, 20.5, 20.6, 28.6, 30.1, 31.4, 38.3, 44.2, 45.8, 48.1, 155.6, 170.8.

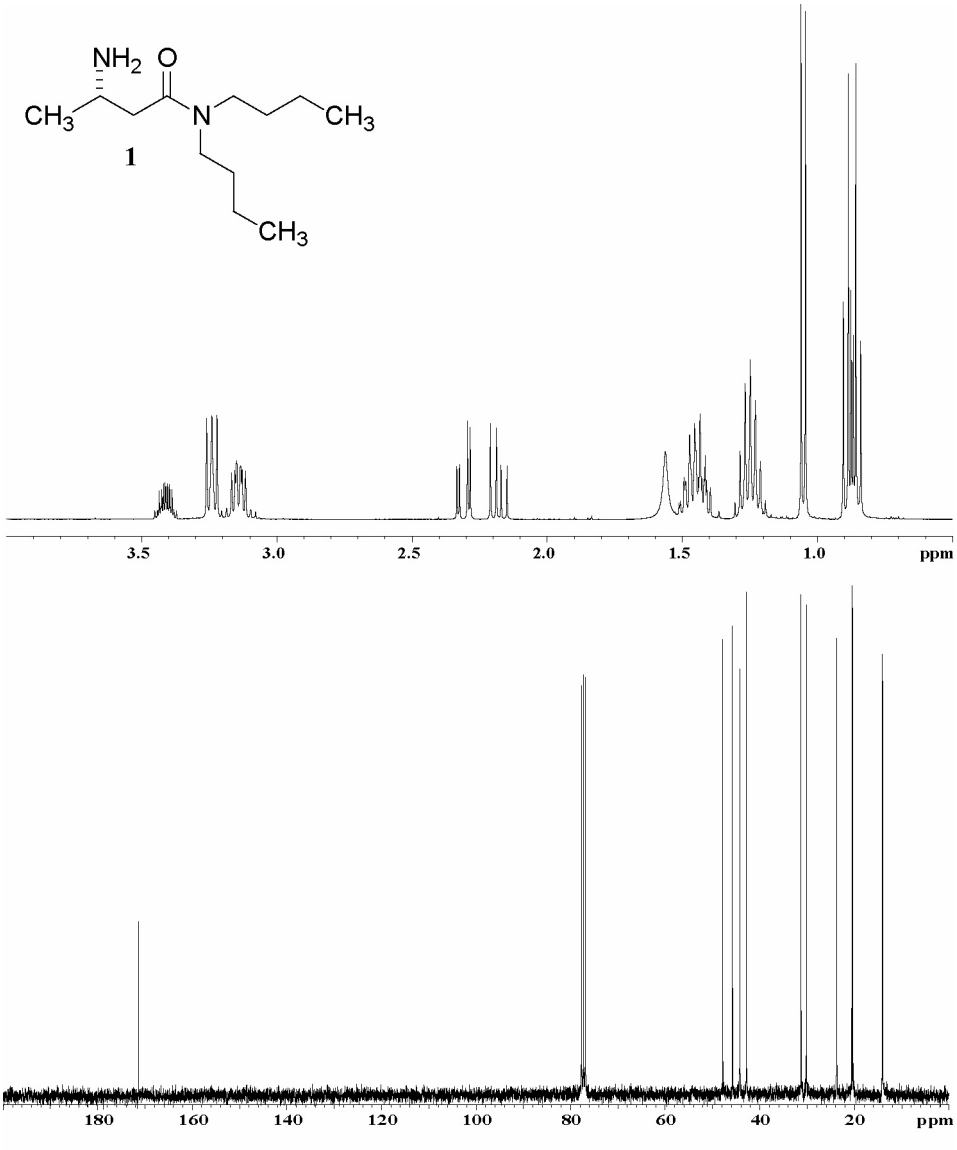

Figure S2. ^{1}H NMR (400 MHz, $CDCl_3$): δ 0.86 (t, *J* = 7.6 Hz, 3H), 0.89 (t, *J* = 7.2 Hz, 3H), 1.05 (d, *J* = 6.4 Hz, 3H), 1.25 (sept, *J* = 7.6 Hz, 4H), 1.45 (sept, *J* = 5.6 Hz, 4H), 1.56 (bs, 2H), 2.18 (dd, *J* = 9.2, 16 Hz, 1H), 2.31 (dd, *J* = 4, 16 Hz, 1H), 3.13 (m, 2H), 3.24 (t, *J* = 7.6 Hz, 2H), 3.41 (ddt, *J* = 3.6, 6.4, 10.4 Hz, 1H). ^{13}C NMR (75 MHz, $CDCl_3$): δ 14.0, 14.1, 20.3, 20.5, 23.7, 30.1, 31.3, 42.8, 44.2, 45.8, 47.8, 171.4.

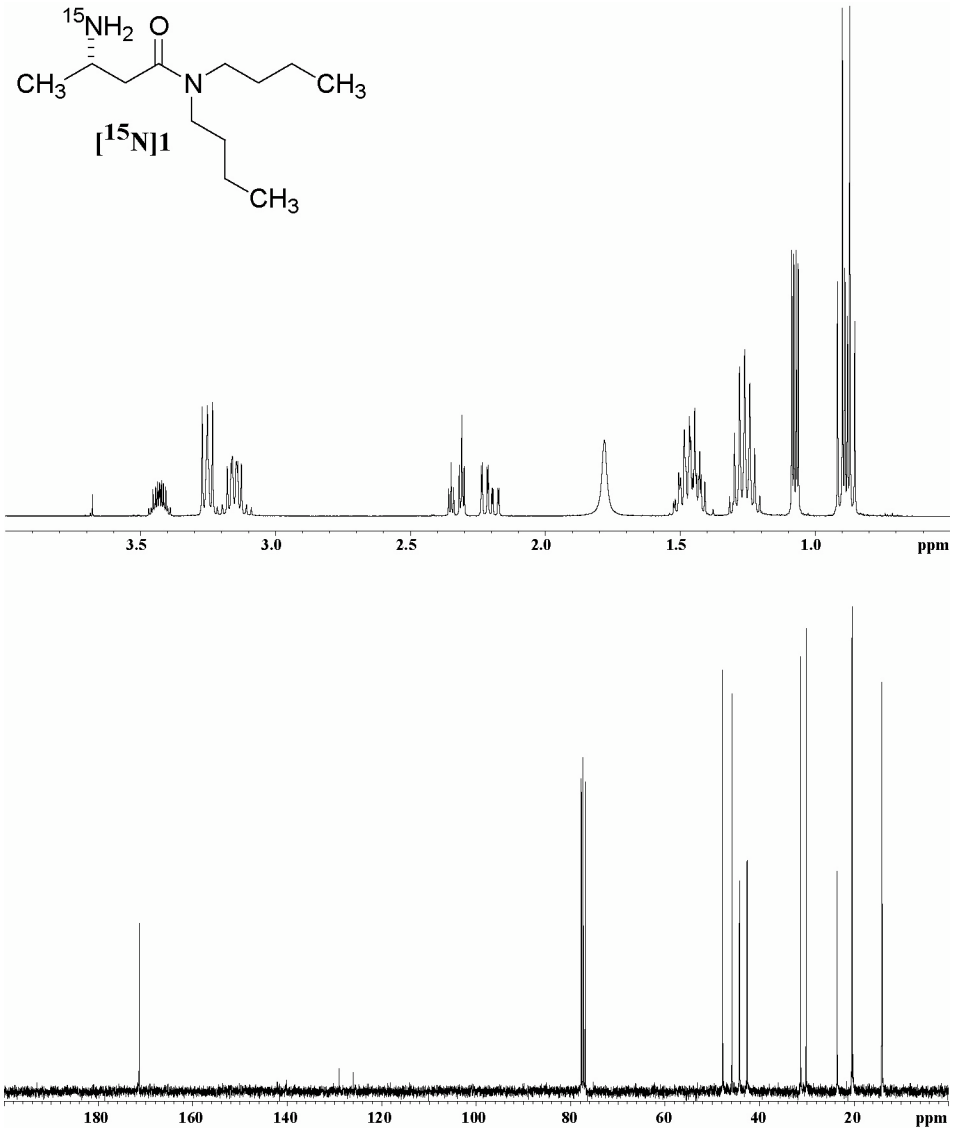

Figure S3. ^{1}H NMR (400 MHz, $CDCl_3$): δ 0.87 (t, *J* = 7.2 Hz, 3H), 0.90 (t, *J* = 7.2 Hz, 3H), 1.07 (dd, *J* = 2.8, 6.4 Hz, 3H), 1.26 (sept, *J* = 7.6 Hz, 4H), 1.45 (m, 4H), 1.78 (bs, 2H), 2.20 (ddd, *J* = 1.6, 8.8, 15.6 Hz, 1H), 2.33 (dt, *J* = 3.6, 16 Hz, 1H), 3.13 (m, 2H), 3.43 (dd, *J* = 7.6, 8 Hz, 2H), 3.41 (m, 1H). ^{13}C NMR (75 MHz, $CDCl_3$): δ 14.0, 14.1, 20.3, 20.5, 23.6 (*J* = 2.3 Hz), 30.1, 31.3, 42.6 (*J* = 2.3 Hz), 44.2 (*J* = 4.0 Hz), 45.8, 47.8, 171.4.

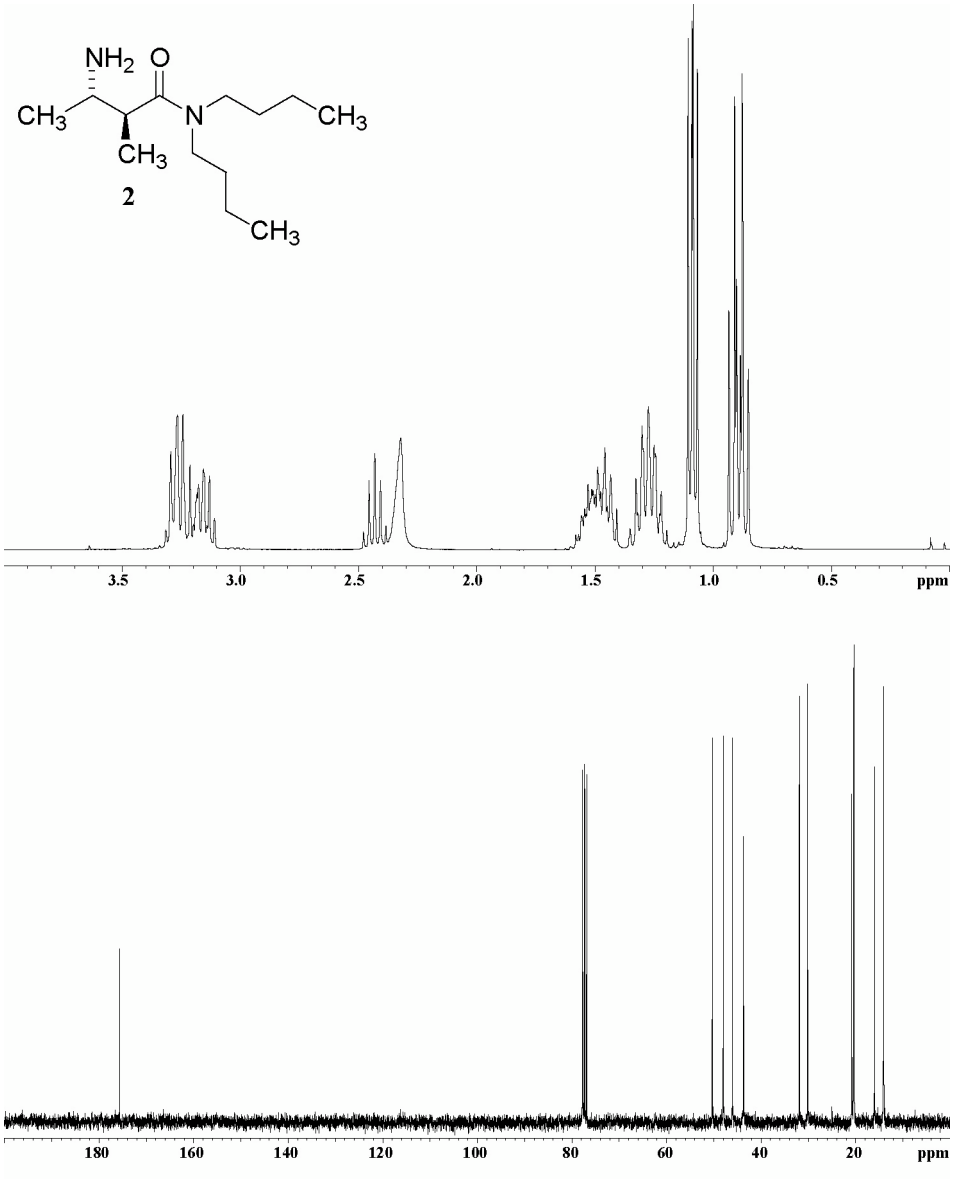

Figure S4. ^{1}H NMR (300 MHz, $CDCl_3$): δ 0.88 (t, *J* = 7.5 Hz, 3H), 0.91 (t, *J* = 7.5 Hz, 3H), 1.07 (d, *J* = 5.1 Hz, 3H), 1.10 (d, *J* = 4.8 Hz, 3H), 1.27 (sept, *J* = 7.5 Hz, 4H), 1.49 (sept, *J* = 7.5 Hz, 4H), 2.32 (bs, 2H), 2.43 (quin, *J* = 7.2, 1H), 3.15 (q, J = 6.6 Hz, 2H), 3.18 (m, 1H), 3.25 (q, *J* = 6.9 Hz, 2H). ^{13}C NMR (75 MHz, $CDCl_3$): δ 14.0, 14.1, 15.9, 20.3, 20.5, 20.8, 30.1, 31.9, 43.7, 46.0, 48.0, 50.3, 175.6.

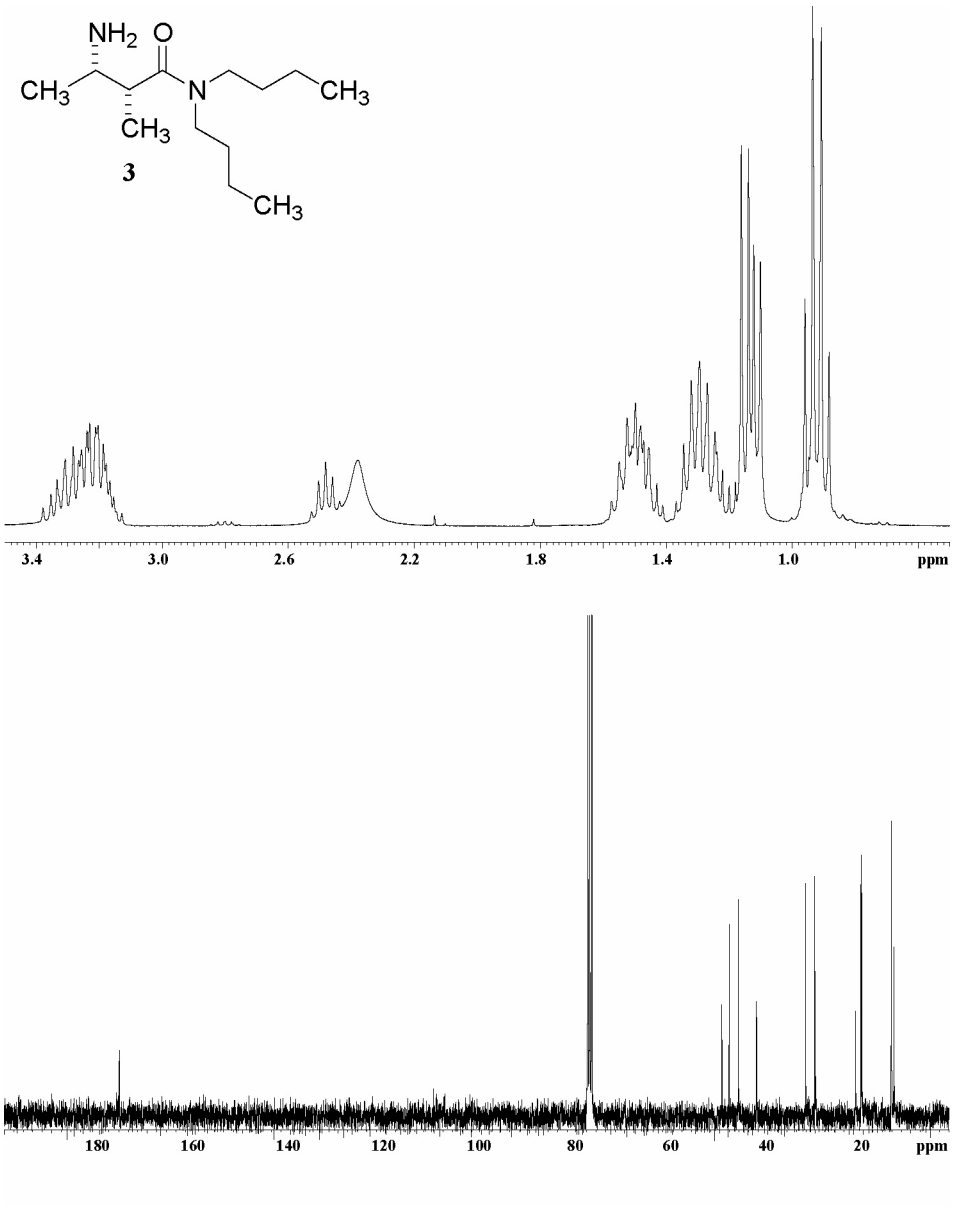

Figure S5. ^{1}H NMR (300 MHz, $CDCl_3$): δ 0.91 (t, J = 7.2 Hz, 3H), 0.94 (t, J = 7.2 Hz, 3H), 1.11 (d, J = 6.6 Hz, 3H), 1.15 (d, J = 6.9 Hz, 3H), 1.29 (sept, J = 7.8 Hz, 4H), 1.50 (sept, J = 7.8 Hz, 4H), 2.38 (bs, 2H), 2.43 (quin, J = 6.9, 1H), 3.22 (m, 2H), 3.24 (m, 1H), 3.28 (m, 2H). ^{13}C NMR (75 MHz, $CDCl_3$): δ 13.5, 14.0, 14.1, 20.3, 20.5, 21.6, 30.1, 32.0, 42.3, 46.2, 48.1, 49.6, 175.9.

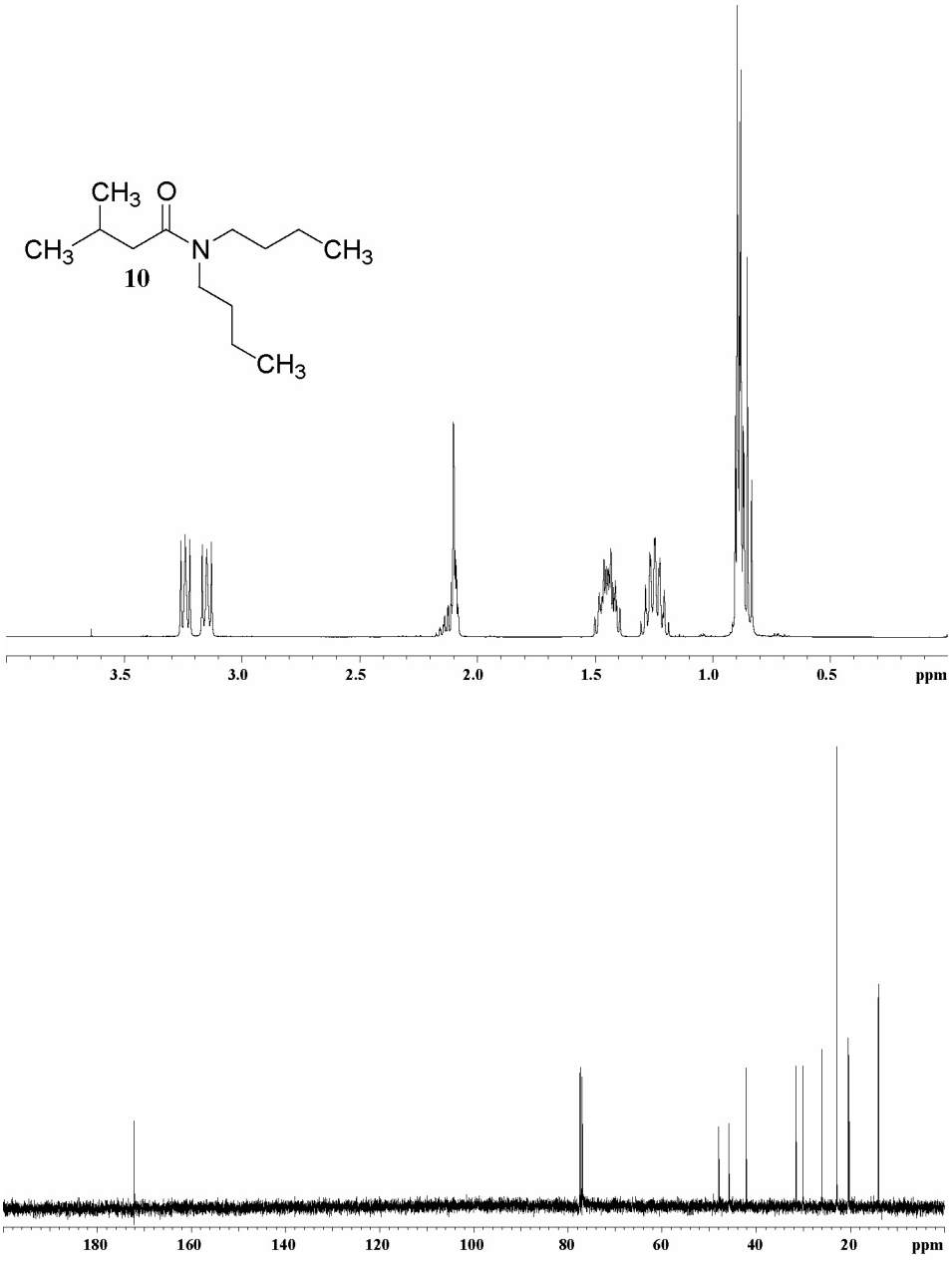

Figure S6. ^{1}H NMR (400 MHz, $CDCl_3$): δ 0.85 (t, *J* = 7.2 Hz, 3H), 0.89 (d, *J* = 6.4 Hz, 6H), 0.90 (t, *J* = 7.2 Hz, 3H), 1.25 (m, 4H), 1.44 (m, 4H), 2.09 (m, 1H), 2.10 (t, *J* = 7.2 Hz, 2H), 3.15 (t, *J* = 7.8 Hz, 2H), 3.24 (t, *J* = 7.6 Hz, 2H). ^{13}C NMR (100 MHz, $CDCl_3$): δ 14.0, 14.1, 20.3, 20.5, 22.9, 26.0, 30.1, 31.5, 42.1, 45.8, 47.9, 172.2.

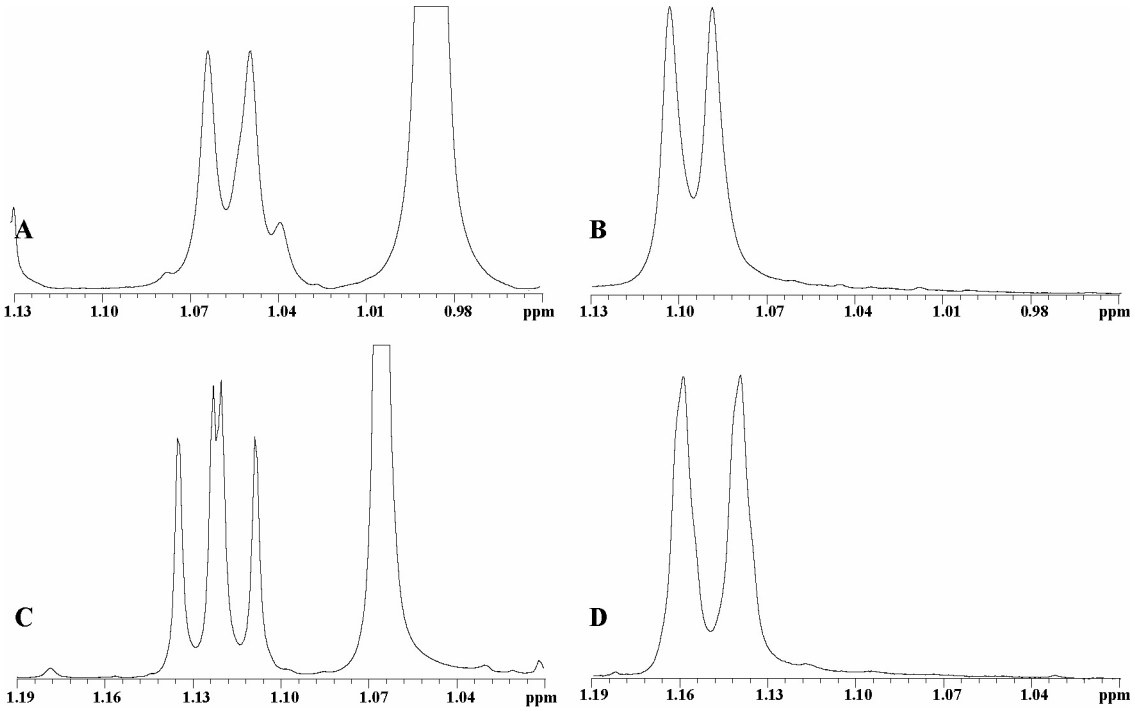

Figure S7. ^{1}H NMR spectra ($CDCl_3$) recorded on the product of reaction of (*S*)-**1** (0.10 M, 100% ee) with LiHMDS (0.10 M) in 0.075 M THF/toluene at 20 ^{o}C: (A) and (B) 2 h; (C) and (D) 24 h. Spectra A and C were recorded with addition of 1 equiv of (+)-TADDOL.

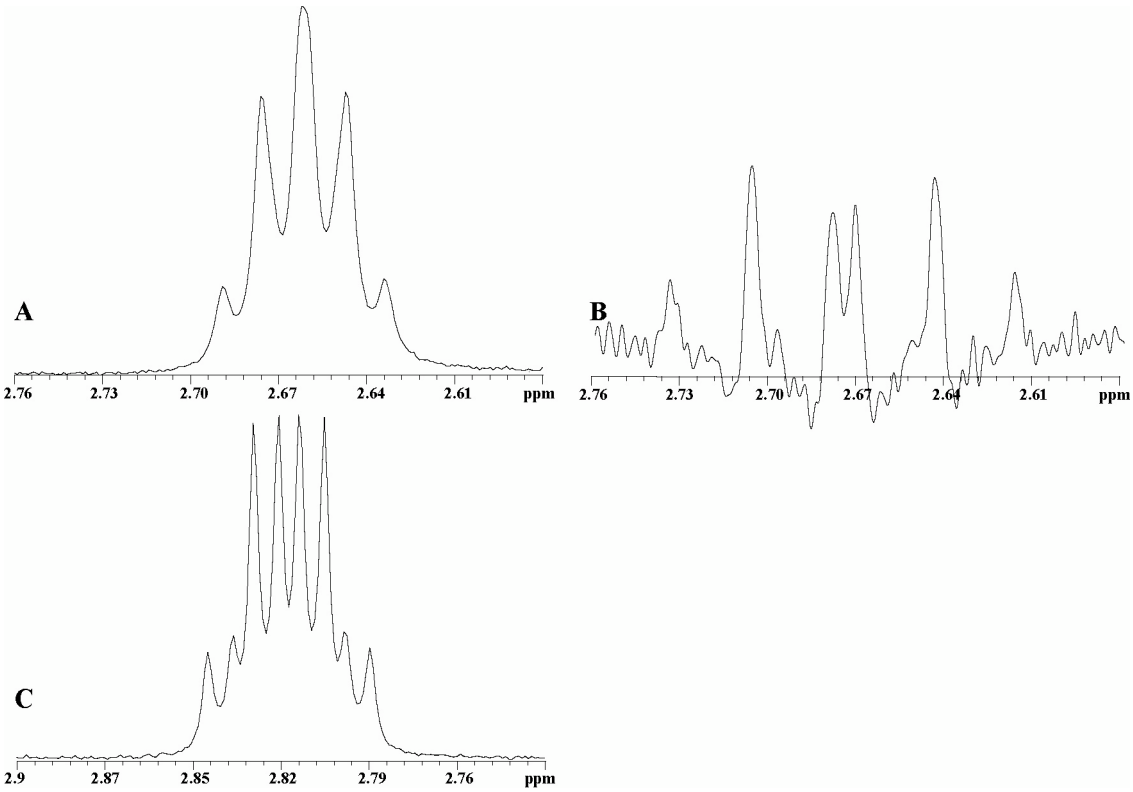

Figure S8. ^{1}H NMR spectra (500 MHz, d_8-THF) recorded on (A) *N*-Boc **3**; (B) *N*-Boc **3** (J = 7, 8.8 Hz) with an unshifted squared sinusoidal weighting function; (C) *N*-Boc **2** (J = 3.5, 6.5 Hz). **2** and **3** were separated by column chromatography (80/20 petroleum ether/EtOAc) after Boc protection of the amine.

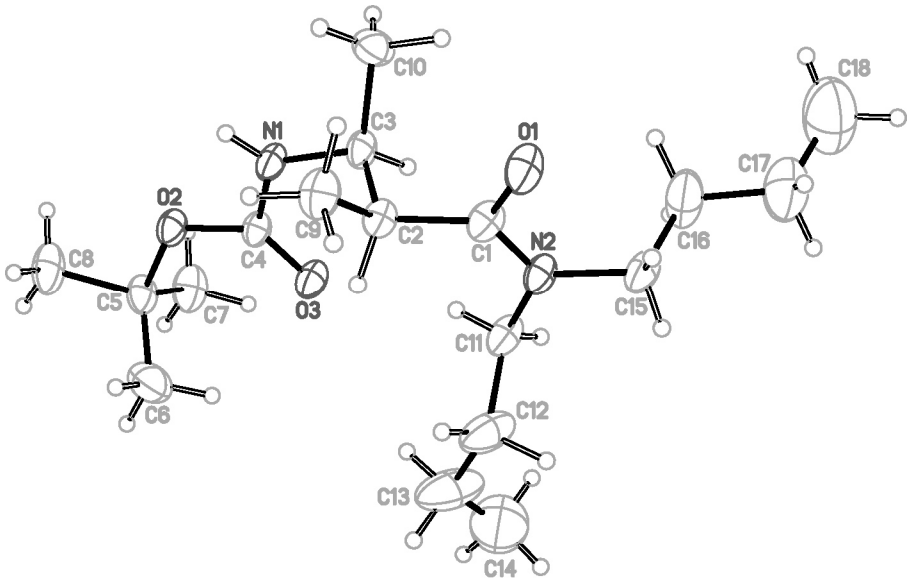

Figure S9. ORTEP of the *N*-Boc derivative of **2**.

Experimental: Crystals of *N*-Boc **2** were obtained from an EtOAc solution by evaporation at ambient temperature. A single crystal suitable for X-ray diffraction was transferred to the goniometer head of a Bruker X8 APEX II diffractometer (λ = 0.71073 Å, T = 173 K). The crystal belongs to the space group P2(1). 1093 frames were collected using 0.5 deg. omega and phi scans ($2\theta_{max}$ = 49.42 º). The data were processed with Bruker SAINT and SADABS programs to yield a total of 6869 unique reflections (R(int)=0.0173). The structure was solved using direct method (SHELXS) completed by subsequent Fourier synthesis and refined by full-matrix least-squares procedures (SHELXL). At final convergence, R(1) = 0.0757 for 3433 Fo > 4sig(Fo) and GOF = 1.067 for 505 parameters.

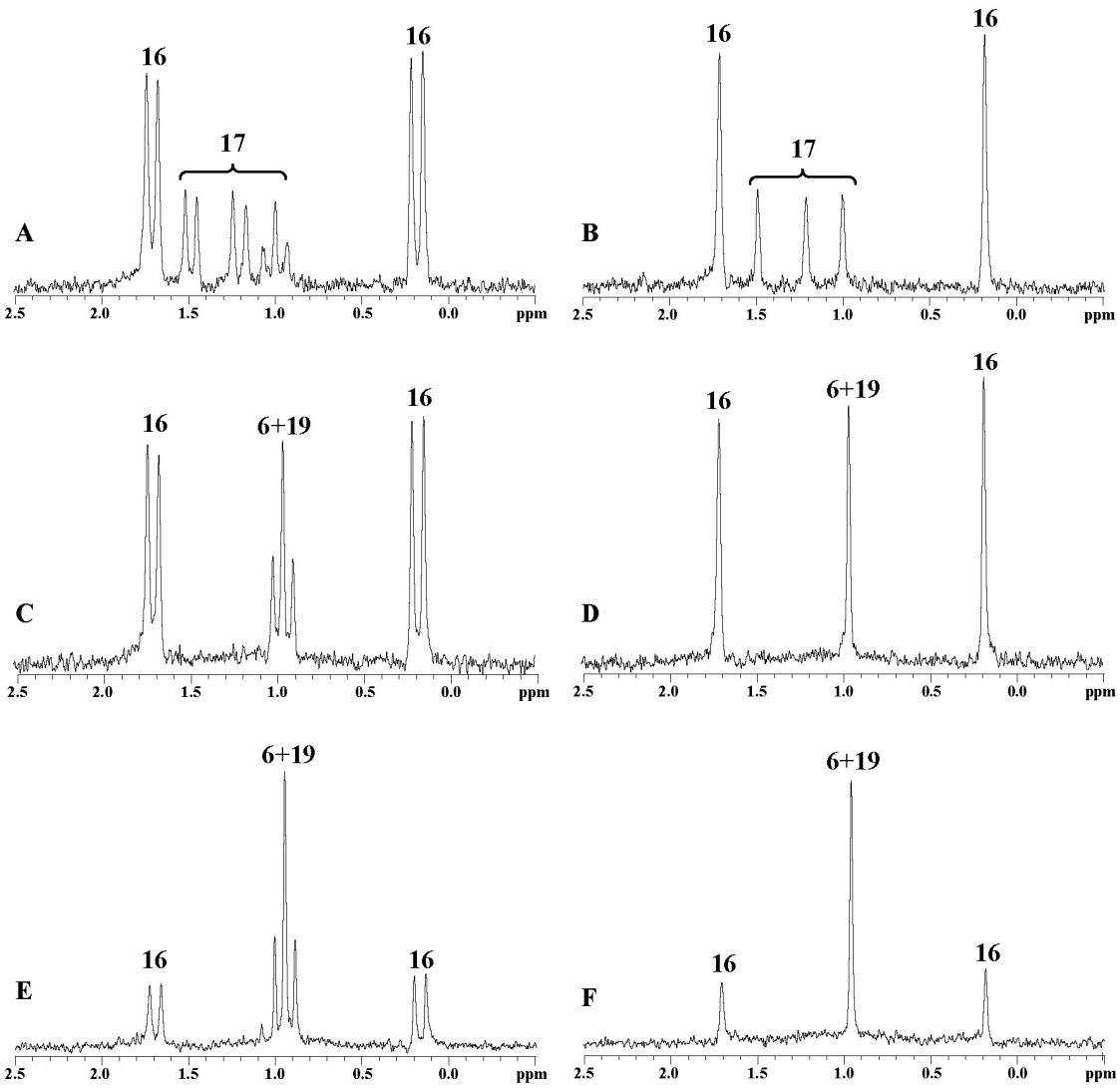

Figure S10. ^{6}Li NMR spectra recorded on [^{6}Li,^{15}N]LiHMDS (0.08 M) and **1** (0.023 M) at various THF concentrations with toluene at -75 ^{o}C: (A) and (B) 0.0 M; (C) and (D) 0.01 M; (E) and (F) 0.02 M; (G) and (H) 0.04 M; (I) and (J) 0.06 M; (K) and (L) 0.08 M. Spectra B, D, F, H, J, and L were recorded with ^{15}N broad-band decoupling.

Figure S10 (continued)

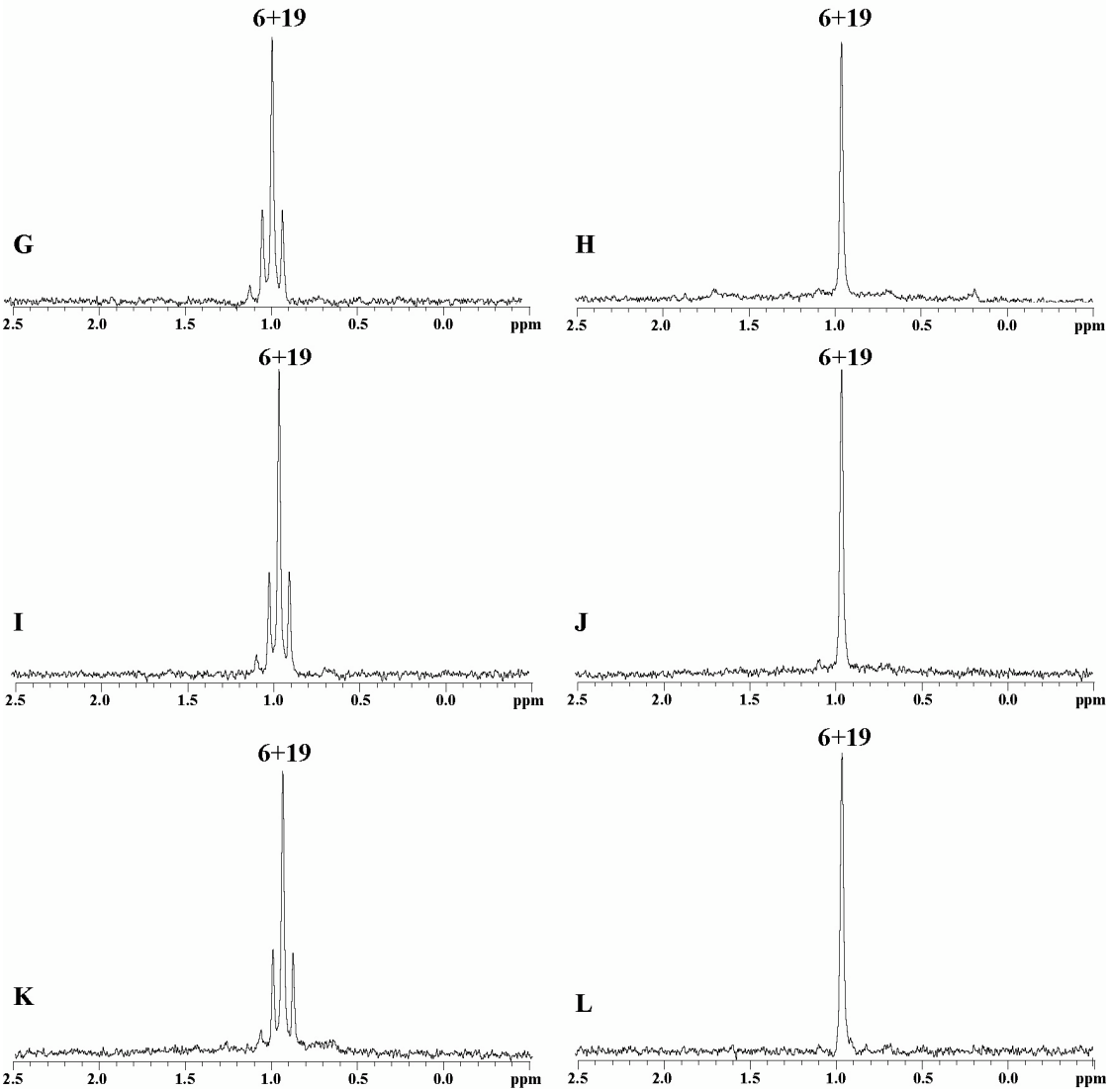

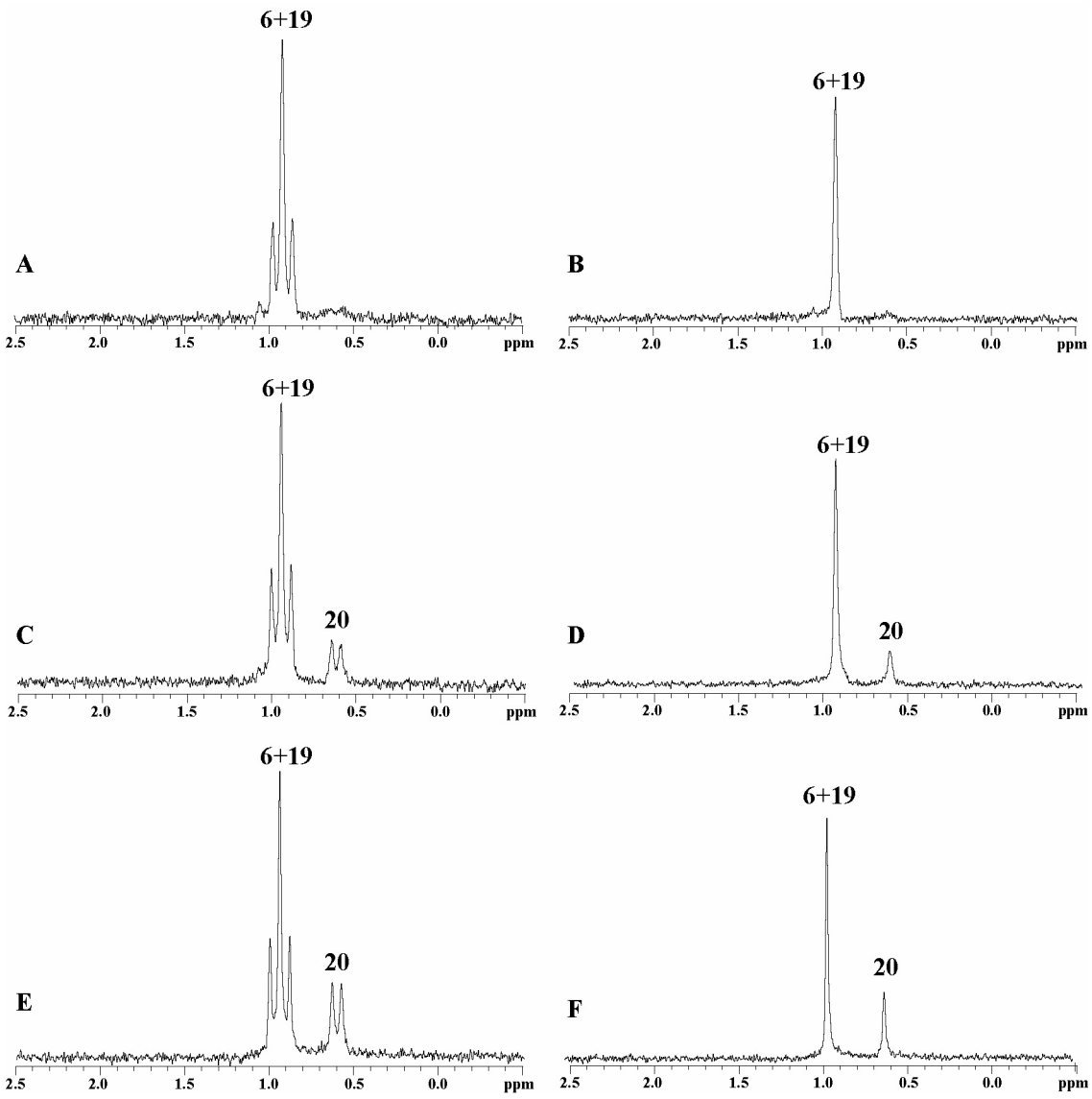

Figure S11. ^{6}Li NMR spectra recorded on [^{6}Li,^{15}N]LiHMDS (0.08 M) and **1** (0.023 M) at various THF concentrations with toluene at -75 ^{o}C: (A) and (B) 0.1 M; (C) and (D) 0.3 M; (E) and (F) 0.5 M; (G) and (H) 0.7 M; (I) and (J) 1.0 M. Spectra B, D, F, H, and J were recorded with ^{15}N broad-band decoupling.

Figure S11 (continued)

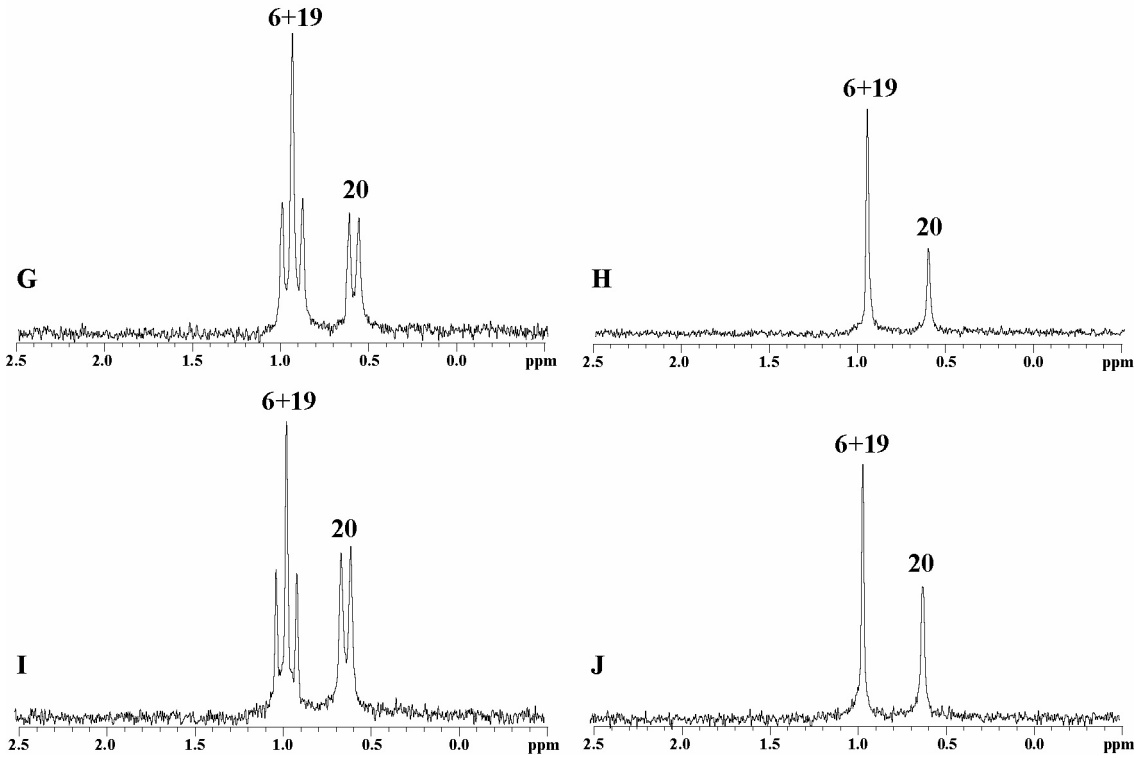

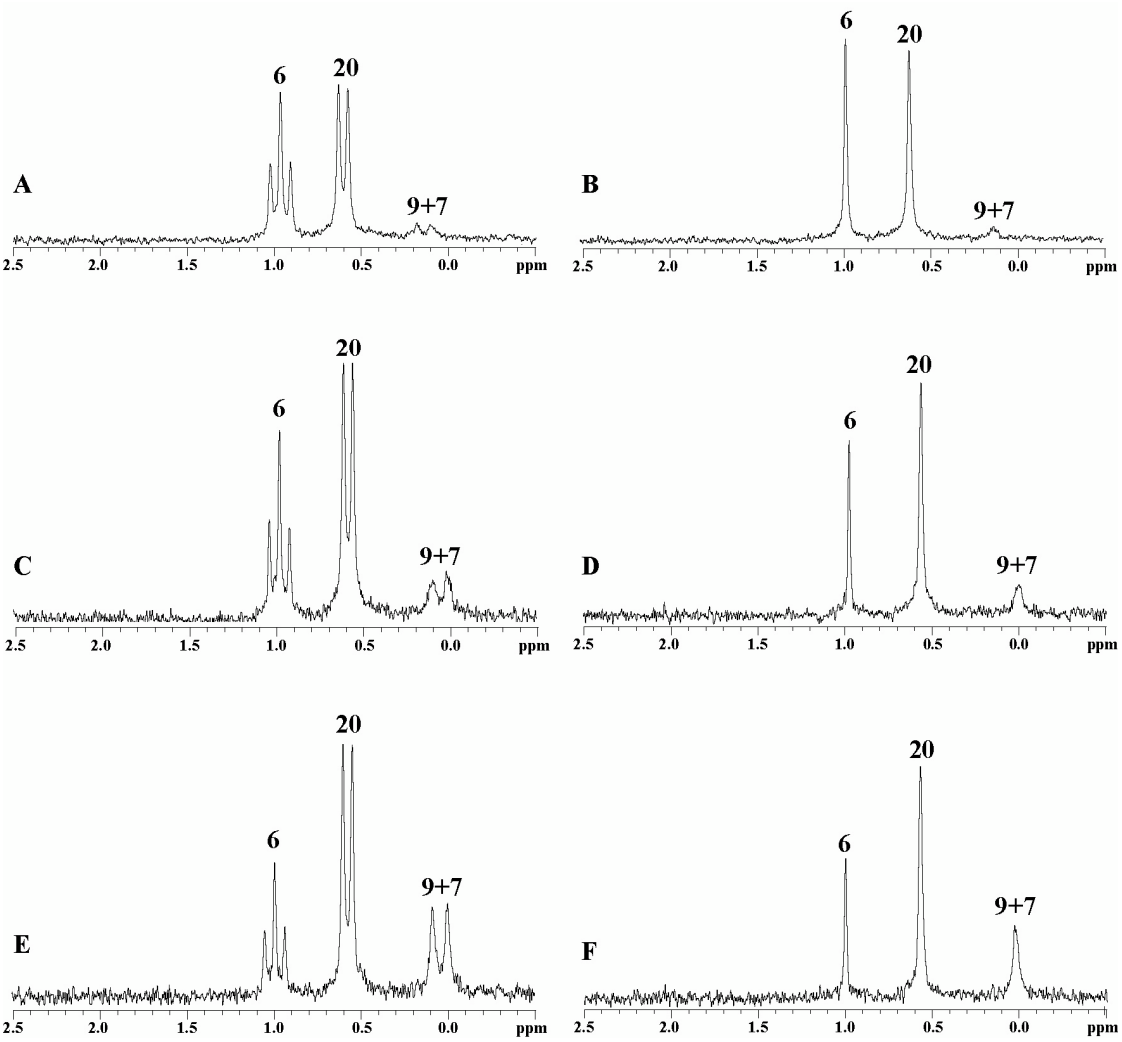

Figure S12. ^{6}Li NMR spectra recorded on [^{6}Li,^{15}N]LiHMDS (0.08 M) and **1** (0.023 M) at various THF concentrations with toluene at -75 ^{o}C: (A) and (B) 2.0 M; (C) and (D) 3.0 M; (E) and (F) 4.0 M; (G) and (H) 6.0 M; (I) and (J) 8.0 M. Spectra B, D, F, H, and J were recorded with ^{15}N broad-band decoupling.

Figure S12 (continued)

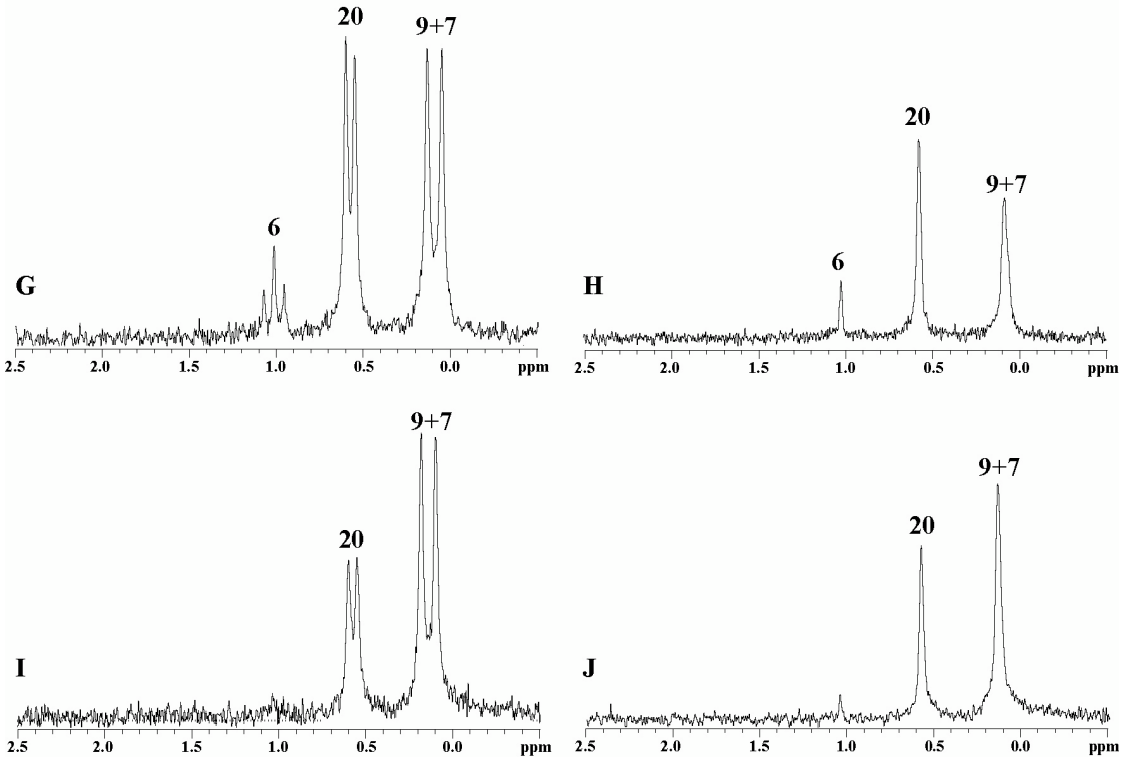

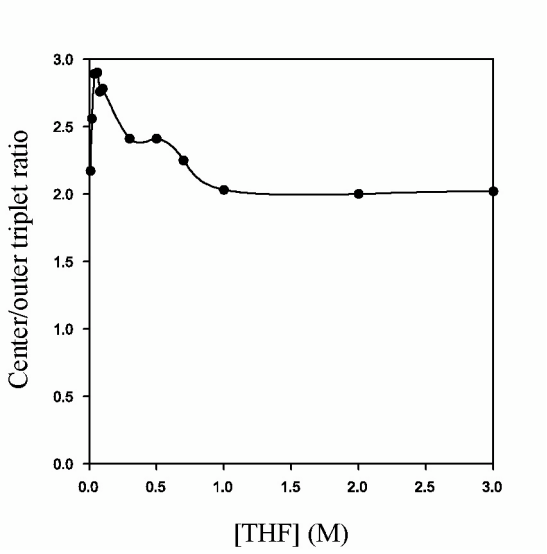

Figure S13. Plot of the relative integration of the center/outer triplet resonances versus [THF] (M) for solutions of [^{6}Li,^{15}N]LiHMDS (0.08 M) and **1** (0.023 M) in THF/toluene solutions at -78 ^{o}C.

Table S1. Data for plot in Figure S13.

[THF] (M)	Relative ratio
0.00	0.00
0.01	2.17
0.02	2.56
0.04	2.89
0.06	2.90
0.08	2.76
0.10	2.78
0.30	2.41
0.50	2.41
0.70	2.25
1.0	2.03
2.0	2.00
3.0	2.02
4.0	1.97

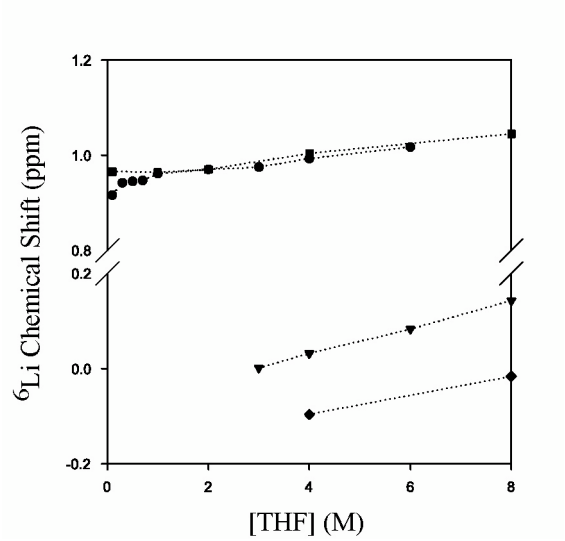

Figure S14. Plot of the ^{6}Li chemical shift (ppm) versus [THF] (M) with toluene for solutions of [^{6}Li,^{15}N]LiHMDS [dimer (■), monomer (♦)] and [^{6}Li,^{15}N]LiHMDS/**1** [dimer (●), monomer (▼)] at -75 ^{o}C.

Table S2. Data for the plot in Figure S14.

[THF] (M)	dimer (■)	monomer (♦)	dimer (●)	monomer (▼)
0.1	0.966	–	0.916	–
0.3	–	–	0.942	–
0.5	–	–	0.945	–
0.7	–	–	0.947	–
1	0.964	–	0.961	–
2	0.97	–	0.97	–
3	–	–	0.975	0.001
4	1.004	-0.096	0.993	0.032
6	–	–	1.017	0.083
8	1.045	-0.016	–	0.143

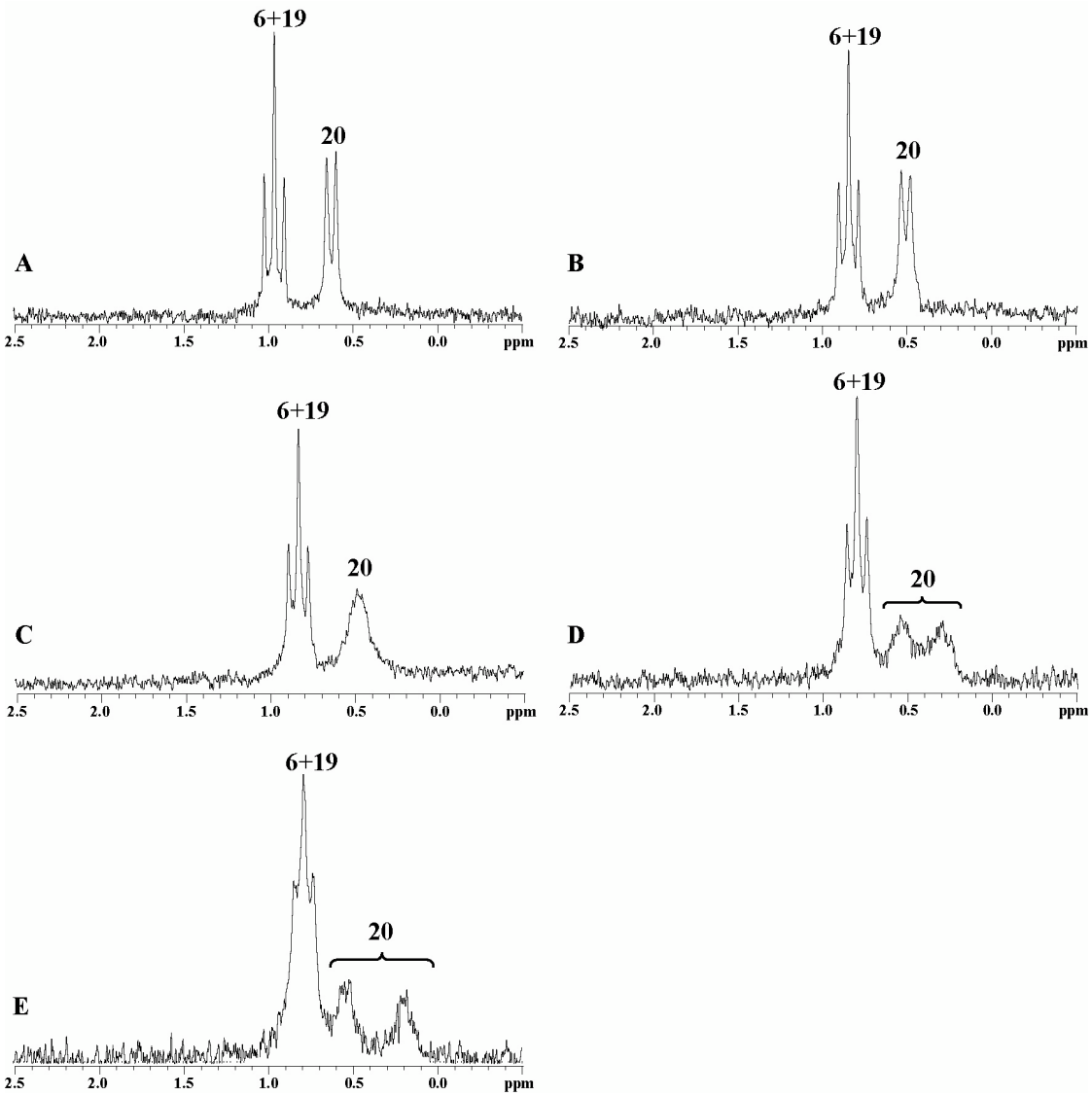

Figure S15. ^{6}Li NMR spectra recorded on [^{6}Li,^{15}N]LiHMDS (0.08 M) and **1** (0.023 M) at 1.0 M THF/toluene at various temperatures: (A) -75 ^{o}C; (B) -85 ^{o}C; (C) -95 ^{o}C; (D) -105 ^{o}C; (E) -115 ^{o}C.

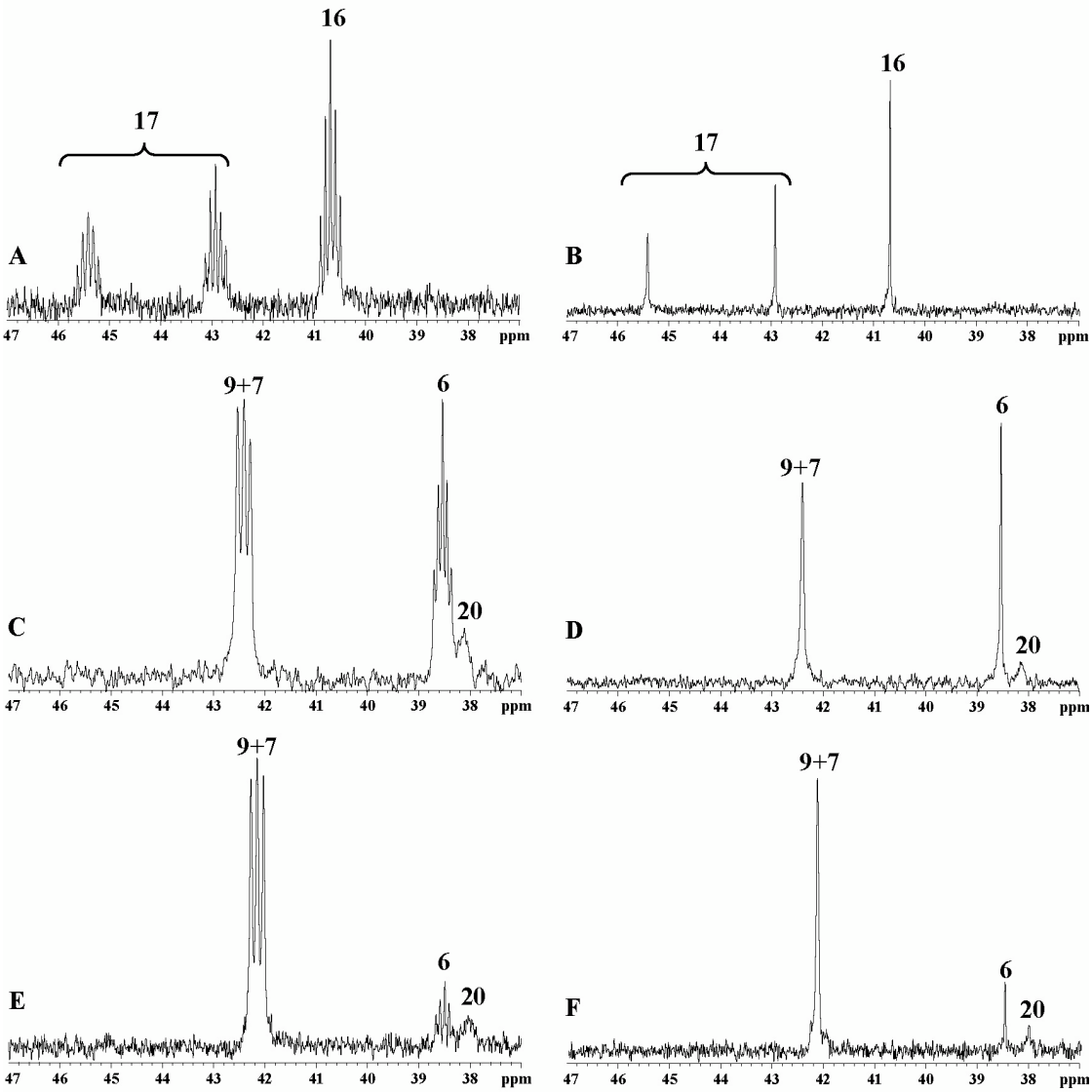

Figure S16. ^{15}N NMR spectra recorded on [^{6}Li,^{15}N]LiHMDS (0.08 M) and **1** (0.023 M) at various THF concentrations with toluene at -75 ^{o}C: (A) and (B) 0.0 M; (C) and (D) 4.0 M; (E) and (F) 6.0 M. Spectra B, D, and F were recorded with ^{6}Li broad-band decoupling. (Note: The relative intensities of the ^{15}N resonances for mixed dimer **20** are attenuated relative to the LiHMDS dimer and monomer in these INEPT spectra.)

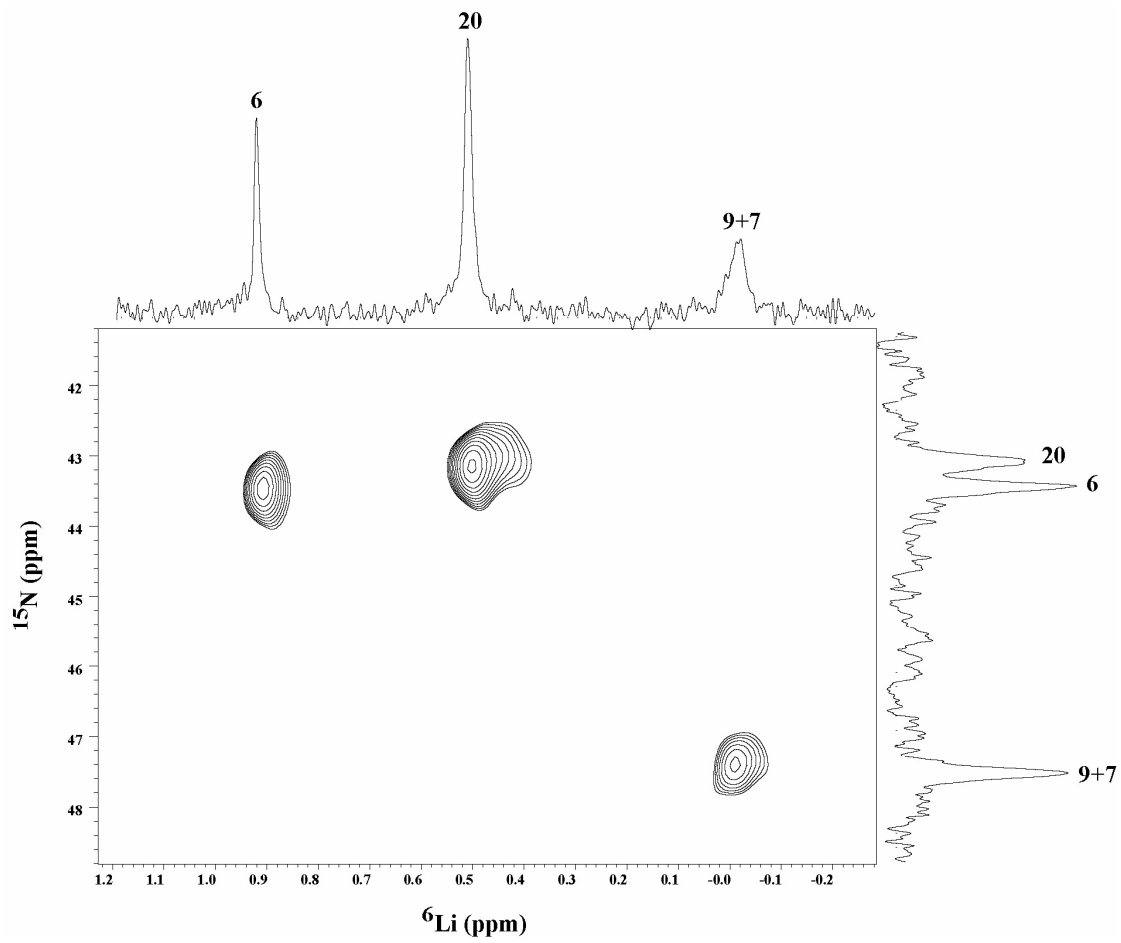

Figure S17. ^{6}Li,^{15}N-heteronuclear single quantum correlation (HSQC) spectrum recorded on [^{6}Li,^{15}N]LiHMDS (0.08 M) and **1** (0.023 M) at 4.0 M THF/toluene at -75 ^{o}C. (Note: The ^{15}N resonances of mixed dimer **20** accurately reflect their abundance in the sample in this direct detect spectrum.)

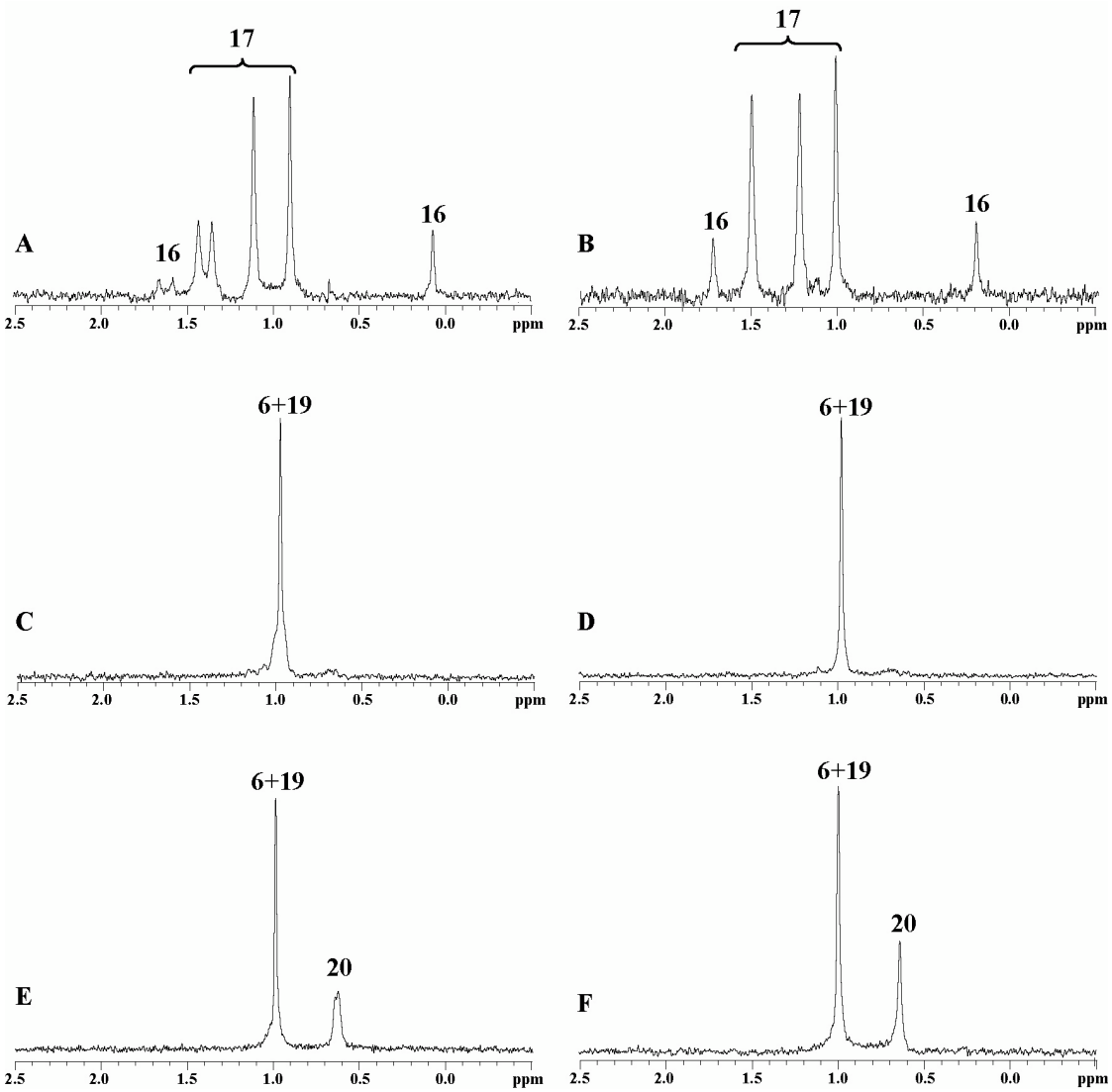

Figure S18. ^{6}Li NMR spectra recorded on [^{6}Li]LiHMDS (0.08 M) and [^{15}N]**1** (0.023 M) at various THF concentrations with toluene at -75 ^{o}C: (A) and (B) 0.0 M; (C) and (D) 0.1 M; (E) and (F) 1.0 M; (G) and (H) 3.0 M; (I) and (J) 6.0 M. Spectra B, D, F, H, and J were recorded with ^{15}N broad-band decoupling.

Figure S18 (continued)

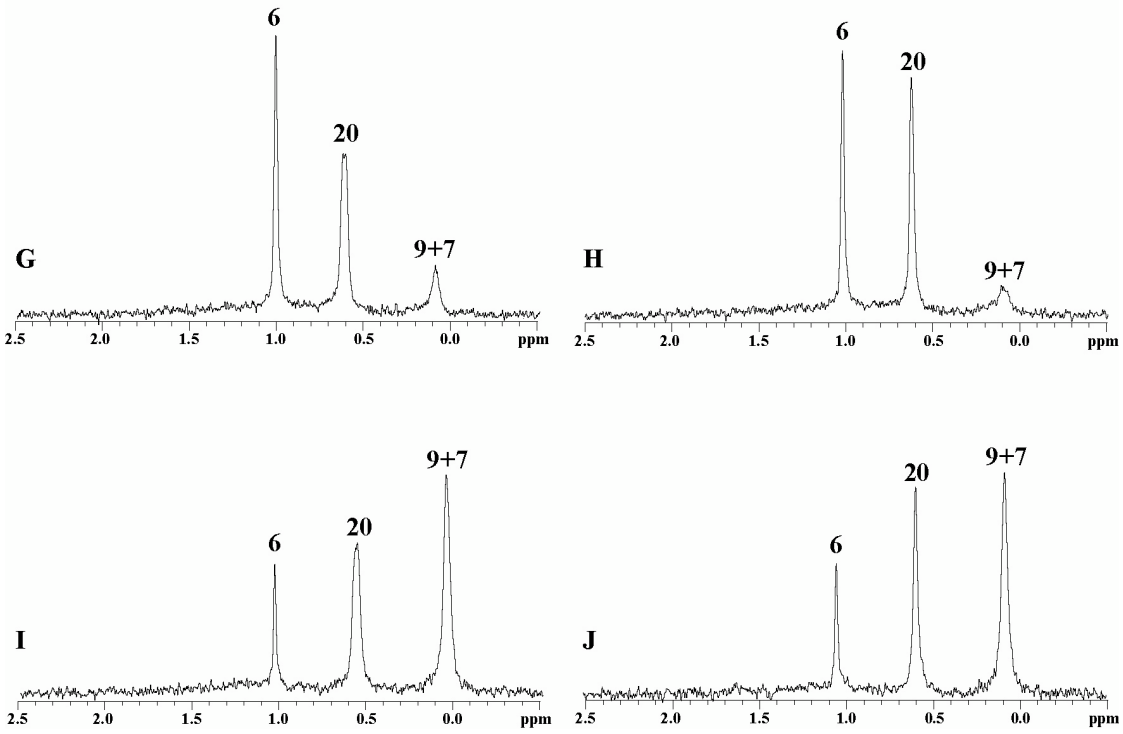

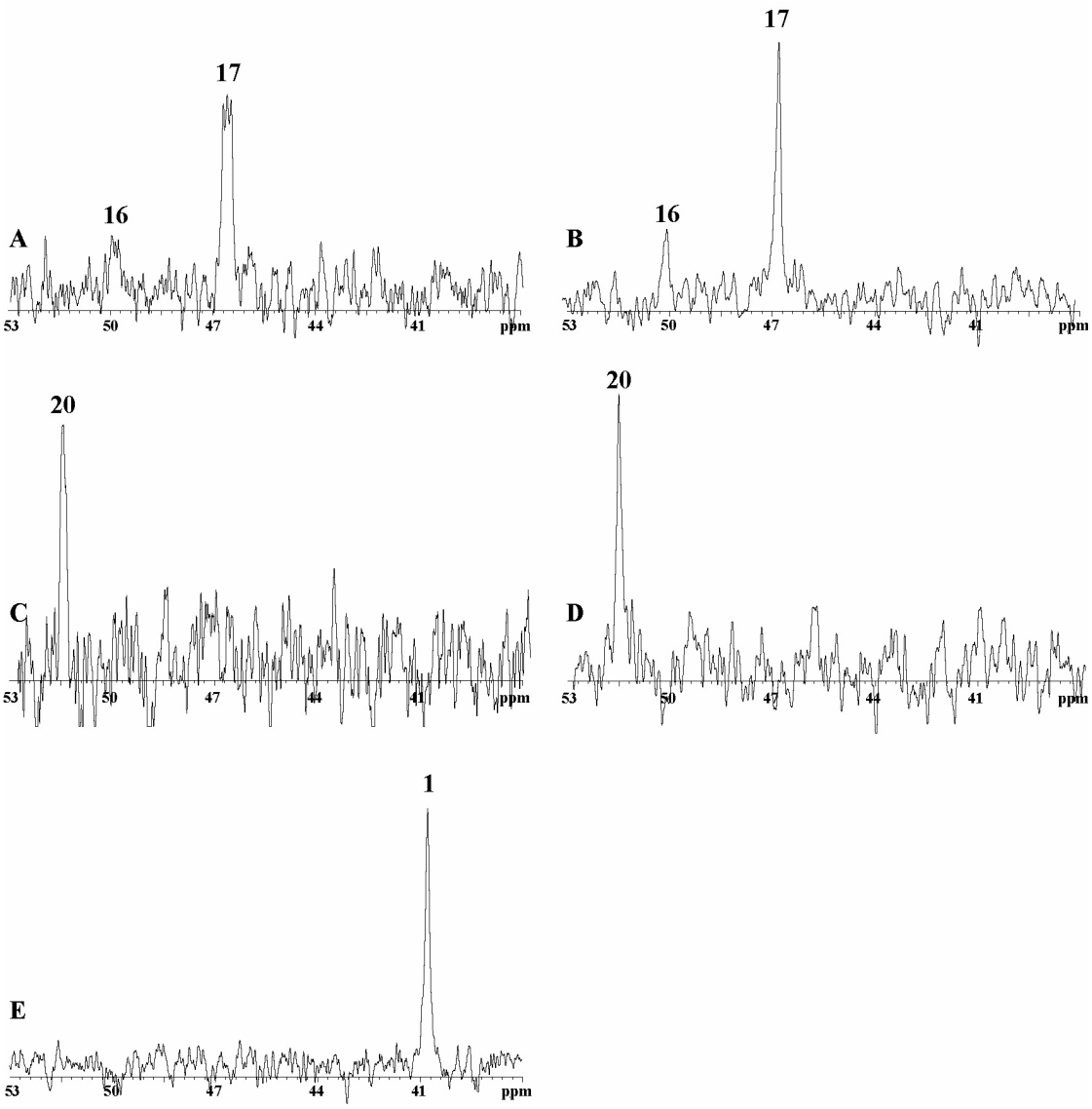

Figure S19. ^{15}N NMR spectra recorded on [^{6}Li]LiHMDS (0.08 M) and [^{15}N]**1** (0.023 M) at various THF concentrations with toluene at -75 ^{o}C: (A) and (B) 0.0 M; (C) and (D) 3.0 M; (E) 0.0 M (only [^{15}N]**1**). Spectra B and D were recorded with ^{6}Li broad-band decoupling.

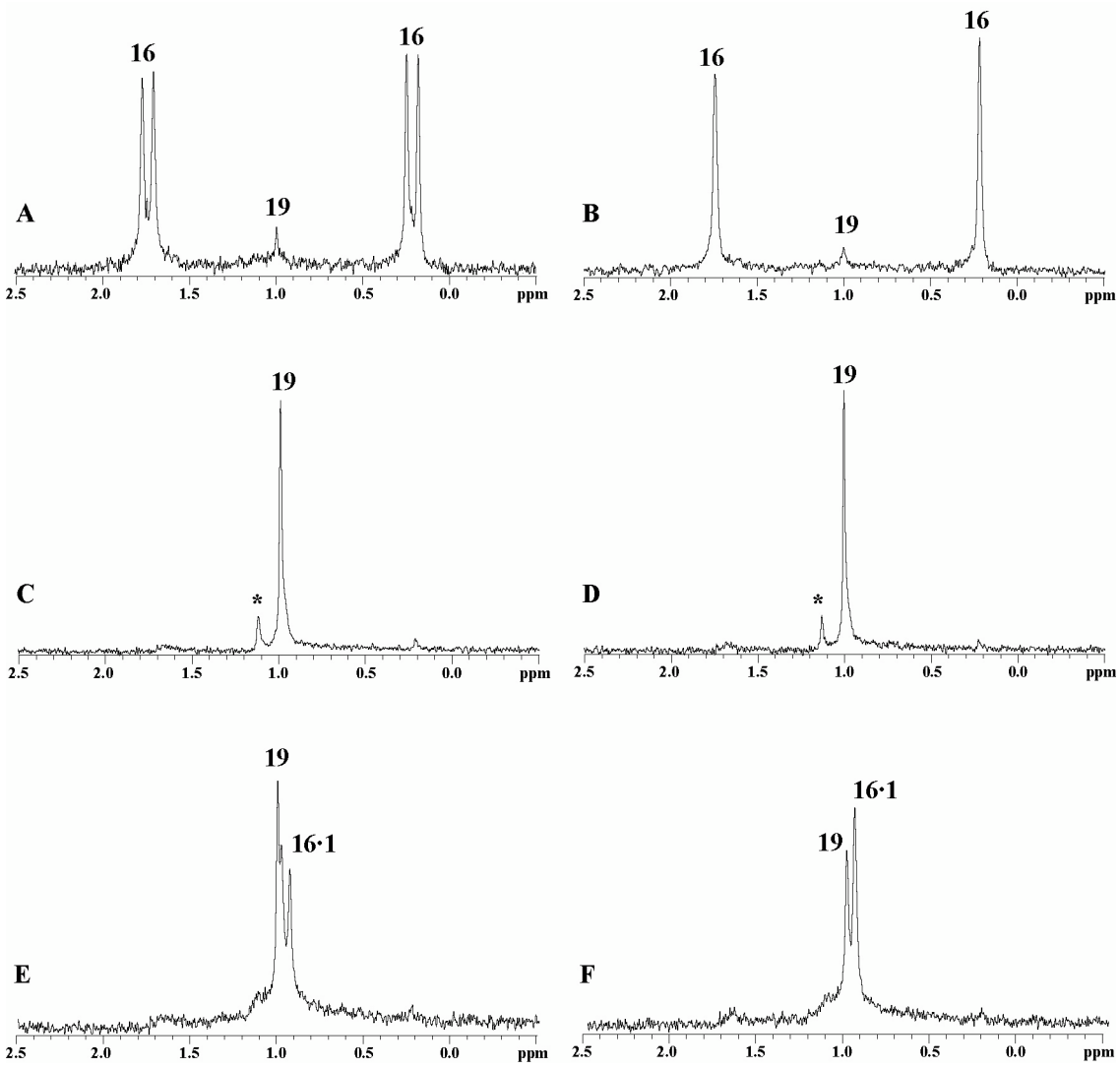

Figure S20. ^{6}Li NMR spectra recorded on [^{6}Li,^{15}N]LiHMDS (0.08 M) and varying concentrations of **1** in neat toluene at -75 ^{o}C: (A) and (B) 0.04 M; (C) and (D) 0.08 M; (E) and (F) 0.12 M. Spectra B, D, and F were recorded with ^{15}N broad-band decoupling. (*denotes an unassigned resonance.)

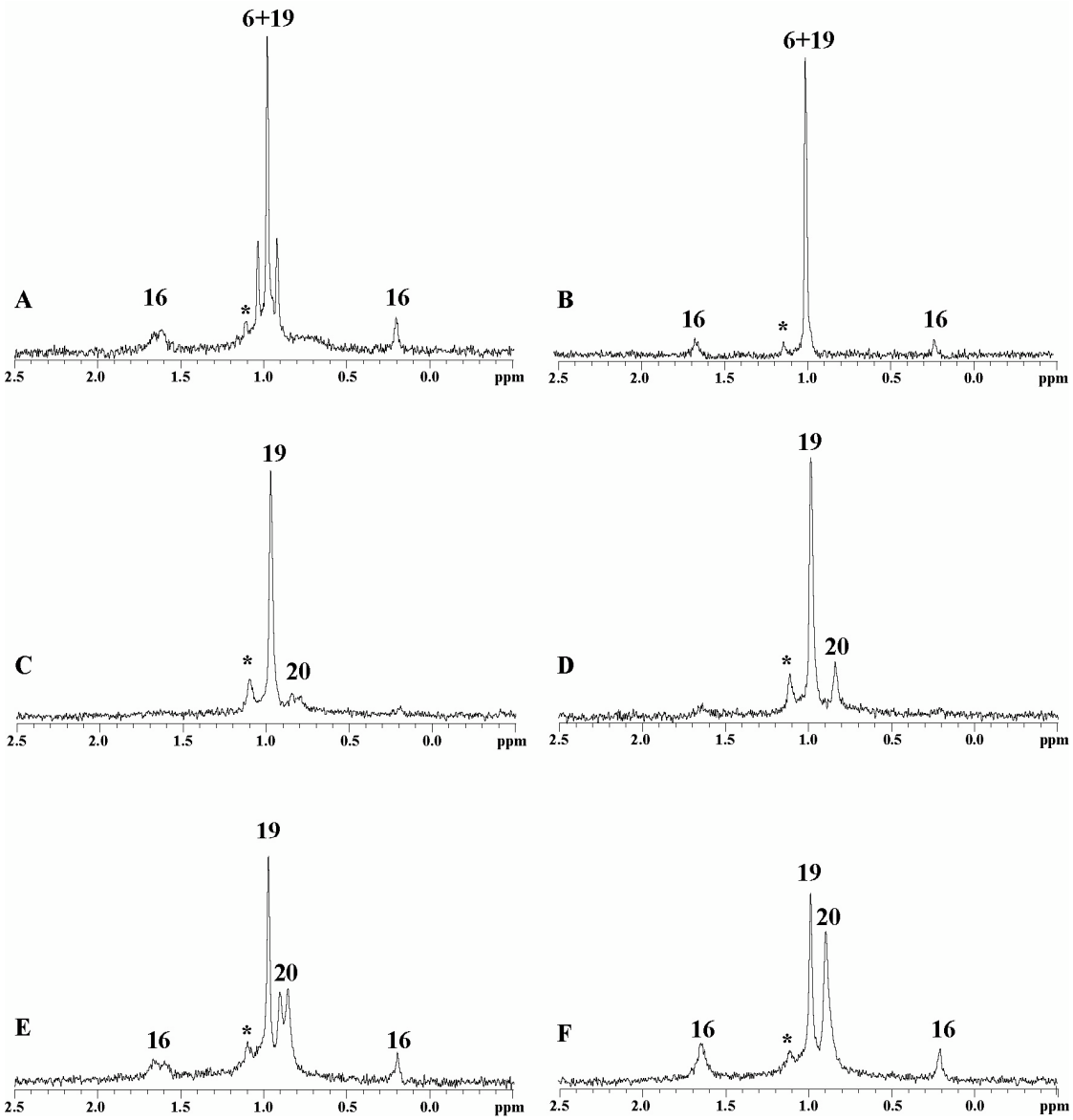

Figure S21. ^{6}Li NMR spectra recorded on [^{6}Li,^{15}N]LiHMDS (0.08 M) and varying concentrations of **1** at 0.06 M THF/toluene at -75 ^{o}C: (A) and (B) 0.04 M; (C) and (D) 0.08 M; (E) and (F) 0.12 M. Spectra B, D, and F were recorded with ^{15}N broad-band decoupling. (*denotes an unassigned resonance.)

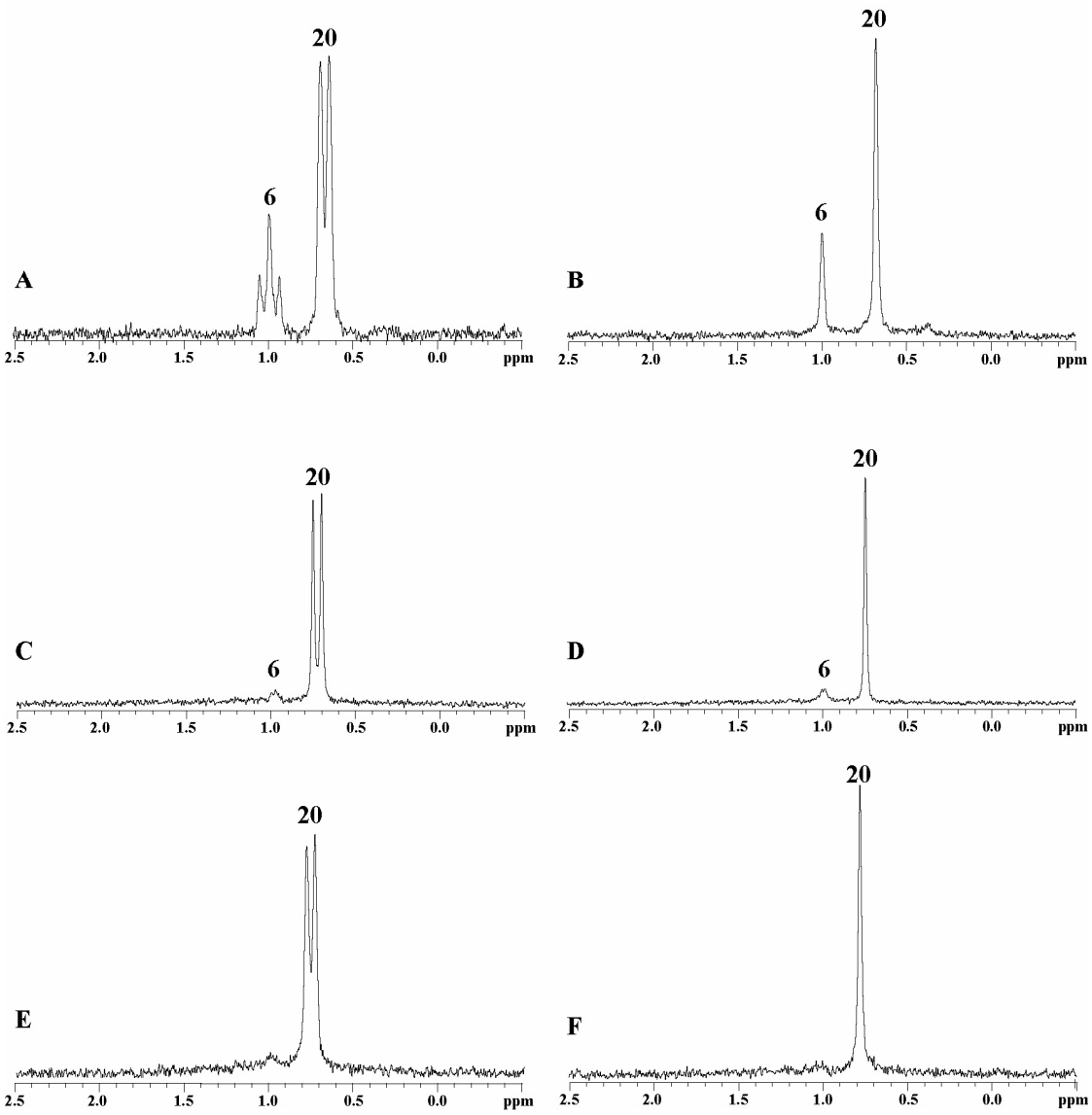

Figure S22. ^{6}Li NMR spectra recorded on [^{6}Li,^{15}N]LiHMDS (0.08 M) and varying concentrations of **1** at 2.0 M THF/toluene at -75 ^{o}C: (A) and (B) 0.04 M; (C) and (D) 0.08 M; (E) and (F) 0.12 M. Spectra B, D, and F were recorded with ^{15}N broad-band decoupling.

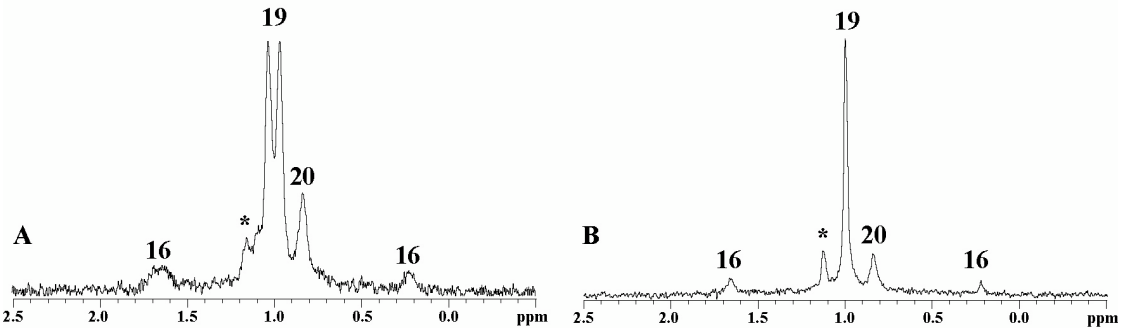

Figure S23. ^{6}Li NMR spectra recorded on [^{6}Li]LiHMDS (0.08 M) and [^{15}N]**1** (0.08 M) at 0.06 M THF/toluene at -75 ^{o}C. Spectrum B was recorded with ^{15}N broad-band decoupling. (*denotes an unassigned resonance.)

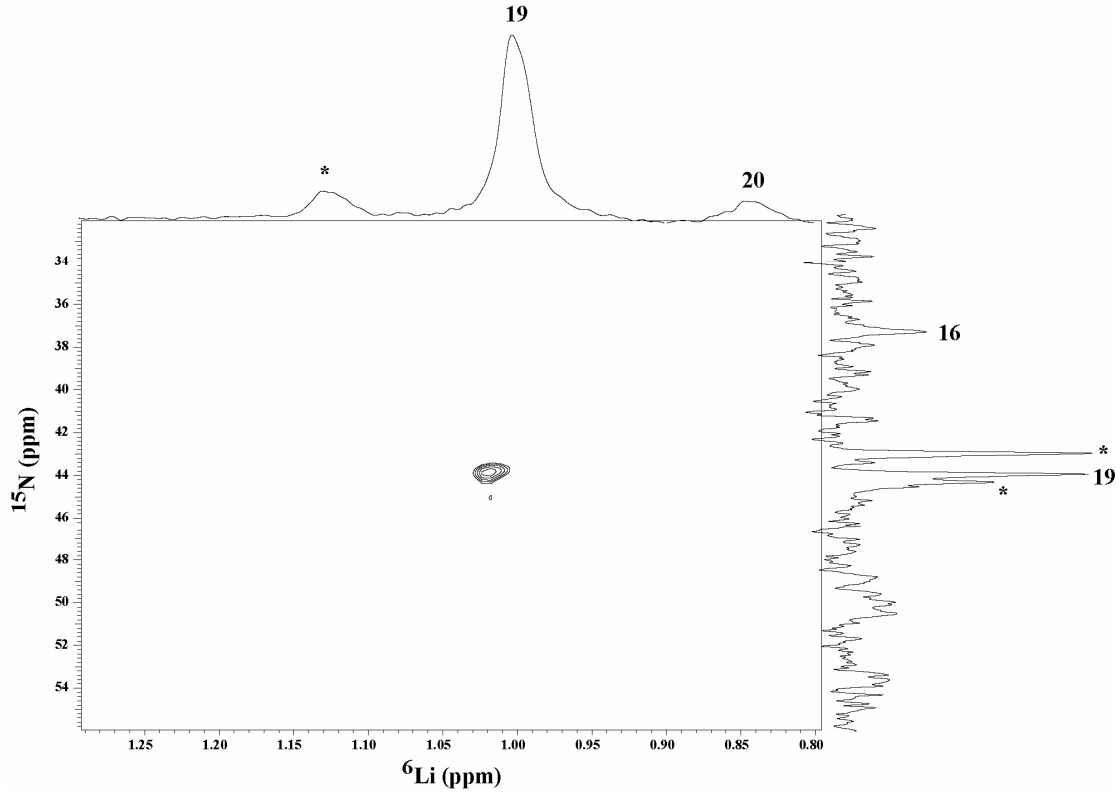

Figure S24. ^{6}Li,^{15}N-heteronuclear single quantum correlation (HSQC) spectrum recorded on [^{6}Li]LiHMDS (0.08 M) and [^{15}N]**1** (0.08 M) at 0.06 M THF/toluene at -75 ^{o}C. (*denotes an unassigned resonance.)

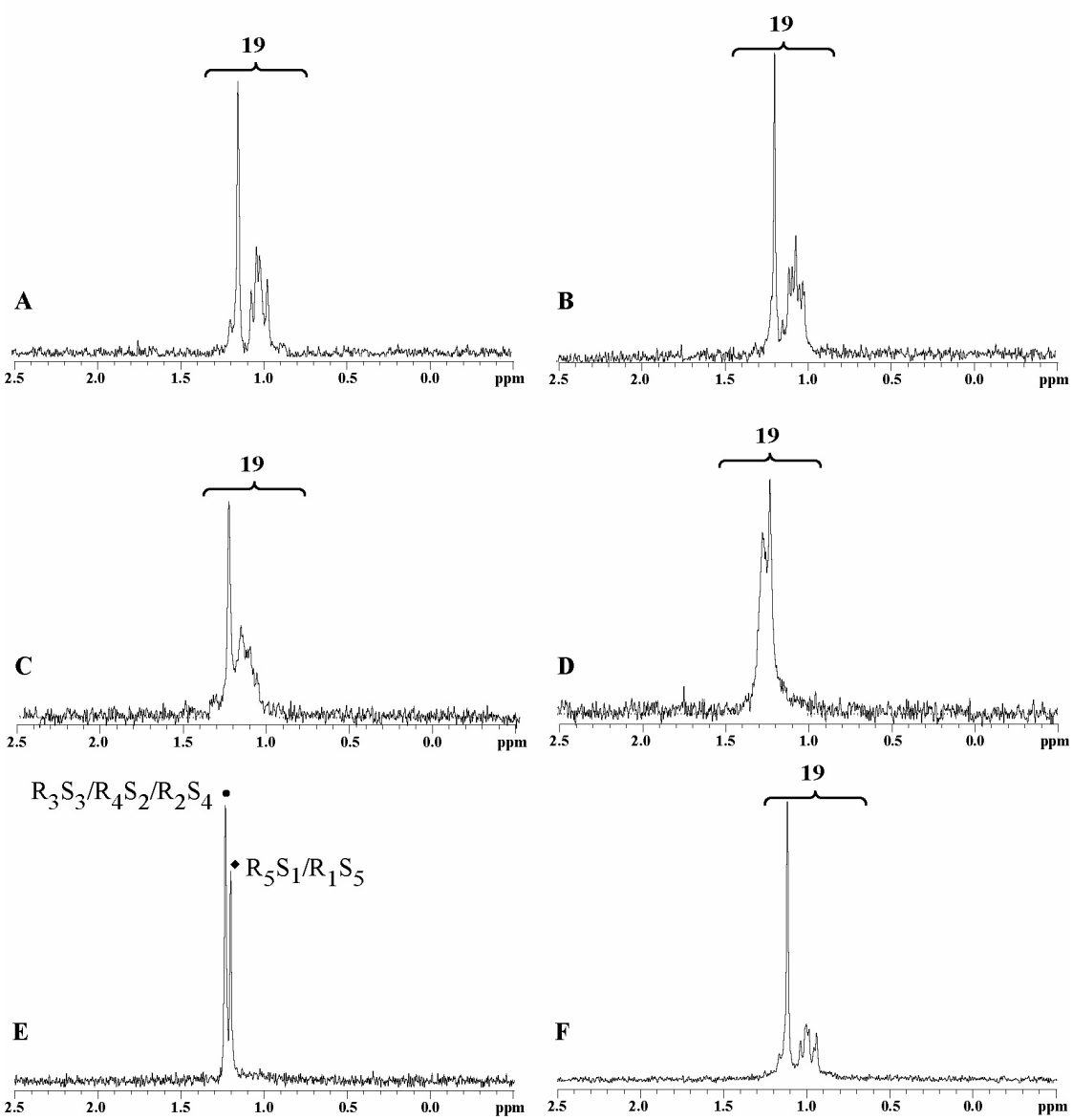

Figure S25. ^{6}Li NMR spectra recorded on [^{6}Li]**4** (0.10 M, X_R = 0.5) at 0.06 M THF/toluene at various temperatures: (A) -75 ^{o}C; (B) -55 ^{o}C; (C) -25 ^{o}C; (D) 0 ^{o}C; (E) 25 ^{o}C; (F) -75 ^{o}C after aging. **R_3S_3/R_4S_2/R_2S_4** (•); **R_5S_1/R_1S_5** (◆); **R_6/S_6** (▪).

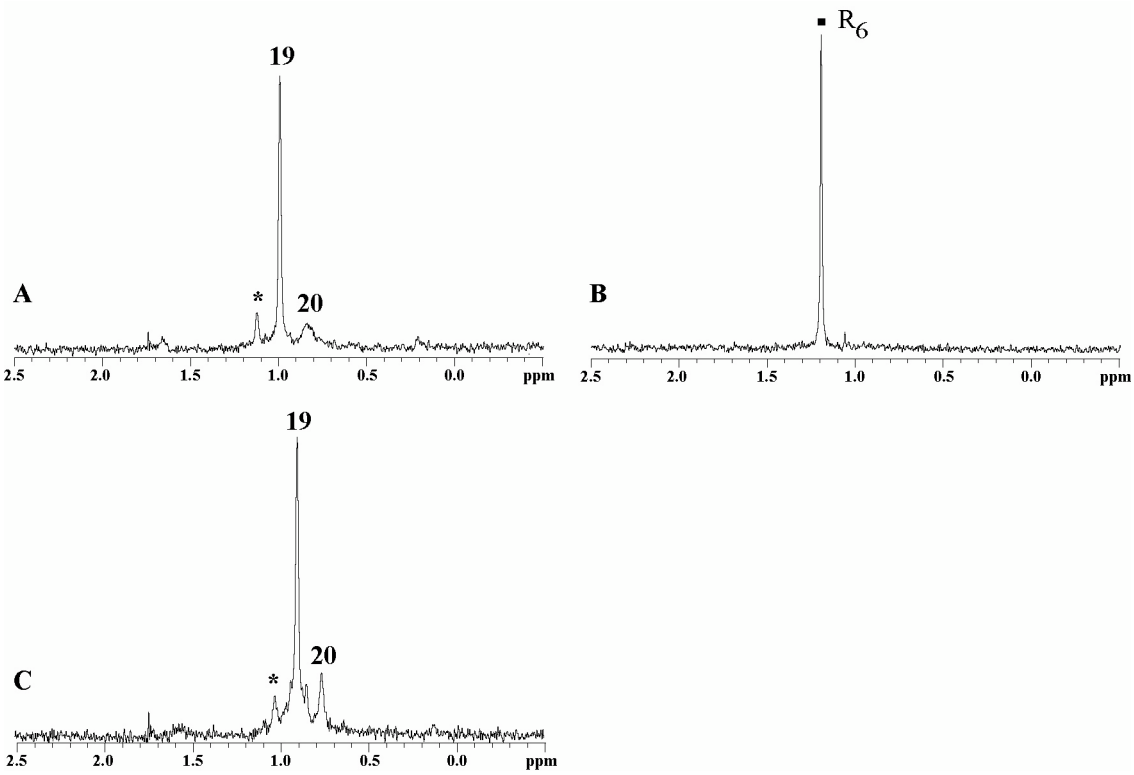

Figure S26. ^{6}Li NMR spectra recorded on [^{6}Li]**4** (0.10 M, X_R = 1.0) at 0.06 M THF/toluene at various temperatures: (A) -75 ^{o}C; (B) 20 ^{o}C; (C) -75 ^{o}C after aging. (*denotes an unassigned resonance.) **R_3S_3/R_4S_2/R_2S_4** (•); **R_5S_1/R_1S_5** (◆); **R_6/S_6** (■).

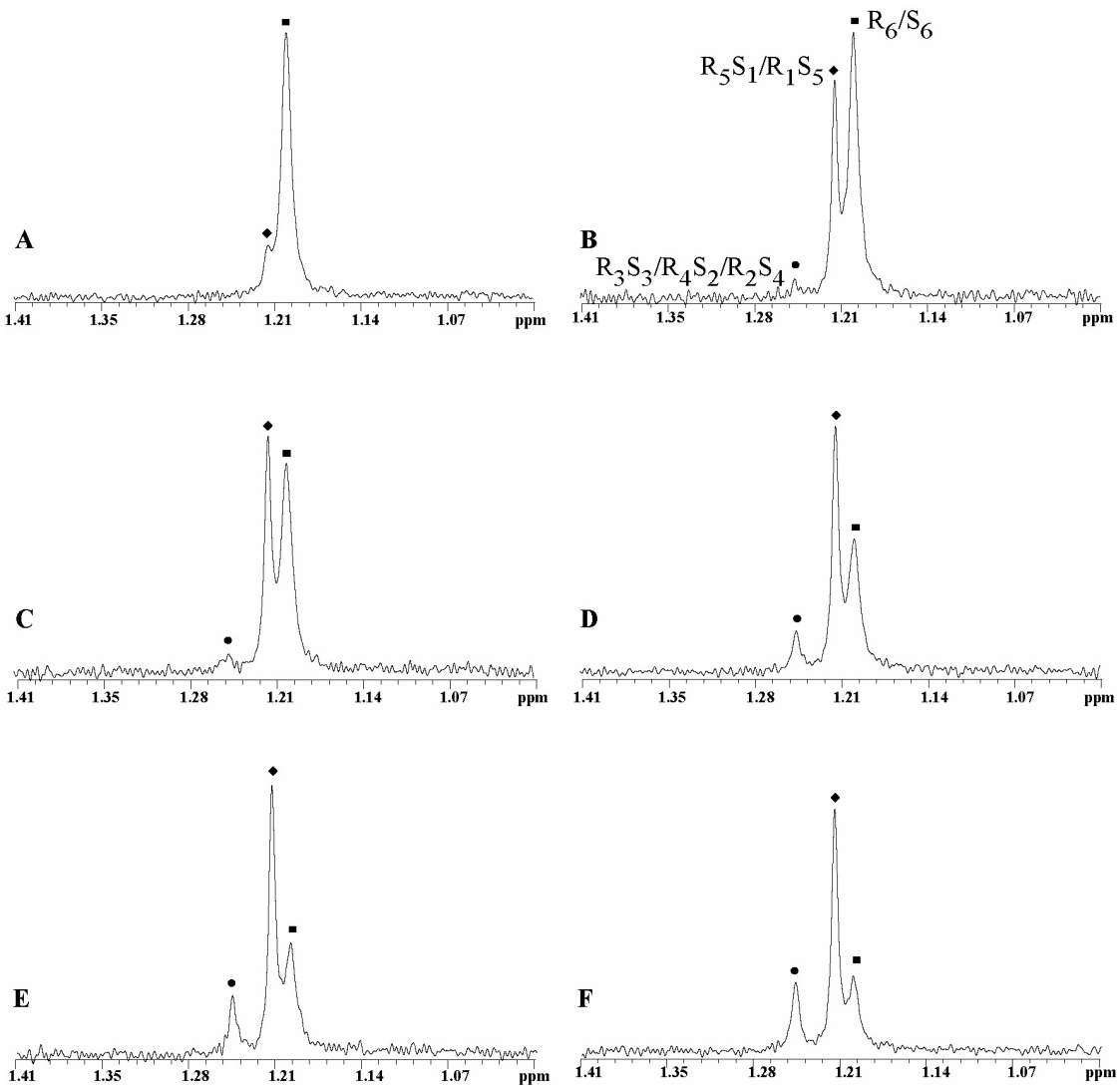

Figure S27. ^{6}Li NMR spectra recorded on [^{6}Li]**4** (0.10 M, X_R = 1.0) at 0.06 M THF/toluene at 30 ^{o}C over 2 h. **$R_3S_3/R_4S_2/R_2S_4$** (●); **R_5S_1/R_1S_5** (◆); **R_6/S_6** (■).

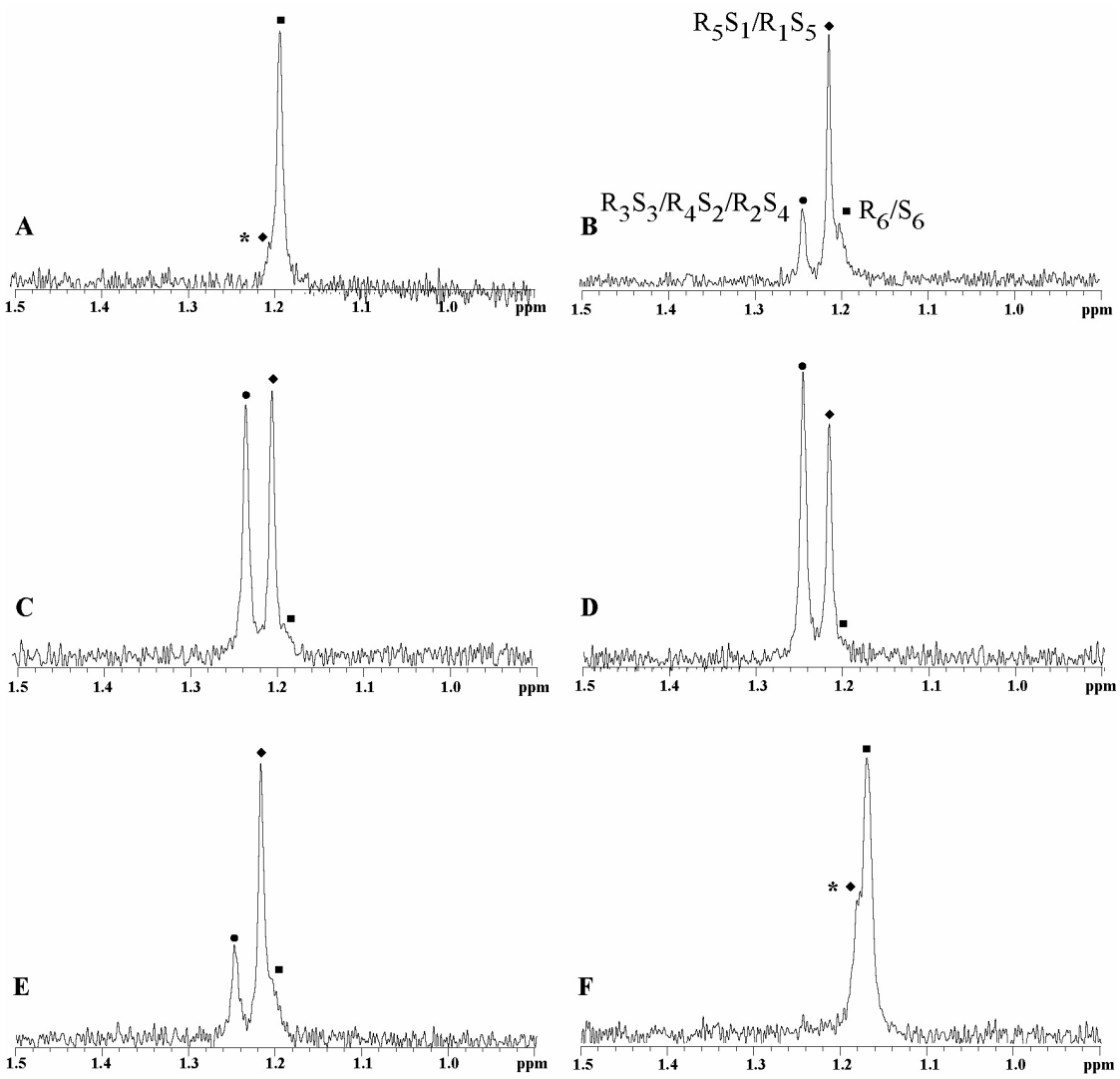

Figure S28. ^{6}Li NMR spectra recorded on [^{6}Li]**4** (0.10 M) at 0.06 M THF/toluene at 30 ^{o}C at various X_R: (A) 1.0; (B) 0.8; (C) 0.6; (D) 0.4; (E) 0.2; and (F) 0.0. **R_3S_3/R_4S_2/R_2S_4** (•); **R_5S_1/R_1S_5** (◆); **R_6/S_6** (■). (*denotes the beginning of racemization)

Table S3. Table of data for Job plot.

X_R	$\mathbf{R_3S_3/R_4S_2/R_2S_4}$	$\mathbf{R_5S_1/R_1S_5}$	$\mathbf{R_6/S_6}$
1	0.00 ± 0.00	0.00 ± 0.00	1.00 ± 0.00
0.9	0.07 ± 0.01	0.46 ± 0.04	0.46 ± 0.05
0.85	0.166 ± 0.002	0.59 ± 0.02	0.24 ± 0.02
0.8	0.23 ± 0.03	0.54 ± 0.05	0.22 ± 0.06
0.75	0.335 ± 0.002	0.568 ± 0.004	0.097 ± 0.006
0.7	0.42 ± 0.02	0.49 ± 0.04	0.09 ± 0.06
0.6	0.55 ± 0.08	0.43 ± 0.05	0.02 ± 0.02
0.5	0.661 ± 0.004	0.339 ± 0.004	0.00 ± 0.00
0.4	0.569 ± 0.008	0.414 ± 0.003	0.02 ± 0.01
0.3	0.40 ± 0.01	0.54 ± 0.01	0.05 ± 0.02
0.25	0.287 ± 0.008	0.59 ± 0.02	0.13 ± 0.03
0.2	0.25 ± 0.04	0.56 ± 0.05	0.19 ± 0.02
0.15	0.22 ± 0.07	0.572 ± 0.007	0.20 ± 0.07
0.1	0.12 ± 0.02	0.56 ± 0.06	0.32 ± 0.07
0	0.00 ± 0.00	0.00 ± 0.00	1.00 ± 0.00

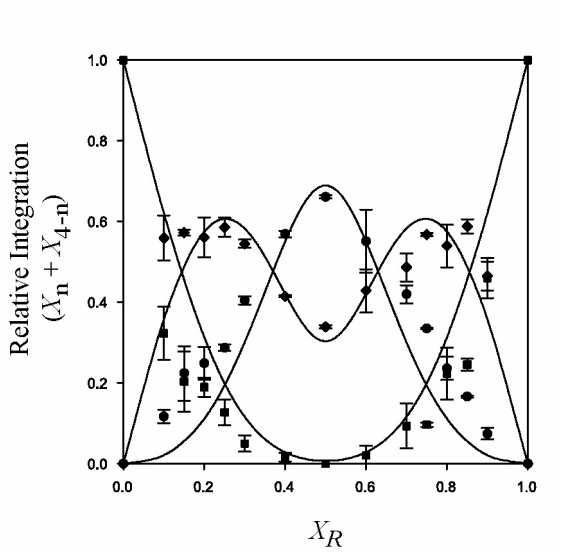

Figure S29. Plot of the mole fraction of the $\mathbf{R_nS_{4-n}/R_{4-n}S_n}$ aggregate ($X_n + X_{4-n}$) versus the mole fraction of *R* enantiomer (X_R) for the tetramer model. $\mathbf{R_2S_2}$ (•); $\mathbf{R_3S_1/R_1S_3}$ (⬥); $\mathbf{R_4/S_4}$ (▪).

Table S4. Best-fit values of φ for the tetramer fit.

φ_0/φ_4	φ_1/φ_3	φ_2
1	10.72	32.44

Table S5. Percent errors in φ_n for the tetramer fit.

n	**0**	**1**	**2**
φ_n/φ_0	0	8.3	13.7
φ_n/φ_1	8.3	0	4.8
φ_n/φ_2	13.7	4.8	0

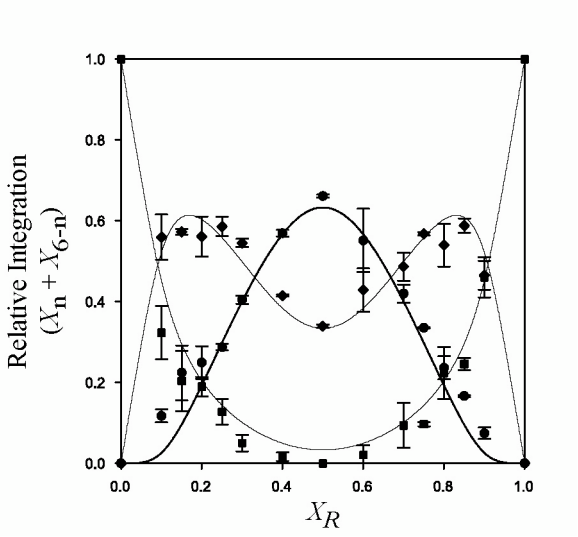

Figure S30. Plot of the mole fraction of the $\mathbf{R_nS_{6-n}/R_{6-n}S_n}$ aggregate ($X_n + X_{6-n}$) versus the mole fraction of *R* enantiomer (X_R) for the hexamer model assuming superposition of $\mathbf{R_5S_1/R_1S_5}$ and $\mathbf{R_4S_2/R_2S_4}$. $\mathbf{R_3S_3}$ (•); $\mathbf{R_5S_1/R_1S_5/R_4S_2/R_2S_4}$ (⬥); $\mathbf{R_6/S_6}$ (▪).

Table S6. Best-fit values of φ for the hexamer fit in Figure S30.

$\varphi_0(\varphi_6)$	$\varphi_1(\varphi_5)$	$\varphi_2(\varphi_4)$	φ_3
1	1.68	0	1.91

Table S7. Percent errors in φ_n for the hexamer fit in Figure S30.

n	0	1	2	3
φ_n/φ_0	0	7.7	73	13.9
φ_n/φ_1	7.7	0	76	5.4
φ_n/φ_2	73	76	0	77
φ_n/φ_3	13.9	5.4	77	0

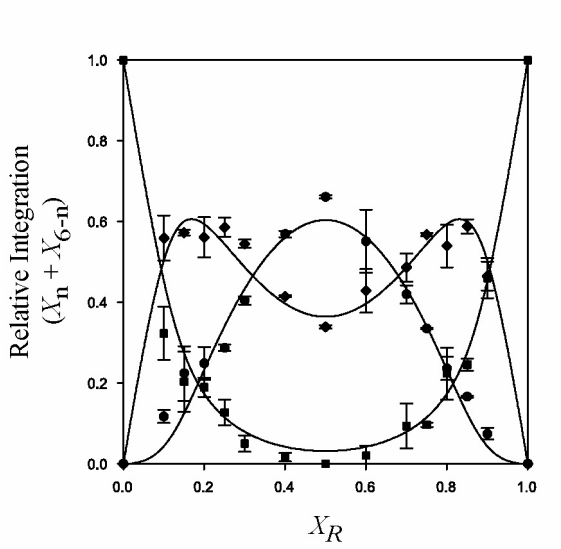

Figure S31. Plot of the mole fraction of the $\mathbf{R_nS_{6-n}/R_{6-n}S_n}$ aggregate ($X_n + X_{6-n}$) versus the mole fraction of *R* enantiomer (X_R) for the hexamer model assuming superposition of $\mathbf{R_3S_3}$ and $\mathbf{R_4S_2/R_2S_4}$. $\mathbf{R_3S_3/R_4S_2/R_2S_4}$ (•); $\mathbf{R_5S_1/R_1S_5}$ (♦); $\mathbf{R_6/S_6}$ (▪).

Table S8. Best-fit values of φ for the hexamer fit in Figure S31.

$\varphi_0(\varphi_6)$	$\varphi_1(\varphi_5)$	$\varphi_2(\varphi_4)$	φ_3
1	1.91	0.53	1.10

Table S9. Percent errors in φ_n for the hexamer fit in Figure S31.

n	0	1	2	3
φ_n/φ_0	0	10.0	20.3	18.0
φ_n/φ_1	10.0	0	12.4	12
φ_n/φ_2	20.3	12.4	0	21.4
φ_n/φ_3	18.0	12	21.4	0

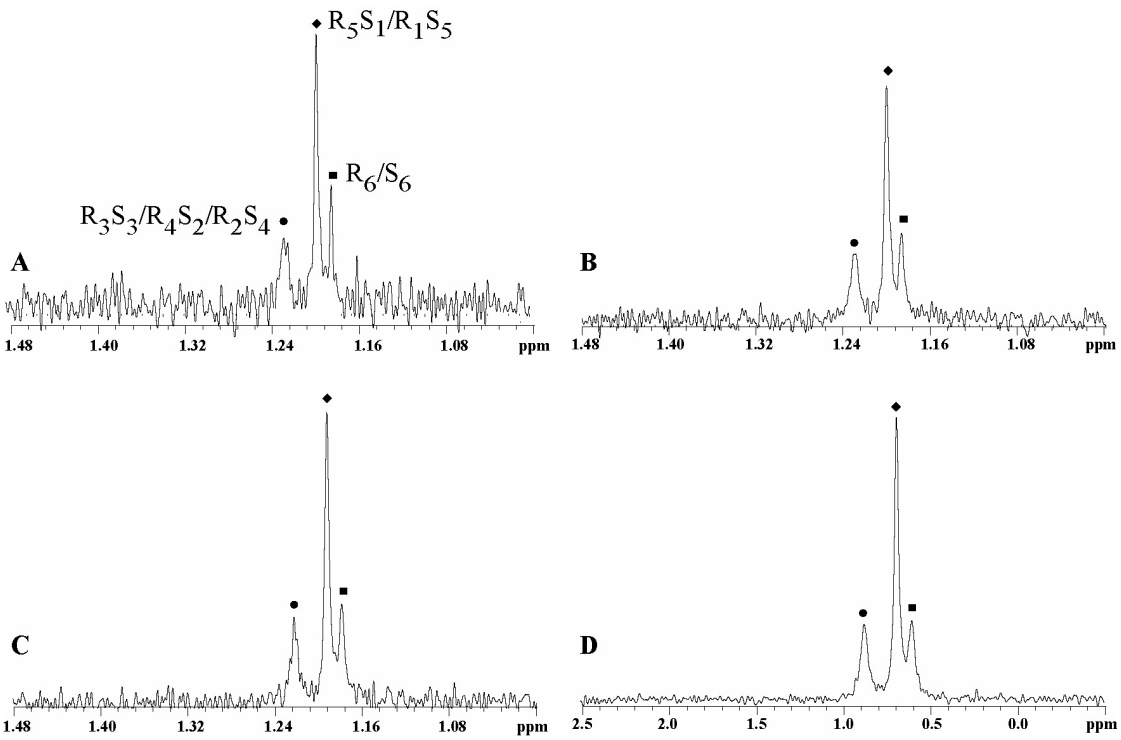

Figure S32. ^{6}Li NMR spectra recorded on varying concentrations of [^{6}Li]**4** (X_R = 0.8) at 0.06 M THF/toluene at 30 ^{o}C: (A) 0.015 M; (B) 0.03 M; (C) 0.06 M; (D) 0.10 M. **R_3S_3/R_4S_2/R_2S_4** (●); **R_5S_1/R_1S_5** (◆); **R_6/S_6** (■).

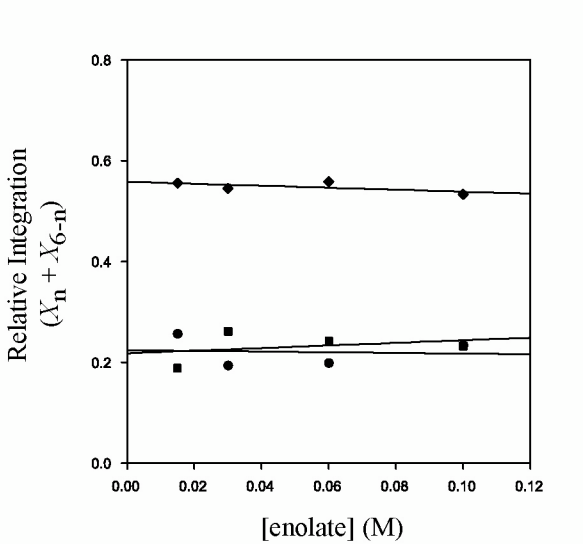

Figure S33. Plot of the mole fraction of the $\mathbf{R_nS_{6-n}/R_{6-n}S_n}$ aggregate ($X_n + X_{6-n}$) versus [enolate] for the spectra in Figure S32. For the case where n = 3, only X_3 is plotted. $\mathbf{R_3S_3/R_4S_2/R_2S_4}$ (•); $\mathbf{R_5S_1/R_1S_5}$ (♦); $\mathbf{R_6/S_6}$ (▪).

Table S10. Table of data for the plot in Figure S33.

[enolate] (M)	$\mathbf{R_3S_3/R_4S_2/R_2S_4}$	$\mathbf{R_5S_1/R_1S_5}$	$\mathbf{R_6/S_6}$
0.015	0.26	0.56	0.19
0.03	0.19	0.55	0.26
0.06	0.20	0.56	0.24
0.10	0.23	0.54	0.23

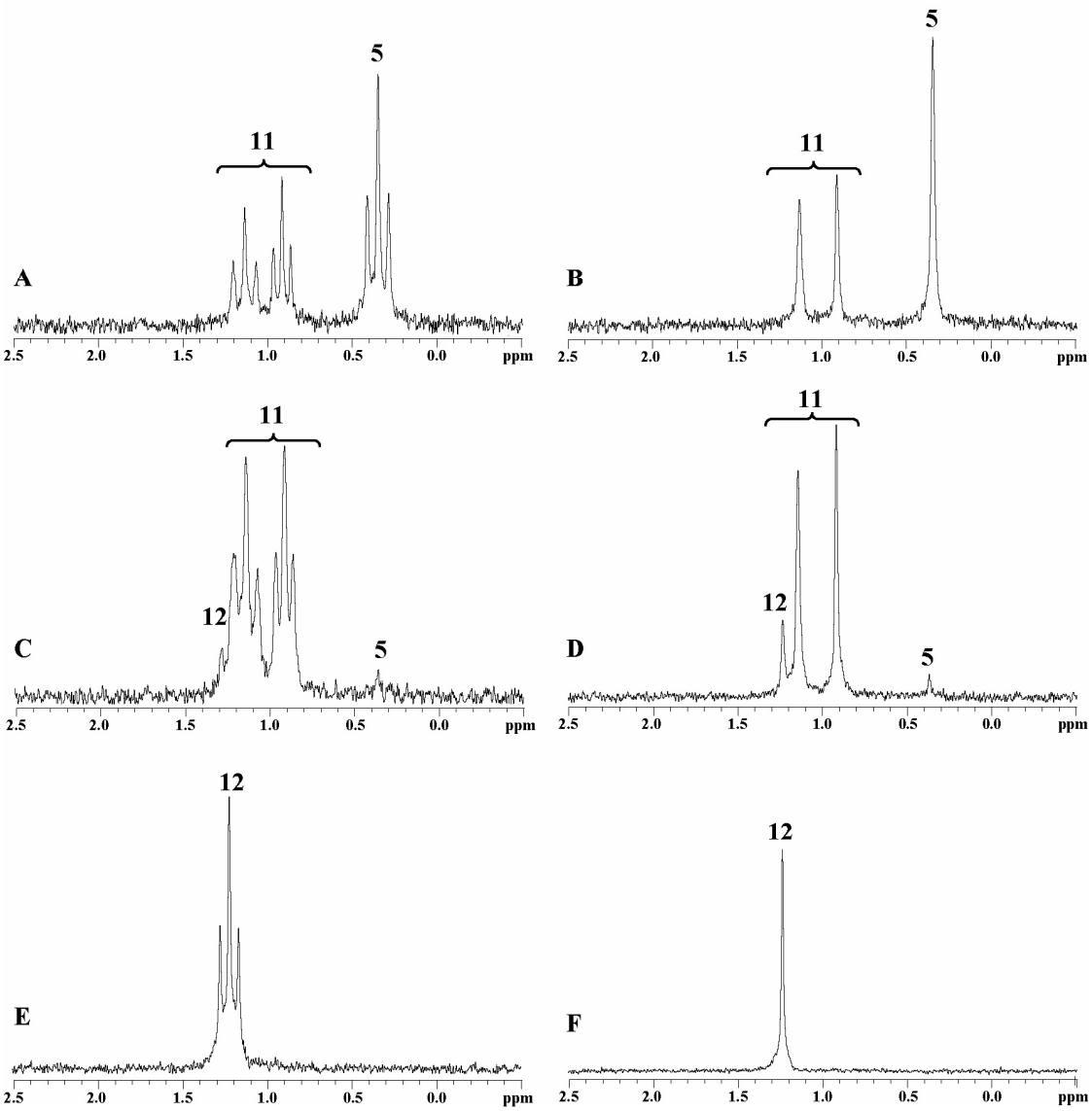

Figure S34. ^{6}Li NMR spectra recorded on [^{6}Li,^{15}N]LiHMDS (0.10 M) and varying concentrations of **10** in toluene at -75 ^{o}C: (A) and (B) 0.02 M; (C) and (D) 0.05 M; (E) and (F) 0.10 M; (G) and (H) 0.20 M; (I) and (J) 0.50 M. Spectra B, D, F, H, and J were recorded with ^{15}N broad-band decoupling.

Figure S34 (continued)

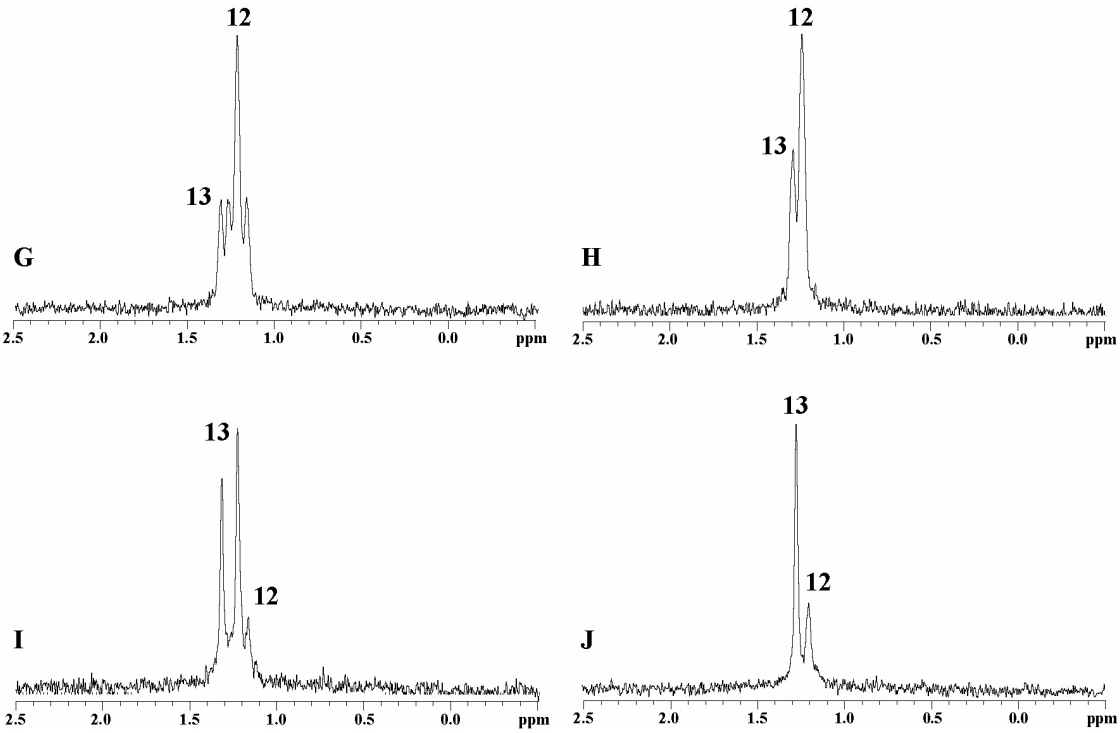

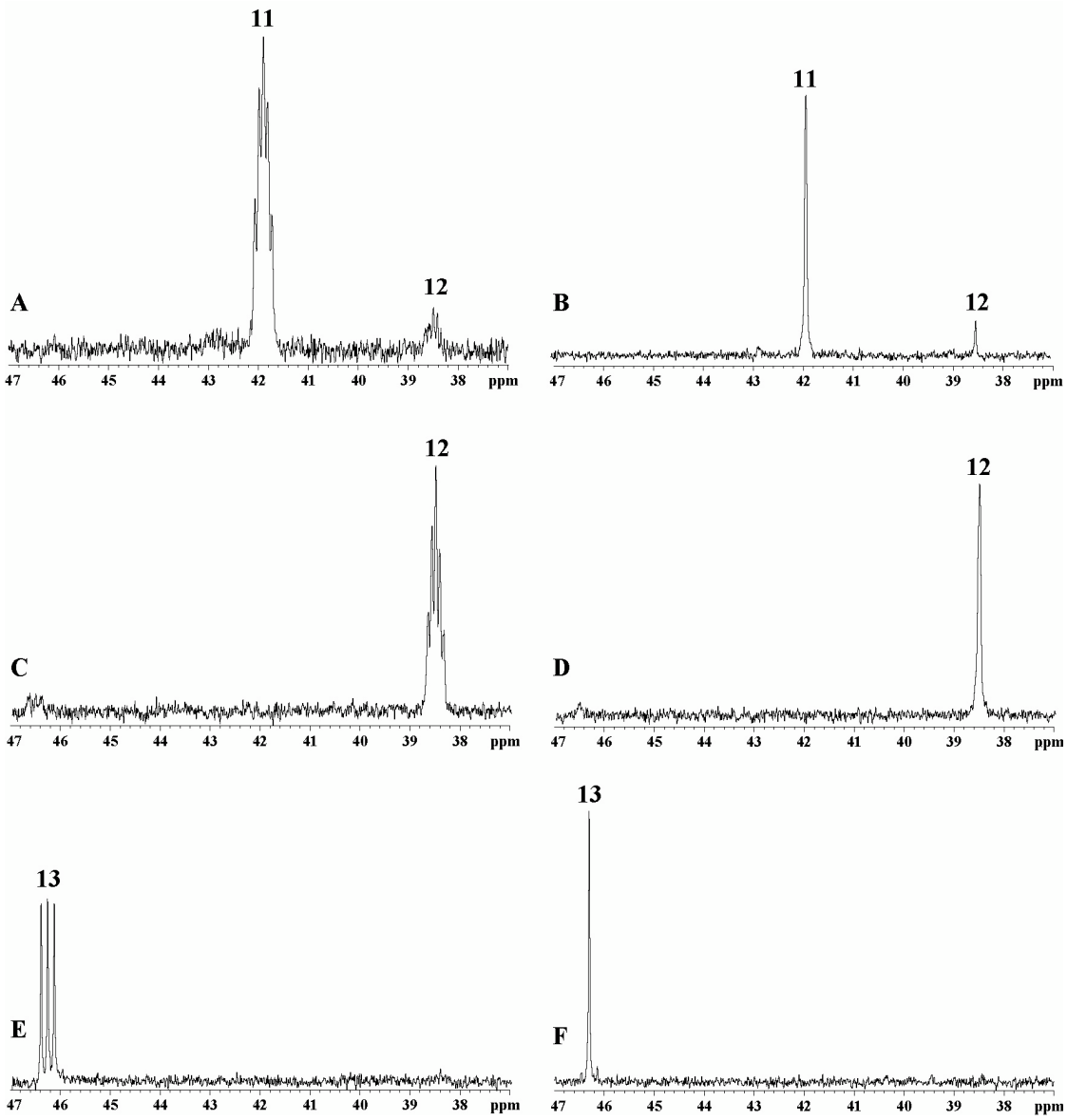

Figure S35. ^{15}N NMR spectra recorded on [^{6}Li,^{15}N]LiHMDS (0.10 M) and varying concentrations of **10** in toluene at -75 ^{o}C: (A) and (B) 0.05 M; (C) and (D) 0.10 M; (E) and (F) 0.50 M. Spectra B, D, and F were recorded with ^{6}Li broad-band decoupling.

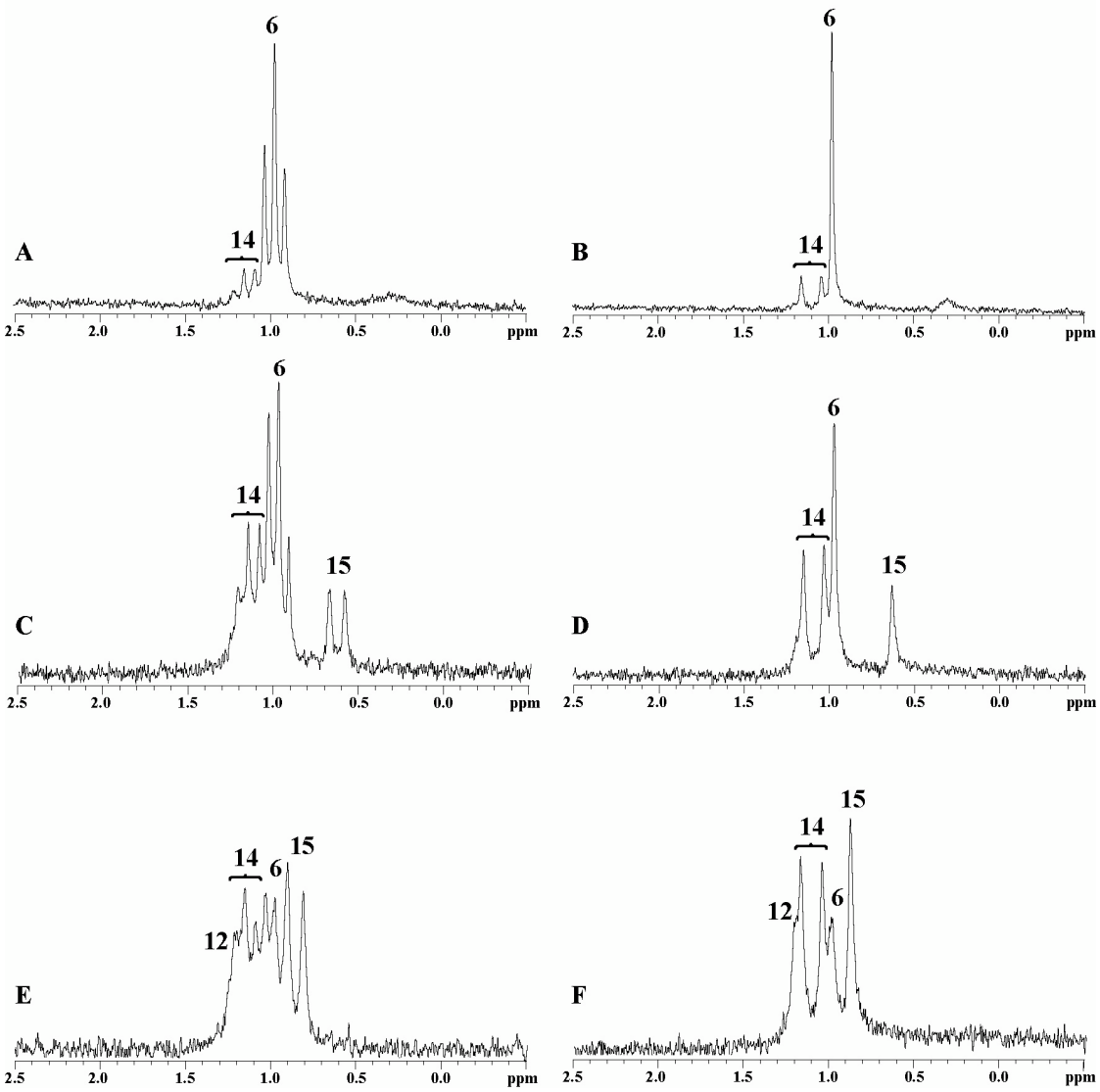

Figure S36. ^{6}Li NMR spectra recorded on [^{6}Li,^{15}N]LiHMDS (0.10 M) and varying concentrations of **10** at 2.0 M THF/toluene at -75 ^{o}C: (A) and (B) 0.02 M; (C) and (D) 0.05 M; (E) and (F) 0.10 M; (G) and (H) 0.20 M; (I) and (J) 0.50 M. Spectra B, D, F, H, and J were recorded with ^{15}N broad-band decoupling.

Figure S36 (continued)

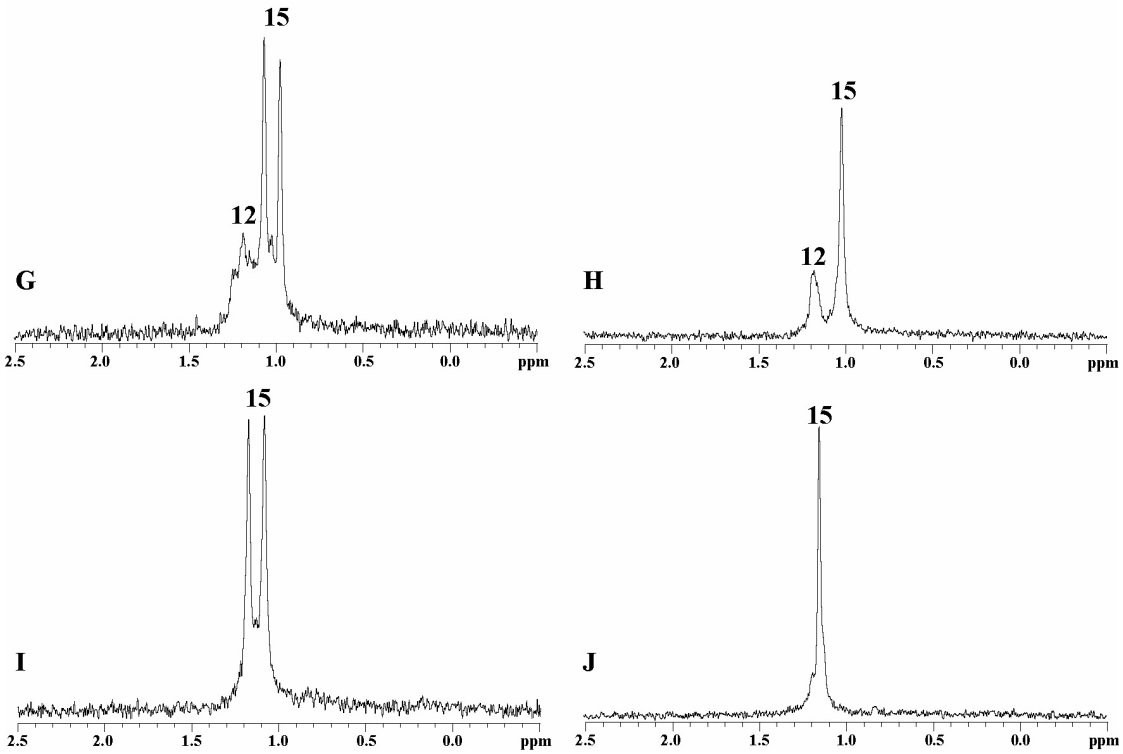

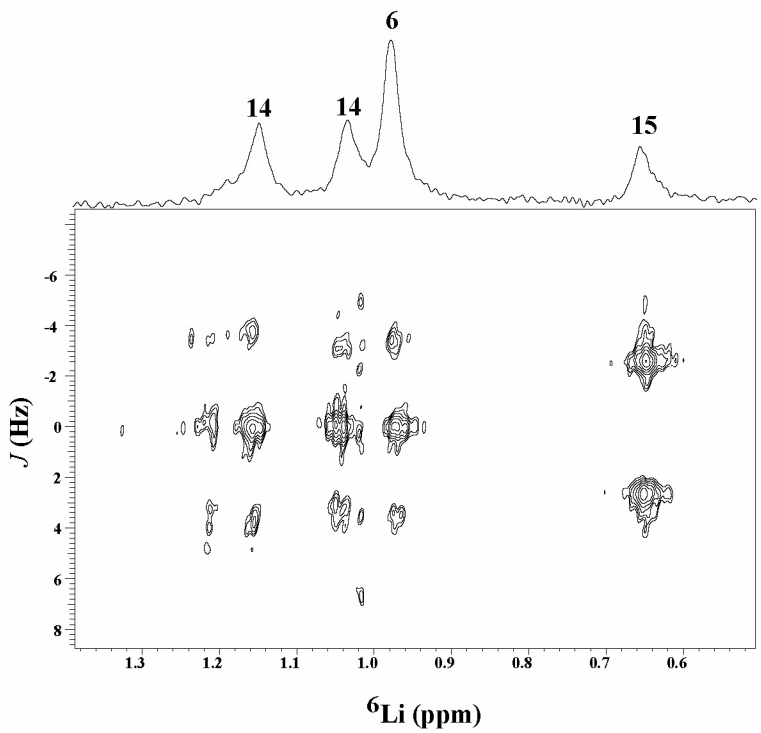

Figure S37. ^{6}Li *J*-resolved spectrum recorded on a solution of [^{6}Li,^{15}N]LiHMDS (0.10 M) and **10** (0.05 M) at 2.0 M THF/toluene at -75 ^{o}C.

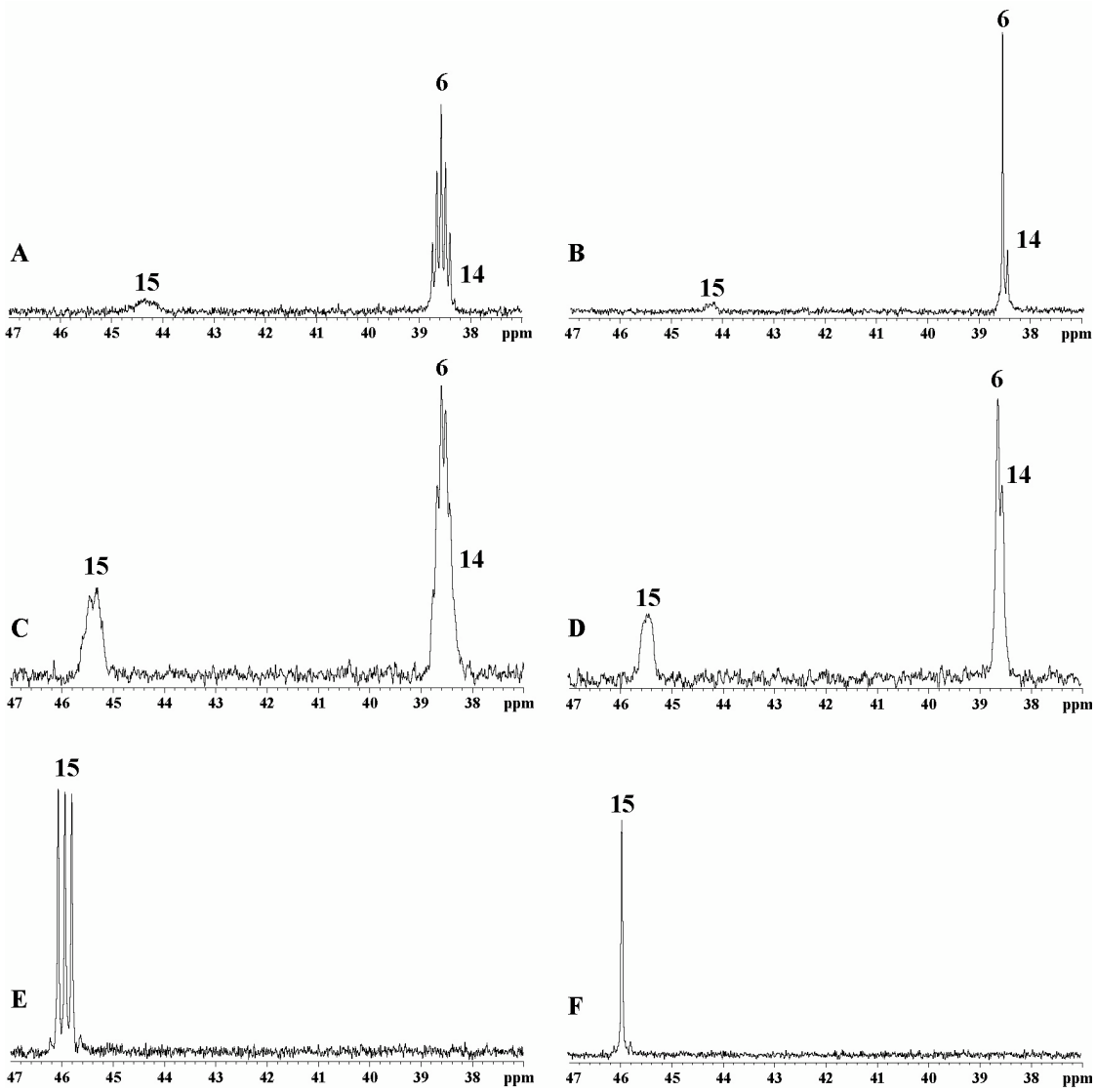

Figure S38. ^{15}N NMR spectra recorded on [^{6}Li,^{15}N]LiHMDS (0.10 M) and varying concentrations of **10** at 2.0 M THF/toluene at -75 ^{o}C: (A) and (B) 0.02 M; (C) and (D) 0.05 M; (E) and (F) 0.50 M. Spectra B, D, and F were recorded with ^{6}Li broad-band decoupling.

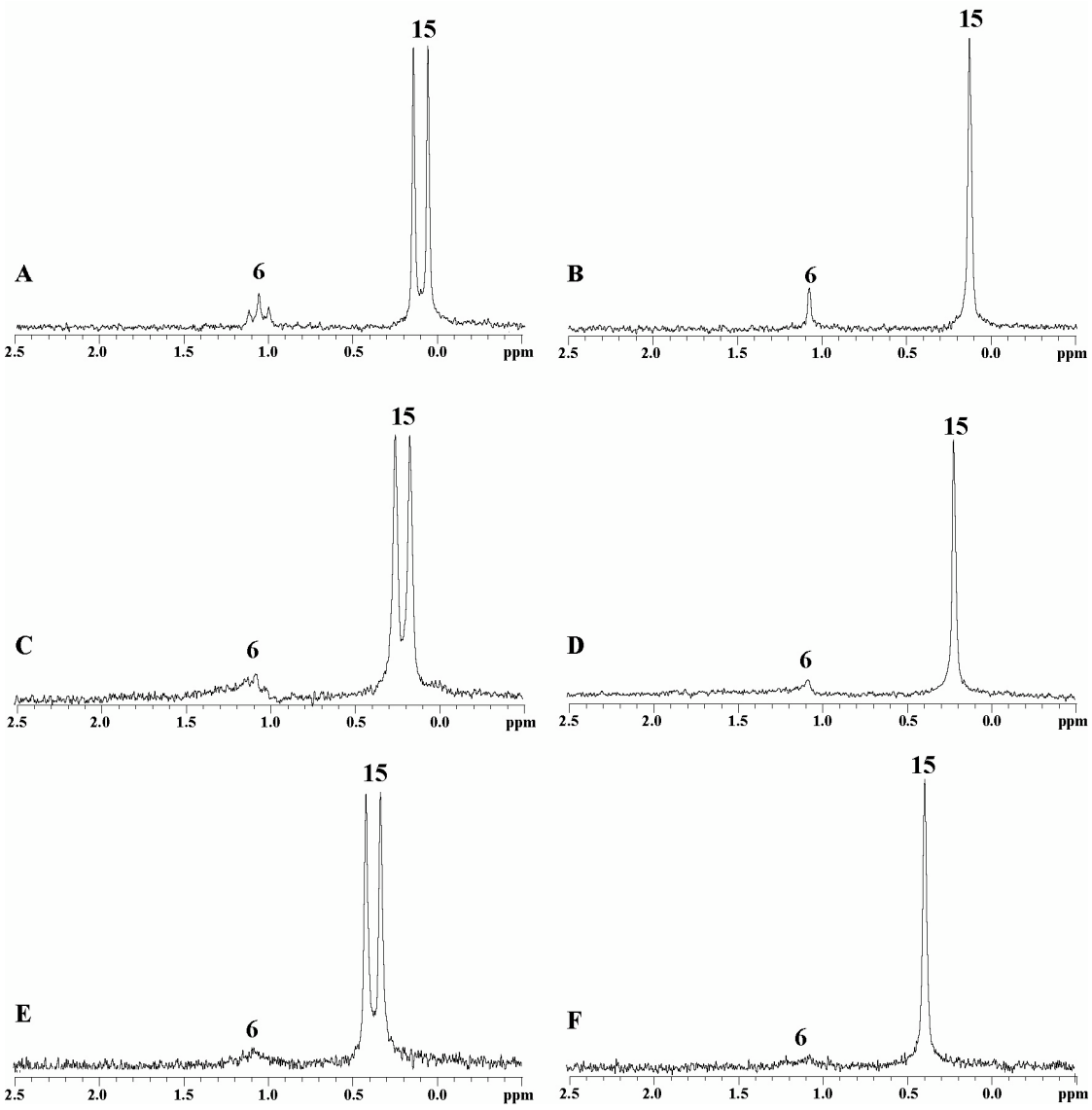

Figure S39. ^{6}Li NMR spectra recorded on [^{6}Li,^{15}N]LiHMDS (0.10 M) and varying concentrations of **10** at 8.0 M THF/toluene at -75 ^{o}C: (A) and (B) 0.02 M; (C) and (D) 0.05 M; (E) and (F) 0.10 M; (G) and (H) 0.20 M; (I) and (J) 0.30 M; (K) and (L) 0.50 M. Spectra B, D, F, H, J, and L were recorded with ^{15}N broad-band decoupling.

Figure S39 (continued)

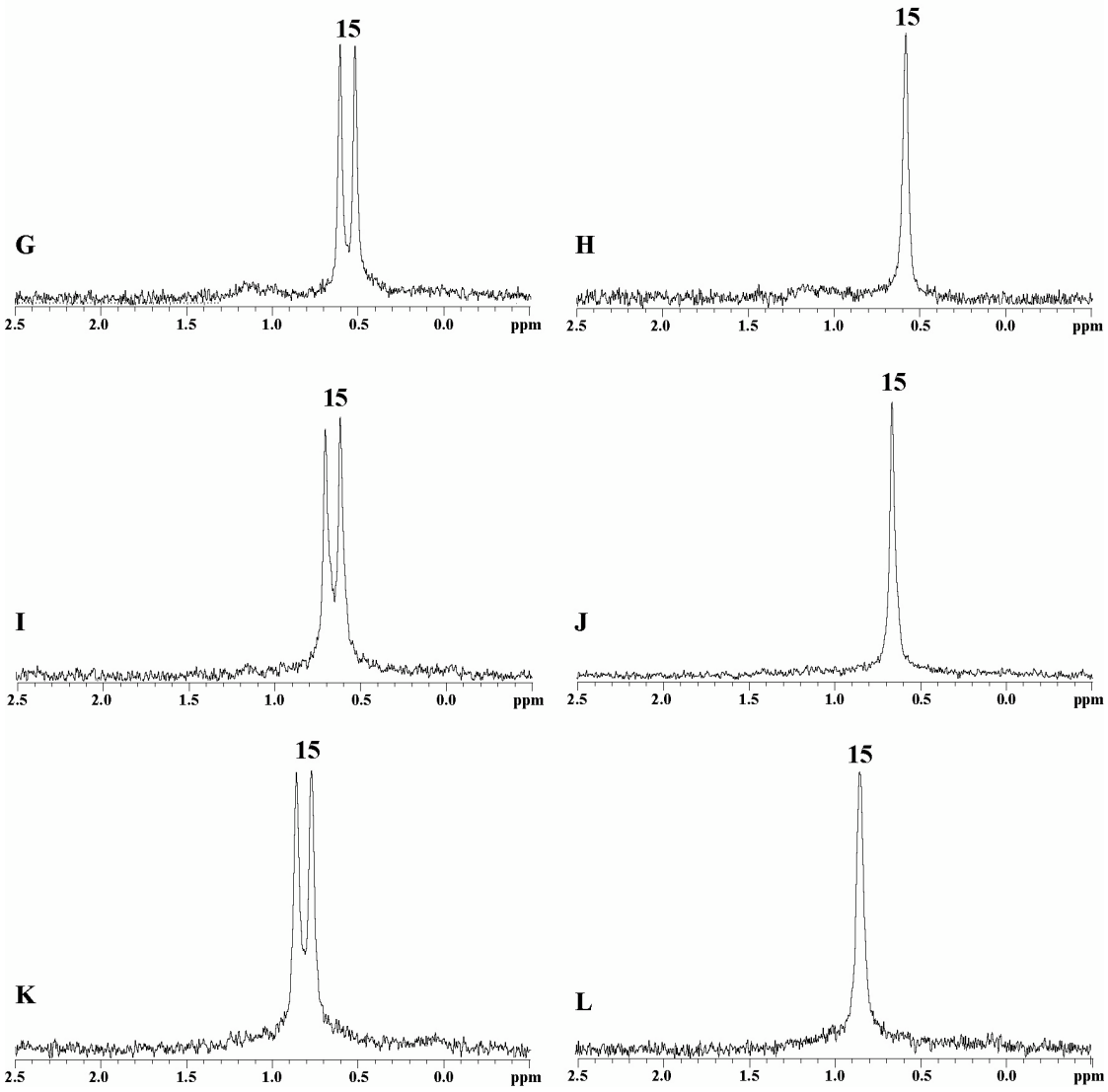

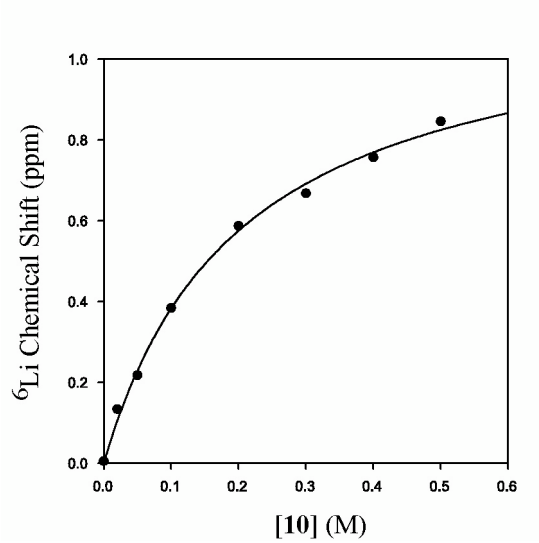

Figure S40. Plot of the ^{6}Li chemical shift (ppm) versus the [**10**] (M) for 0.10 M [^{6}Li,^{15}N]LiHMDS at 8.0 M THF/toluene as shown in Figure S39. The curve depicts an unweighted least-squares fit to $y = (ax)/(1+bx)$, where $a = 5.7 \pm 0.4$ and $b = 4.9 \pm 0.5$.

Table S11. Table of ^{6}Li chemical shifts for the data shown in Figures S39-S40.

[**10**] (M)	Chemical Shift (ppm)	*J* (Hz)
0	0.005	5.0
0.02	0.134	5.1
0.05	0.218	5.1
0.10	0.384	5.1
0.20	0.587	5.1
0.30	0.668	5.1
0.40	0.757	5.2
0.50	0.846	5.2

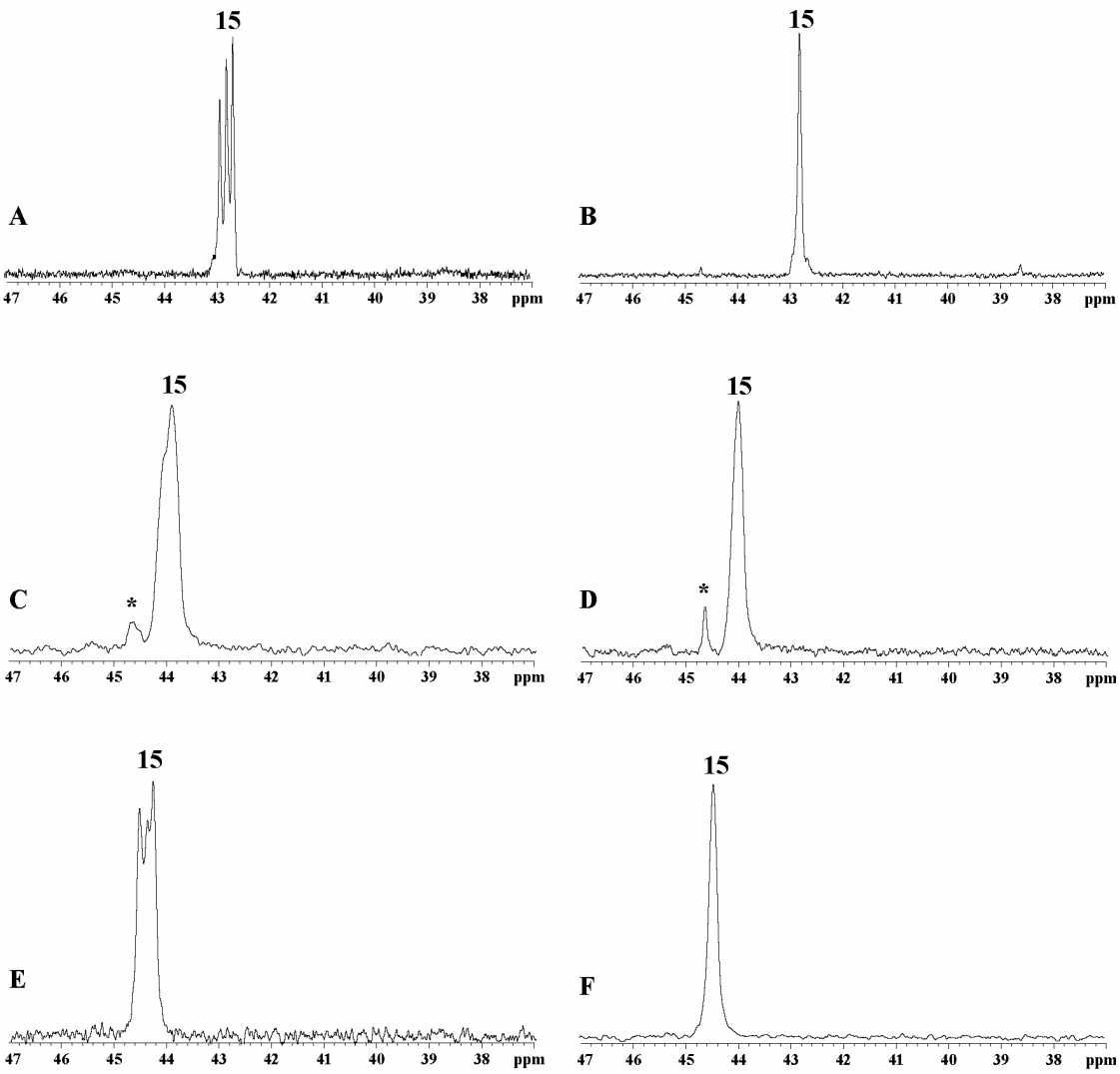

Figure S41. ^{15}N NMR spectra recorded on [^{6}Li,^{15}N]LiHMDS (0.10 M) and varying concentrations of **10** at 8.0 M THF/toluene at -75 ^{o}C: (A) and (B) 0.20 M; (C) and (D) 0.30 M; (E) and (F) 0.40 M. Spectra B, D, and F were recorded with ^{6}Li broad-band decoupling. (*denotes an unassigned resonance.)

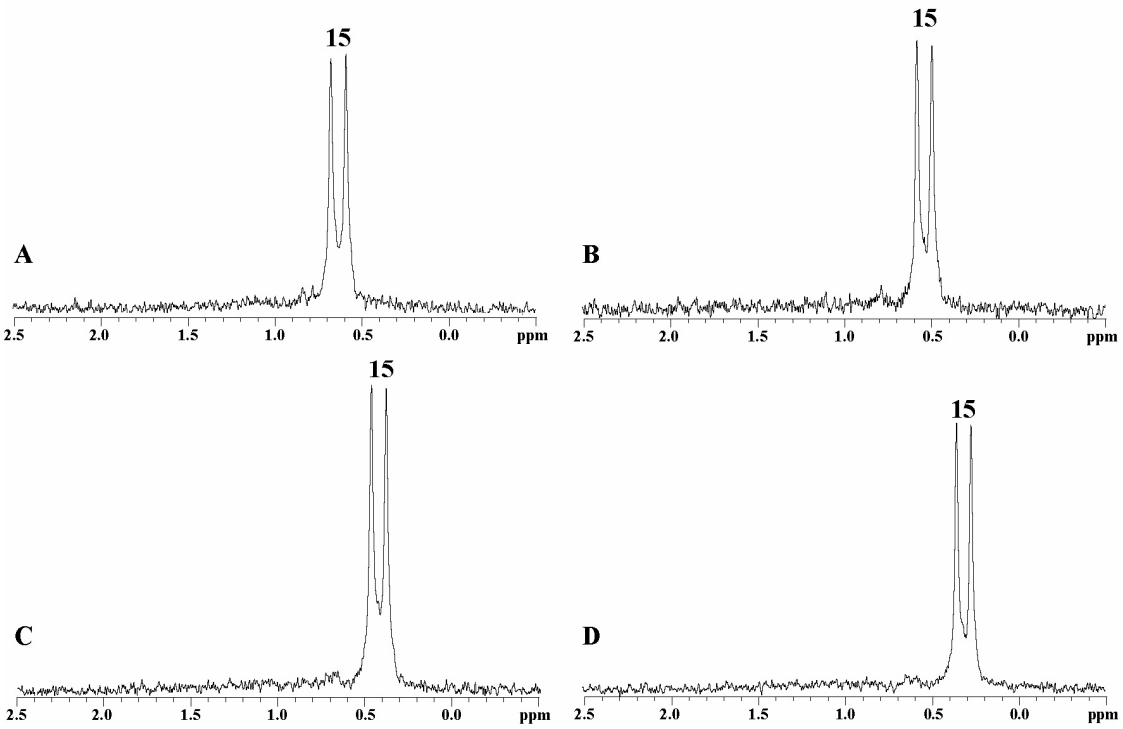

Figure S42. ^{6}Li NMR spectra recorded on [^{6}Li,^{15}N]LiHMDS (0.10 M) and **10** (0.30 M) at 8.0 M THF/toluene at various temperatures: (A) -75 ^{o}C; (B) -85 ^{o}C; (C) -95 ^{o}C; (D) -105 ^{o}C.

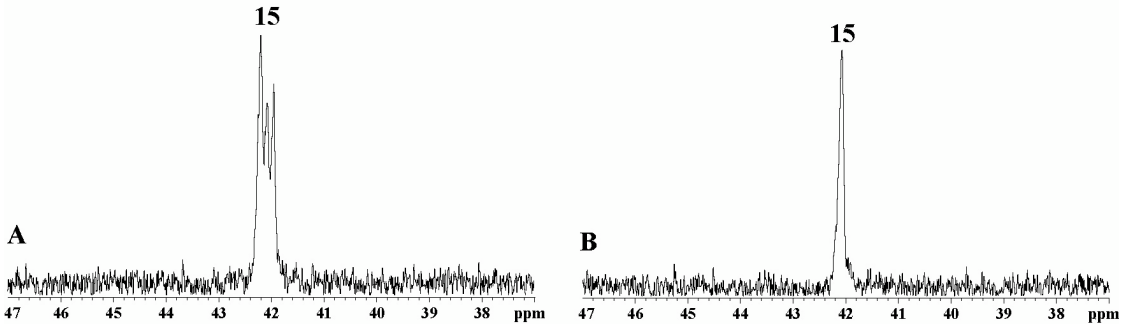

Figure S43. ^{15}N NMR spectra recorded on [^{6}Li,^{15}N]LiHMDS (0.10 M) and **10** (0.30 M) at 8.0 M THF/toluene at -105 ^{o}C. Spectrum B was recorded with ^{6}Li broad-band decoupling.

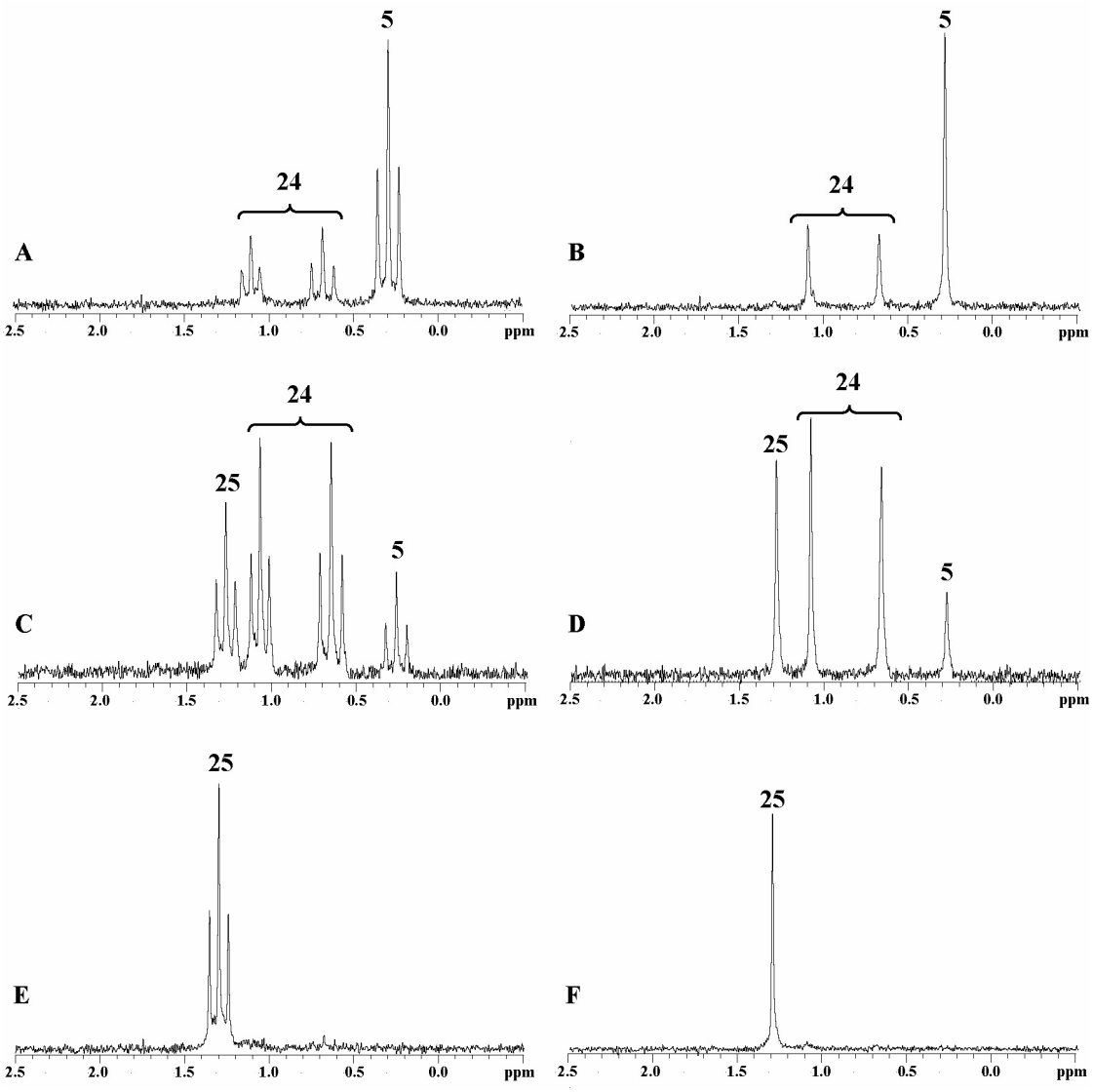

Figure S44. ^{6}Li NMR spectra recorded on [^{6}Li,^{15}N]LiHMDS (0.10 M) and varying concentrations of **23** in neat toluene at -75 ^{o}C: (A) and (B) 0.02 M; (C) and (D) 0.05 M; (E) and (F) 0.10 M; (G) and (H) 0.20 M; (I) and (J) 0.50 M. Spectra B, D, F, H, and J were recorded with ^{15}N broad-band decoupling.

Figure S44 (continued)

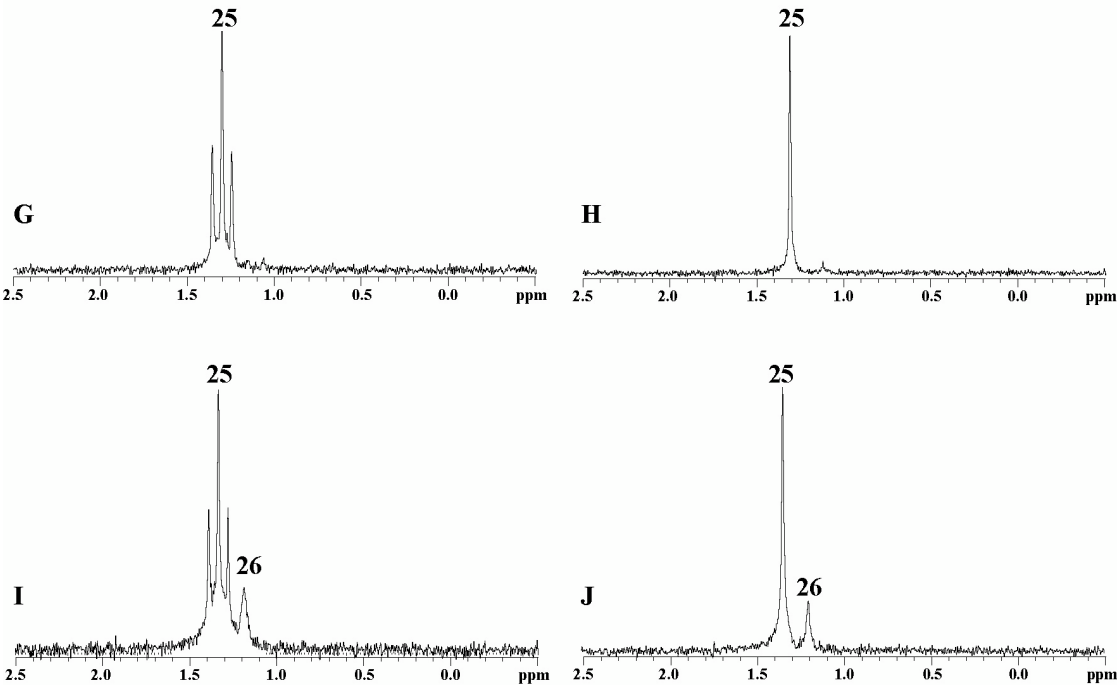

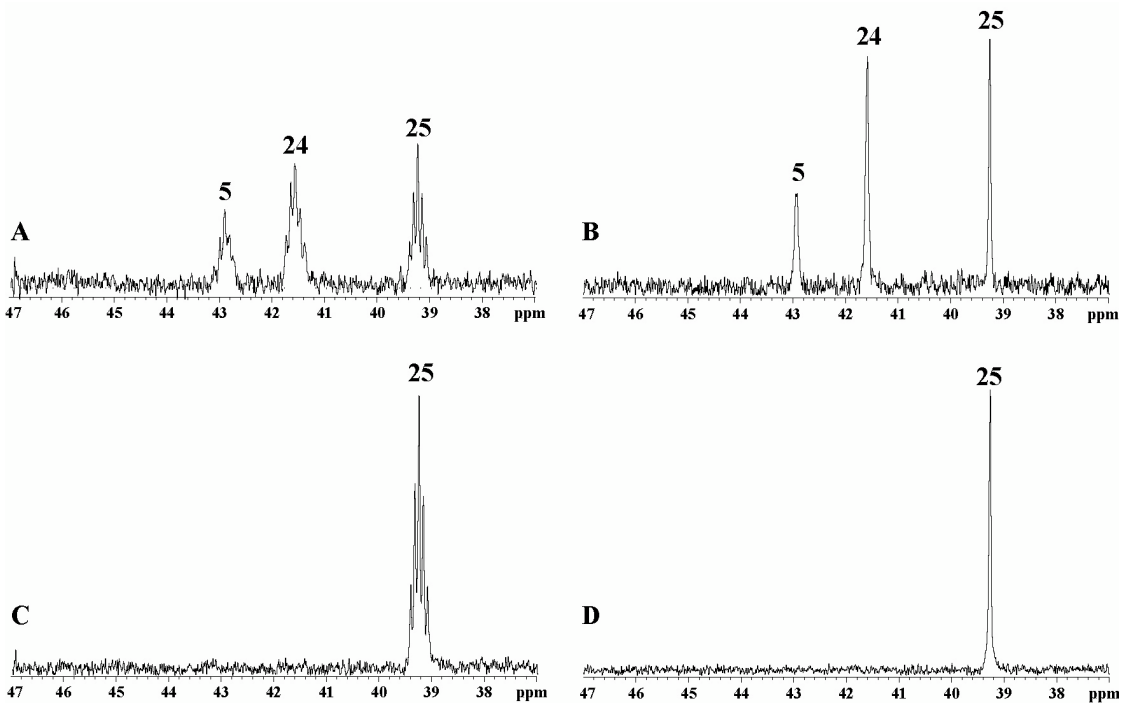

Figure S45. ^{15}N NMR spectra recorded on [^{6}Li,^{15}N]LiHMDS (0.10 M) and varying concentrations of **23** in neat toluene at -75 ^{o}C: (A) and (B) 0.05 M; (C) and (D) 0.20 M. Spectra B and D were recorded with ^{6}Li broad-band decoupling.

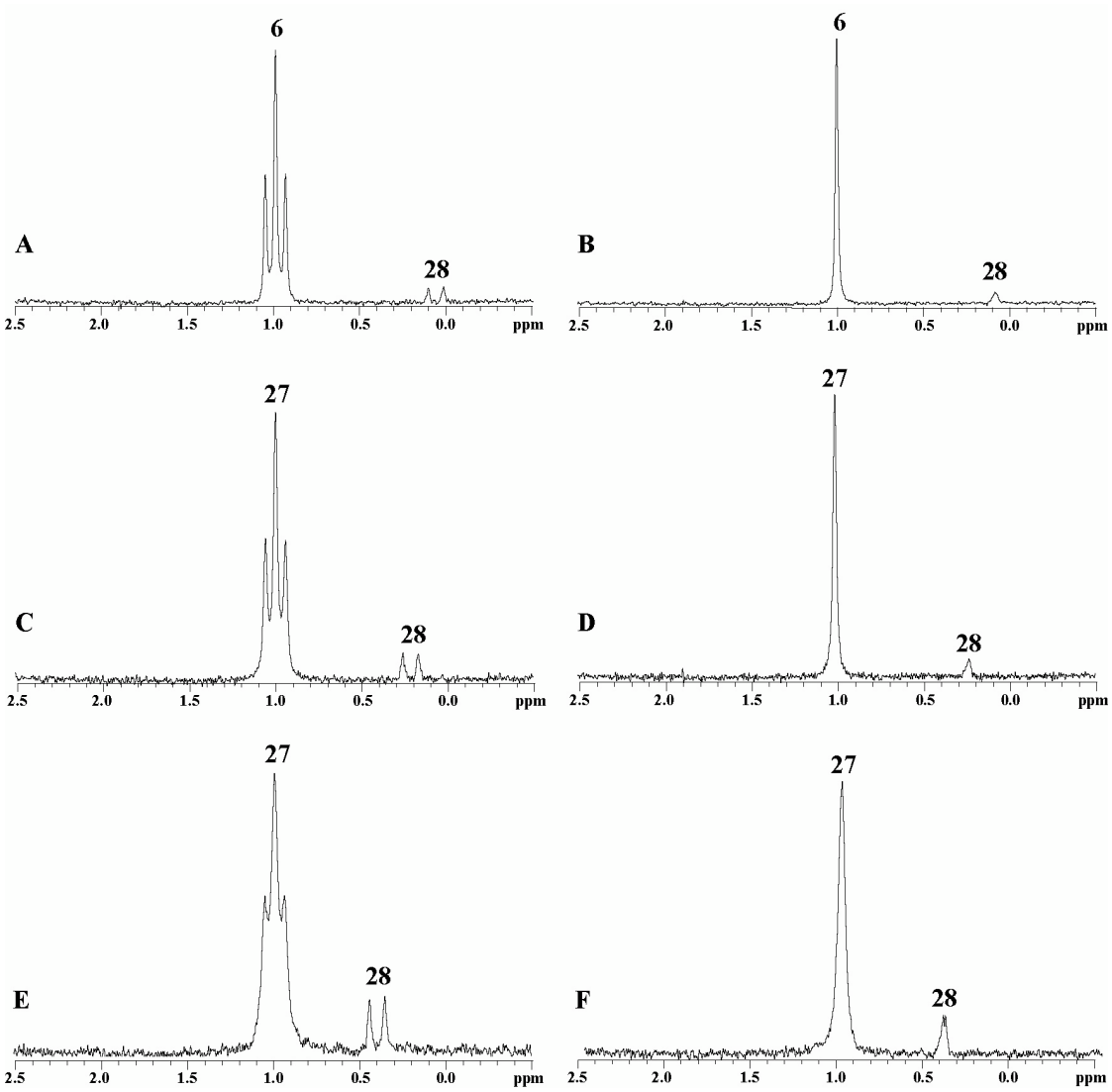

Figure S46. ^{6}Li NMR spectra recorded on [^{6}Li,^{15}N]LiHMDS (0.10 M) and varying concentrations of **23** at 2.0 M THF/toluene at -75 ^{o}C: (A) and (B) 0.02 M; (C) and (D) 0.05 M; (E) and (F) 0.10 M; (G) and (H) 0.20 M; (I) and (J) 0.50 M. Spectra B, D, F, H, and J were recorded with ^{15}N broad-band decoupling.

Figure S46 (continued)

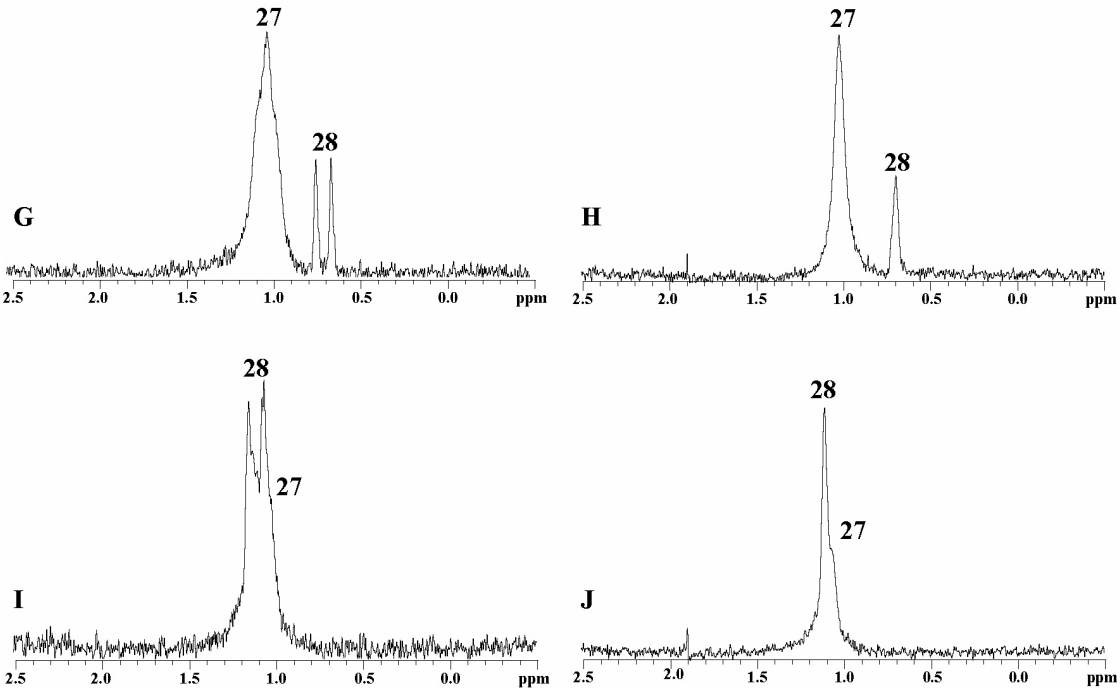

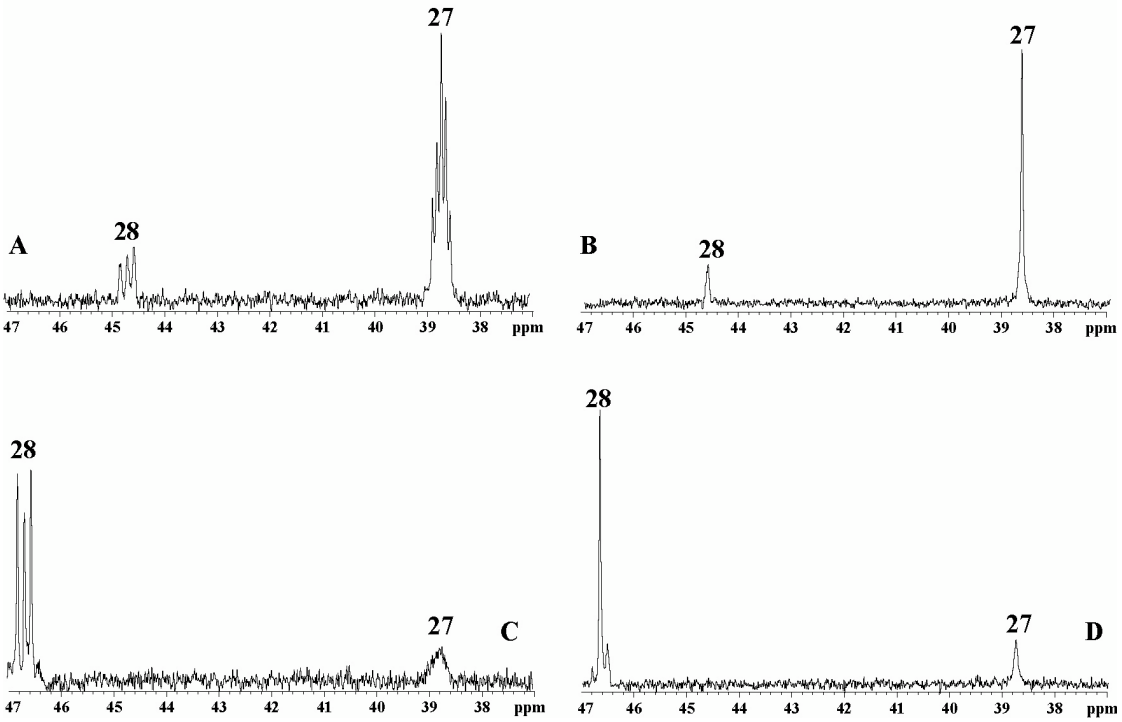

Figure S47. ^{15}N NMR spectra recorded on [^{6}Li,^{15}N]LiHMDS (0.10 M) and varying concentrations of **23** at 2.0 M THF/toluene at -75 ^{o}C: (A) and (B) 0.10 M; (C) and (D) 0.50 M. Spectra B and D were recorded with ^{6}Li broad-band decoupling.

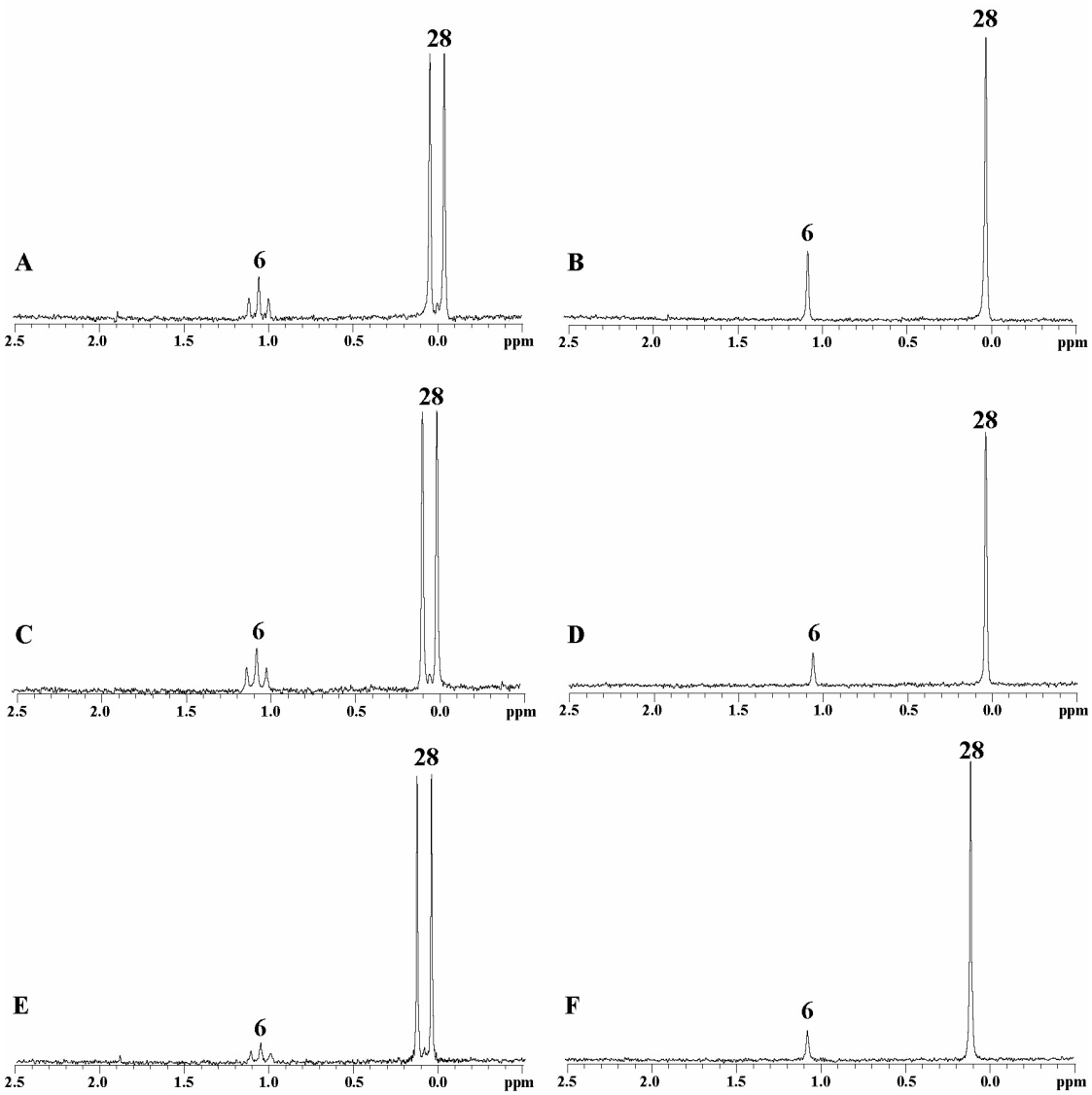

Figure S48. ^{6}Li NMR spectra recorded on [^{6}Li,^{15}N]LiHMDS (0.10 M) and varying concentrations of **23** at 8.0 M THF/toluene at -75 ^{o}C: (A) and (B) 0.02 M; (C) and (D) 0.05 M; (E) and (F) 0.10 M; (G) and (H) 0.20 M; (I) and (J) 0.50 M. Spectra B, D, F, H, and J were recorded with ^{15}N broad-band decoupling.

Figure S48 (continued)

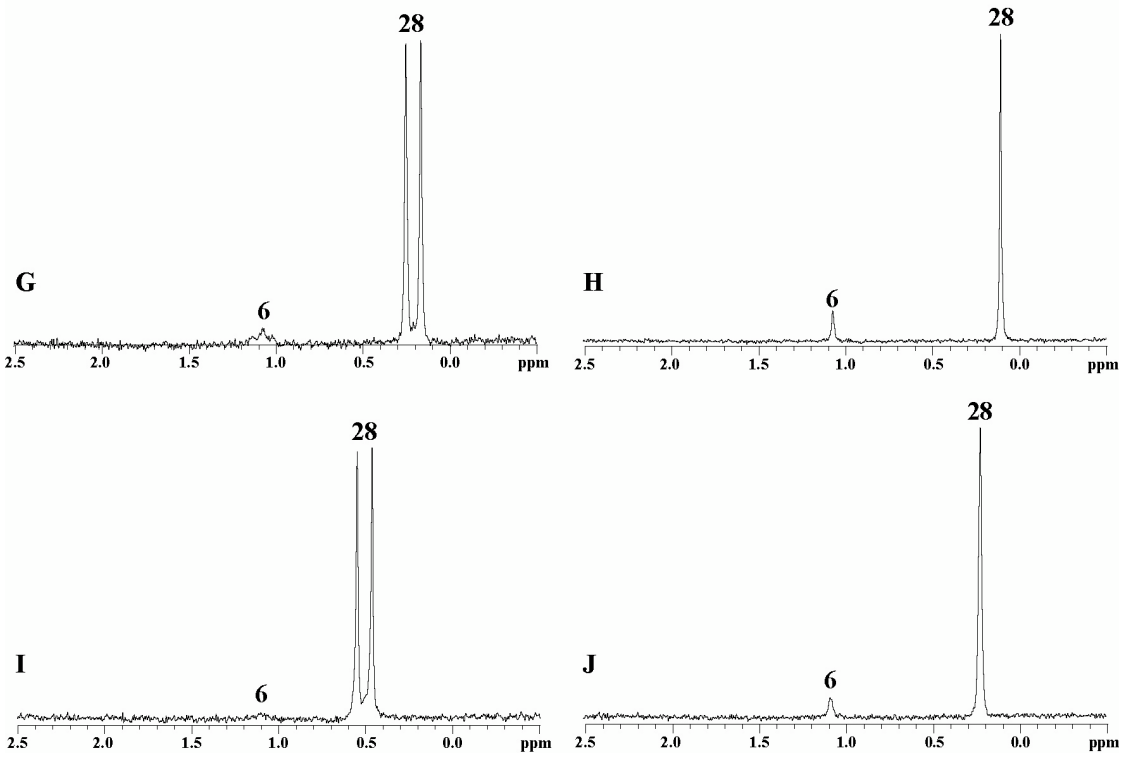

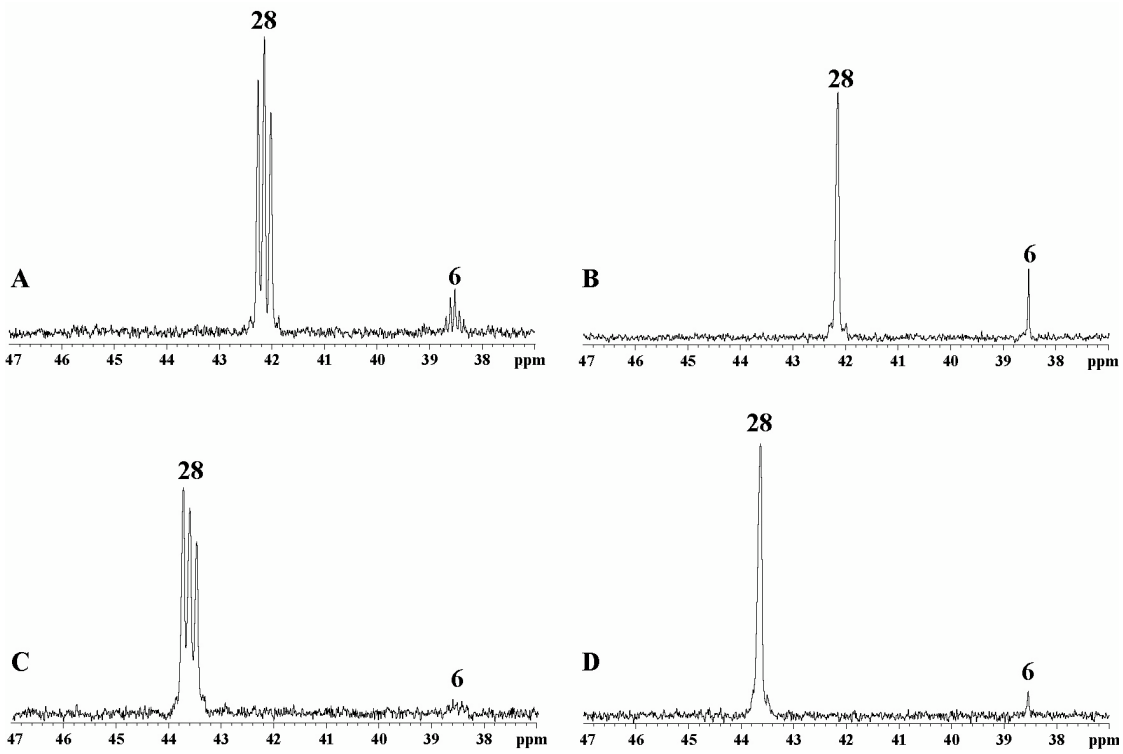

Figure S49. ^{15}N NMR spectra recorded on [^{6}Li,^{15}N]LiHMDS (0.10 M) and varying concentrations of **23** at 8.0 M THF/toluene at -75 ^{o}C: (A) and (B) 0.05 M; (C) and (D) 0.50 M. Spectra B and D were recorded with ^{6}Li broad-band decoupling.

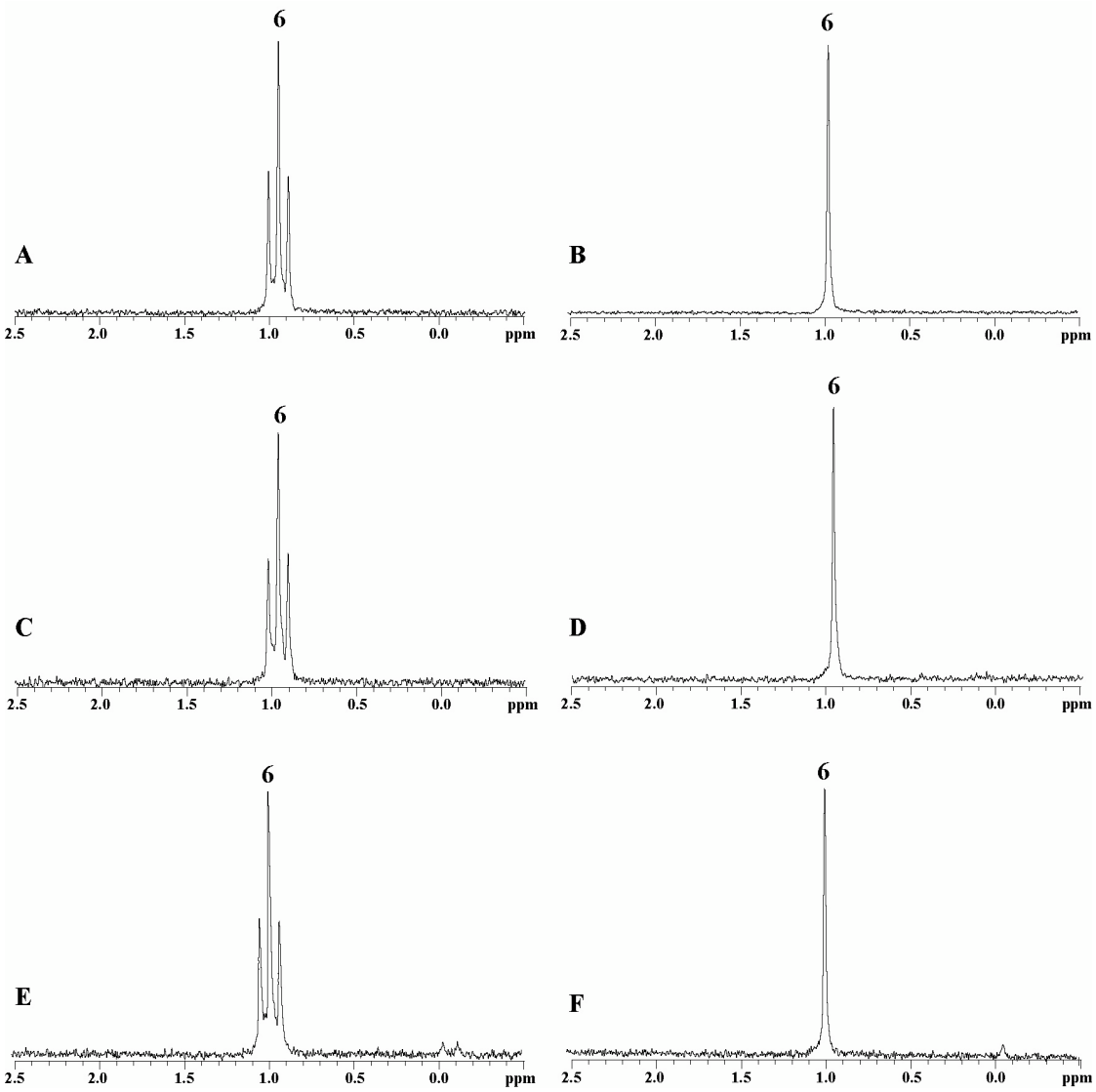

Figure S50. ^{6}Li NMR spectra recorded on [^{6}Li,^{15}N]LiHMDS (0.10 M) at varying THF concentrations with toluene at -75 ^{o}C: (A) and (B) 0.10 M; (C) and (D) 1.0 M; (E) and (F) 2.0 M; (G) and (H) 4.0 M; (I) and (J) 8.0 M. Spectra B, D F, H, and J were recorded with ^{15}N broad-band decoupling.

Figure S50 (continued)

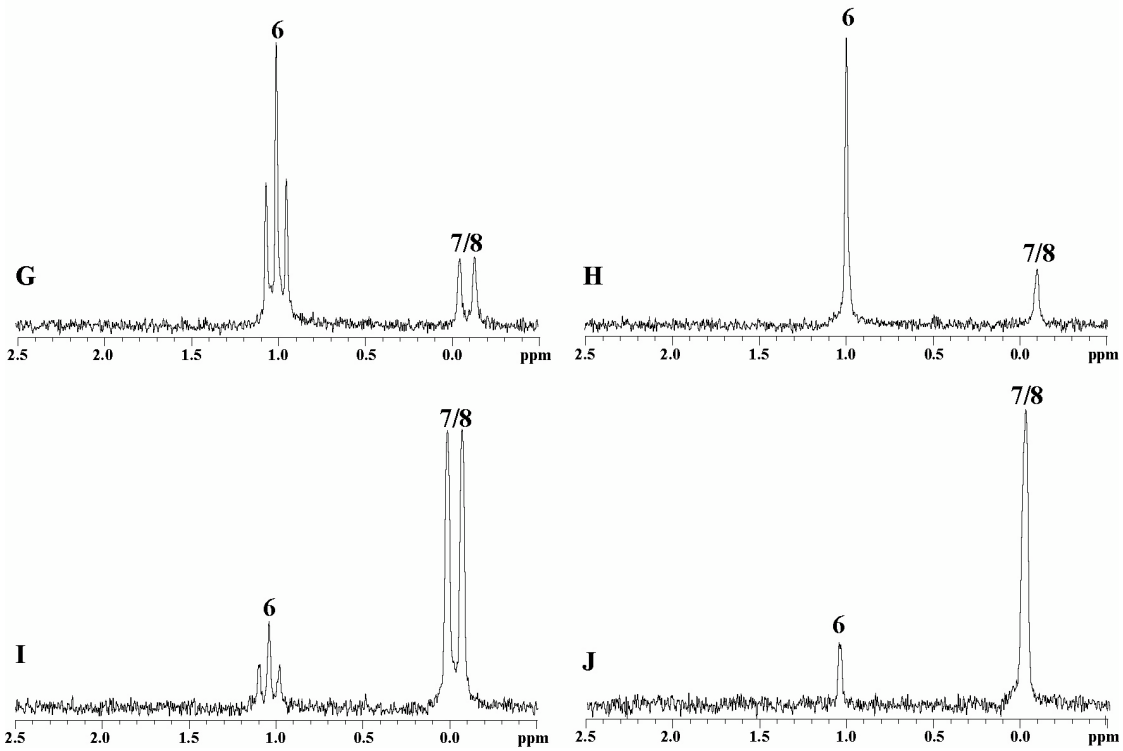

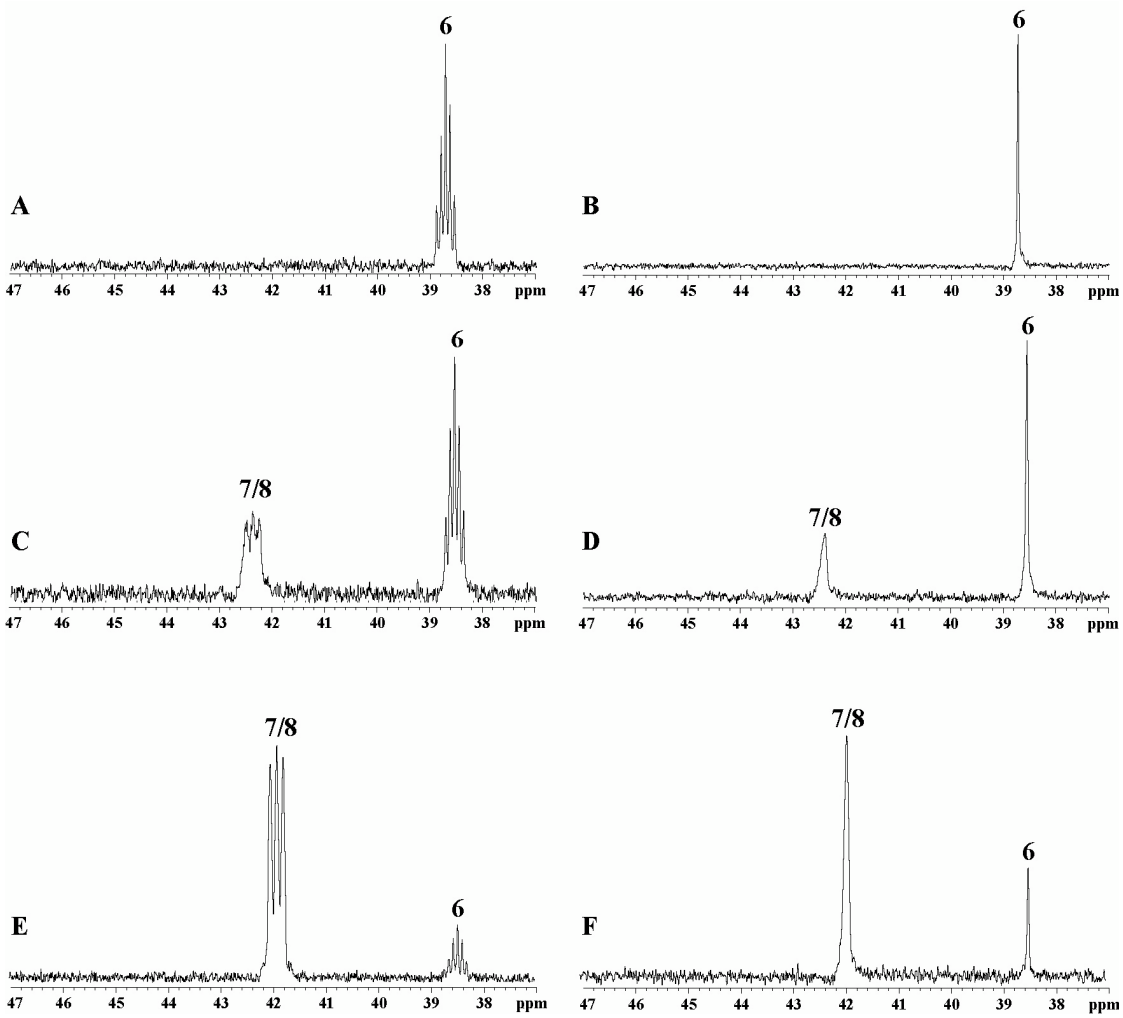

Figure S51. ^{15}N NMR spectra recorded on [^{6}Li,^{15}N]LiHMDS (0.10 M) in varying THF concentrations with toluene at -75 ^{o}C: (A) and (B) 0.10 M; (C) and (D) 4.0 M; (E) and (F) 8.0 M. Spectra B, D, and F were recorded with ^{6}Li broad-band decoupling.

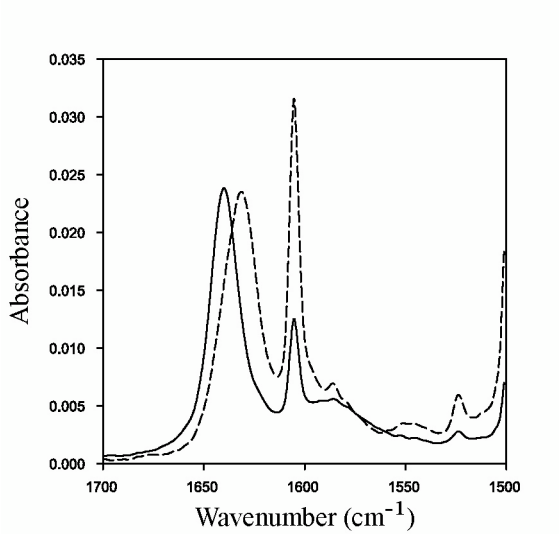

Figure S52. IR spectra recorded on **1** (1640 cm^{-1}, solid, 0.01 M) and LiHMDS/**1** (1630 cm^{-1}, dashed, 0.02/0.01 M) at 11.7 M THF/toluene at -78 ^{o}C.

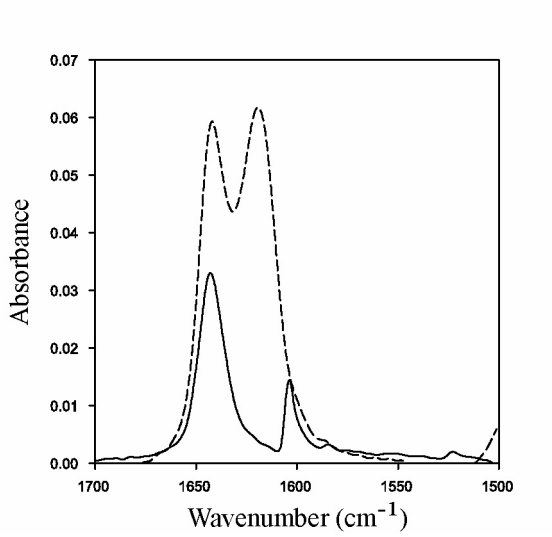

Figure S53. IR spectra recorded on **10** (1640 cm^{-1}, solid, 0.01 M) and LiHMDS/**10** (1640 and 1620 cm^{-1}, dashed, 0.10/0.05 M) at 8.0 M THF/toluene at -78 ^{o}C.

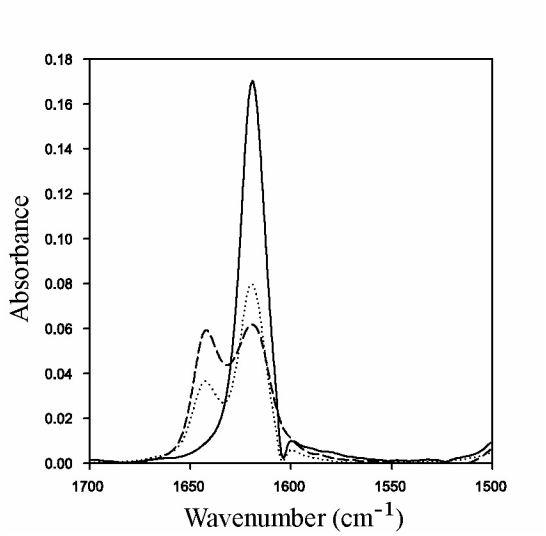

Figure S54. IR spectra recorded on solutions of LiHMDS (0.10 M) and **10** (0.05 M) at various THF concentrations with toluene at -78 ^{o}C: 0.0 M (1618 cm^{-1}, solid); 2.0 M (1640 and 1620 cm^{-1}, dotted); 8.0 M (1640 and 1620 cm^{-1}, dashed).

Alkylation Diastereoselectivities

Sample procedure. LiHMDS (117 mg, 0.7 mmol) was dissolved in 0.07 M THF (60 μL THF) and toluene (9.9 mL) and cooled to -78 ^{o}C. β-Amino amide **1** (41.3 mg, 0.2 mmol) was added neat. After 30 min, CH_3I (20 μL, 0.3 mmol) was added to the flask. After 30 min at -78 ^{o}C, the reaction was quenched with H_2O and warmed to ambient temperature. The slurry was extracted with Et_2O (3 x 25 mL), and the organic layer was dried over $MgSO_4$ and concentrated in vacuo. GC analysis of the crude reaction mixture shows a 59:1 ratio of **2**:**3** in 90% conversion. Column chromatography (90/10 CH_2Cl_2/MeOH) yields 30.6 mg of **2** (69%).

Table S12. Alkylation Diastereoselectivities using 1.5 equiv CH_3I.

Entry	equiv LiHMDS	[THF]	Temp. (^{o}C)	**2**:**3**	% Yield[a,b]
1	1.2	12.3 M	0	6:1	70[b]
2	2.0	12.3 M	0	7:1	80[b]
3	3.0	0.0 M	0	33:1	75[a]
4	3.5	1 equiv	-78	135:1	78[a]
5	3.5	1 equiv	-78	72:1	87[a]
6	3.5	1 equiv	-78	59:1	90[a], 69[b]
7	3.5	5 equiv	-78	87:1	79[a]
8	3.5	6.0 M	-78	79:1	80[a]
9	3.5	0.0 M	-78	55:1	81[a]
10	3.5	0.01 M	-78	59:1	69[a]
11	3.5	0.04 M	-78	27:1	93[a]
12	3.5	0.5 M	-78	56:1	76[a]
13	3.5	4.0 M	-78	61:1	84[a]
14	3.5	11.0 M	-78	40:1	91[a]
15	1.0	0.0 M	-78	61:1	88[a]
16	2.0	0.0 M	-78	74:1	80[a]
17	3.0	0.0 M	-78	80:1	88[a]
18	3.5	8.0 M	-78	46:1	87[a], 78[b]
19	1.0	0.5 equiv	25	11:1	98[a]
20	1.0	0.0 M	25	11:1	98[a]

[a]Yield determined by GC integration relative to remaining **1**. [b]Isolated yield after column chromatography.